NUREG/CR-1504
ANL-80-47

NUREG/CR-1504
ANL-80-47

A User's Guide to EPIC, a Computer Program to Calculate the Motion of Fuel and Coolant Subsequent to Pin Failure in an LMFBR

by

P. A. Pizzica, P. L. Garner,
and P. B. Abramson

ARGONNE NATIONAL LABORATORY

ARGONNE NATIONAL LABORATORY, ARGONNE, ILLINOIS

Prepared for the U. S. NUCLEAR REGULATORY COMMISSION
under Interagency Agreement DOE 40-550-75

The facilities of Argonne National Laboratory are owned by the United States Government. Under the terms of a contract (W-31-109-Eng-38) among the U. S. Department of Energy, Argonne Universities Association and The University of Chicago, the University employs the staff and operates the Laboratory in accordance with policies and programs formulated, approved and reviewed by the Association.

MEMBERS OF ARGONNE UNIVERSITIES ASSOCIATION

The University of Arizona
Carnegie-Mellon University
Case Western Reserve University
The University of Chicago
University of Cincinnati
Illinois Institute of Technology
University of Illinois
Indiana University
The University of Iowa
Iowa State University
The University of Kansas
Kansas State University
Loyola University of Chicago
Marquette University
The University of Michigan
Michigan State University
University of Minnesota
University of Missouri
Northwestern University
University of Notre Dame
The Ohio State University
Ohio University
The Pennsylvania State University
Purdue University
Saint Louis University
Southern Illinois University
The University of Texas at Austin
Washington University
Wayne State University
The University of Wisconsin-Madison

Available from

GPO Sales Program
Division of Technical Information and Document Control
U. S. Nuclear Regulatory Commission
Washington, D.C. 20555

and

National Technical Information Service
Springfield, Virginia 22161

NUREG/CR-1504
ANL-80-47

(Distribution
Code: R7)

ARGONNE NATIONAL LABORATORY
9700 South Cass Avenue
Argonne, Illinois 60439

A User's Guide to EPIC, a Computer Program to Calculate the Motion of Fuel and Coolant Subsequent to Pin Failure in an LMFBR

by

P. A. Pizzica, P. L. Garner,
and P. B. Abramson

Applied Physics Division

October 1979

Prepared for the Division of Reactor Safety Research
Office of Nuclear Regulatory Research
U. S. Nuclear Regulatory Commission
Washington, D. C. 20555
Under Interagency Agreement DOE-40-550-75

NRC FIN No. A2015

A User's Guide to EPIC, a Computer Program to Calculate the Motion of Fuel and Coolant Subsequent to Pin Failure in an LMFBR

by

P. A. Pizzica
P. L. Garner
R. B. Abramson

ABSTRACT

The computer code EPIC models fuel and coolant motion which results from internal fuel pin pressure (from fission gas or fuel vapor) and possibly from the generation of sodium vapor pressure in the coolant channel subsequent to pin failure in a liquid-metal fast breeder reactor. The EPIC model is restricted to conditions where fuel pin geometry is generally preserved and is not intended to treat the total disruption of the pin structure. The modeling includes the ejection of molten fuel from the pin into a coolant channel with any amount of voiding through a clad breach which may be of any length or which may extend with time. One-dimensional Eulerian hydrodynamics is used to treat the motion of fuel and fission gas inside a molten fuel cavity in the fuel pin as well as the mixture of two-phase sodium and fission gas in the coolant channel. Motion of fuel in the coolant channel is tracked with a type of particle-in-cell technique. EPIC is a Fortran-IV program requiring 400K bytes of storage on the IBM 370/195 computer.

NRC FIN No. A2015

Title

Reactor Safety Modeling and Assessment

TABLE OF CONTENTS

LIST OF FIGURES

EXECUTIVE SUMMARY

The EPIC (Eulerian Particle In Cell)computer code was written to calculate material motions following pin failure in a Liquid Metal Cooled Fast Breeder Reactor (LMFBR) during a loss-of-flow (LOF) transient as well as a transient overpower (TOP) accident. EPIC assumes that the pin structure is generally intact after pin failure such as would be the case in the burst failure conditions resulting from fission gas pressure or differential expansion loading of the cladding. This would result in a localized cladding breach allowing communication between the interior of the fuel pin and the coolant channel. The EPIC model is inappropriate for pin failure which involves a massive disruption of pin structure such as would occur when the cladding is in a partially or fully molten state.

The EPIC model is appropriate for pin failures in TOP conditions. It is also capable of modeling pin failures in middle and lower power subassemblies under loss-of-flow-driven TOP (LOF-TOP) conditions. If a fast reactor core voids incoherently enough and if there is sufficient sodium void reactivity insertion from the higher power subassemblies to bring the reactor into the vicinity of prompt-critical, a rapid power rise will result so that middle and lower power subassemblies will experience conditions similar to those in a TOP with some or all of the sodium coolant still present. This LOF-TOP situation is not unusual in larger fast reactors with homogeneous cores. It is not inconceivable that failures near the center of the core may occur, so that the calculation of fuel motion is crucial to the determination of reactivity effects.

To a large extent, EPIC is a parametric code. Our lack of knowledge of the physical processes involved requires this approach. Many of the significant features of the model are parameterized, and often only a partial mechanistic treatment is done. For example, initial cladding rip length, fuel particle size, and most heat transfer rates must be specified as input. This parametric approach provides a certain flexibility in the use of the code, and it also reflects a reluctance to treat highly complicated and poorly understood phenomena with models that are supposedly accurate and well-founded but actually make highly significant but unjustifiable assumptions.

EPIC models a single fuel pin with its associated coolant which represents part of or all of a subassembly or a group of similar subassemblies under pin failure conditions. This is similar to the approach used in the SAS4A accident analysis code (and also for the whole SAS code series). A number of such representative pins can take into account incoherencies within or among subassemblies due to different power levels, voiding histories, coolant flow, etc. The EPIC code begins at the point of cladding failure and models the subsequent events. There must, of course, be some molten fuel in the fuel pin at the start of the calculation since EPIC models the motion of fuel and the concomitant motion of sodium.

A one-dimensional Eulerian calculation of the hydrodynamics inside a molten-fuel cavity is explicitly coupled to a one-dimensional Eulerian calculation in the coolant channel by means of a fuel-ejection model. This ejection model

the Eulerian cell or cells in the fuel pin which delimit the failure length and in the corresponding Eulerian cell or cells in the coolant channel directly in front of the pin failure cells.

EPIC uses a full donor cell spatial differencing scheme with cell-centered densities, pressures and temperatures, and with cell-edge velocities. A combination of explicit, semi-implicit, and fully implicit differencing in time is used. An explicit calculation is done to predict end of time step values; these are then used to compute average values over the step. The average values are in turn used to compute updated end-of-time-step values. There is an option to make the time differencing strictly explicit after a specified time point, as for example, when conditions are no longer changing rapidly. Velocities in both the pin and channel are computed implicitly in time, however. These are computed on each pass which is semi-implicit for the rest of the variables besides velocity or when the calculation is fully explicit in time for the variables besides velocity.

This user's guide describes: the mathematical models used to specify the physical phenomena including the numerical approximations employed the structure of the computer program and the various subprograms the input specifications and output; and a sample problem which will serve as a paradigm for the user.

1. INTRODUCTION

The EPIC (Eulerian Particle In Cell)computer code[1,2] was written to calculate material motions following pin failure in a Liquid Metal Cooled Fast Breeder Reactor (LMFBR) during a loss-of-flow (LOF) transient as well as a transient overpower (TOP) accident. EPIC assumes that the pin structure is generally intact after pin failure such as would be the case in the burst failure conditions resulting from fission gas pressure or differential expansion loading of the cladding. This would result in a localized cladding breach allowing communication between the interior of the fuel pin and the coolant channel. The EPIC model is inappropriate for pin failure which involves a massive disruption of pin structure such as would occur when the cladding is in a partially or fully molten state.

The EPIC model is appropriate for pin failures in TOP conditions. It is also capable of modeling pin failures in middle and lower power subassemblies under loss-of-flow-driven TOP (LOF-TOP) conditions. If a fast reactor core voids incoherently enough and if there is sufficient sodium void reactivity insertion from the higher power subassemblies to bring the reactor into the vicinity of prompt-critical, a rapid power rise will result so that middle and lower power subassemblies will experience conditions similar to those in a TOP with some or all of the sodium coolant still present. This LOF-TOP situation is not unusual in larger fast reactors with homogeneous cores.[3,4] It is not inconceivable that failures near the center of the core may occur,[5] so that the calculation of fuel motion is crucial to the determination of reactivity effects.

To a large extent, EPIC is a parametric code. Our lack of knowledge of the physical processes involved requires this approach. Many of the significant features of the model are parameterized, and often only a partial mechanistic treatment is done. For example, initial cladding rip length, fuel particle size, and most heat transfer rates must be specified as input. This parametric approach provides a certain flexibility in the use of the code, and it also reflects a reluctance to treat highly complicated and poorly understood phenomena with models that are supposedly accurate and well-founded but actually make highly significant but unjustifiable assumptions.

EPIC models a single fuel pin with its associated coolant which represents part of or all of a subassembly or a group of similar subassemblies under pin failure conditions (see Fig. 1). This is similar to the approach used in the SAS4A[6] accident analysis code (and also for the whole SAS code series). A number of such representative pins can take into account incoherencies within or among subassemblies due to different power levels, voiding histories, coolant flow, etc. The EPIC code begins at the point of cladding failure and models the subsequent events. There must, of course, be some molten fuel in the fuel pin at the start of the calculation since EPIC models the motion of fuel and the concomitant motion of sodium.

A one-dimensional Eulerian calculation of the hydrodynamics inside a molten-fuel cavity is explicitly coupled to a one-dimensional Eulerian calculation in the coolant channel by means of a fuel-ejection model This ejection model equilibrates the pressure (instantaneously at the end of a given time step) in

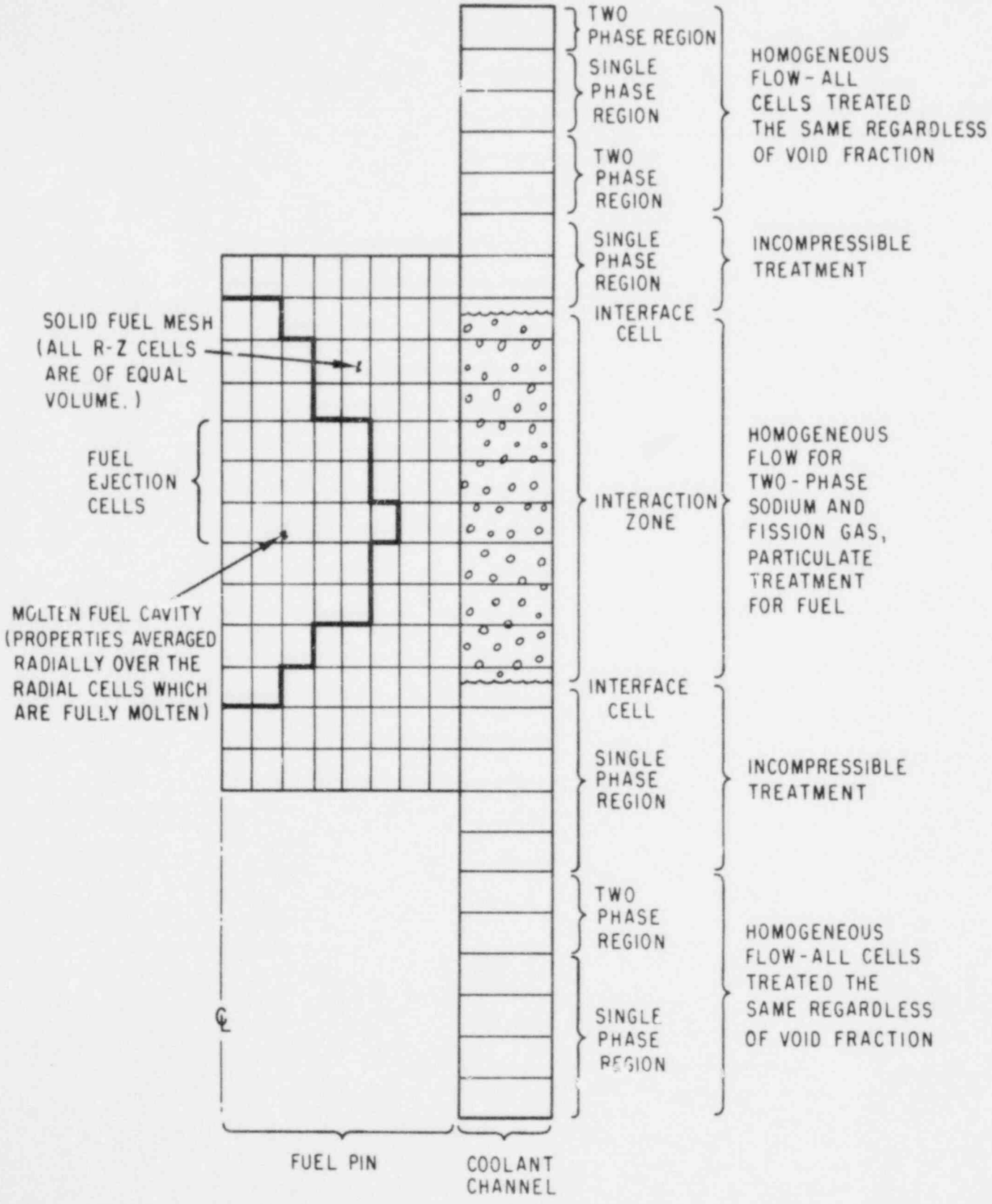

Fig. 1. Schematic of the EPIC Model.

the Eulerian cell or cells in the fuel pin which delimit the failure length and in the corresponding Eulerian cell or cells in the coolant channel directly in front of the pin failure cells.

EPIC uses a full donor cell spatial differencing scheme with cell-centered densities, pressures and temperatures, and with cell-edge velocities. A combination of explicit, semi-implicit,[7] and fully implicit differencing in time is used. An explicit calculation is done to predict end of time step values; these are then used to compute average values over the step. The average values are in turn used to compute updated end-of-time-step values. There is an option to make the time differencing strictly explicit after a specified time point, as for example, when conditions are no longer changing rapidly. Velocities in both the pin and channel are computed implicitly in time, however. These are computed on each pass which is semi-implicit for the rest of the variables besides velocity or when the calculation is fully explicit in time for the variables besides velocity.

This user's guide describes: the mathematical models used to specify the physical phenomena including the numerical approximations employed (Section 2); the structure of the computer program and the various subprograms (Section 3); the input specifications and output (Section 4); and a sample problem which will serve as a paradigm for the user (Section 5).

2. MATHEMATICAL MODELS AND NUMERICAL METHODS

2.1 The Fuel Pin

The time-dependent transient response of the fuel pin is calculated in r-z space as depicted in Fig. 1. This choice of coordinates is appropriate for the cylindrical shape of the undisrupted fuel pin. The space containing the pin is divided into an arbitrary number I of axial cells having equal length. From the axis to the outer surface of the pin, each axial cell is further divided into concentric shells. The partition is done so that an arbitrary number ℓ_{max} of equi-volume radial subdivisions result in each axial cell. The Eulerian mesh in which the calculation of the pin variables is carried out thus contains $I \cdot \ell_{max}$ subcells. The radial subdivisions of each axial cell are referred to as radial subcells. (The option exists to carry out the calculation without radial division of the space containing the pin.)

Unlike the space in which the fuel pin is described, the coolant channel has no defined radial subdivisions. The channel is considered to lie parallel to the fuel pin. There is no connection in the calculation between the fuel outer radius and the cladding inner and outer radius. The cladding outer radius is only used to calculate the coolant flow area. The cladding inner radius is used to calculate the cladding mass for the cladding temperature calcuation. It is assumed that the user's input is realistic and self-consistent, but there is no necessary internal inconsistency in the code between an outer fuel radius which varies axially and inner and outer clad radii which are constant axially. The length of the coolant channel is divided into an integral number of axial cells of the same length as is used in the pin. Each channel cell lies adjacent to its corresponding axial pin cell and is capable of communicating with it when the pin cell contains some molten fuel and is an "ejection cell." Further discussion of the coolant channel is deferred to a later section.

It is assumed that some calculation of the transient prior to pin failure exists, and that initial values at pin failure of all the significant variables associated with each mesh cell are known. An axial power profile together with a time-dependent power function that specifies the instantaneous power as the transient proceeds are provided by the user. It is assumed that there is a pocket of molten fuel in the pin at pin failure (the point where the EPIC calculation begins). This pocket of molten fuel may increase in size during the EPIC calculation. During each time step, the condition of each radial subcell is examined and updated. Whenever a radial subcell becomes fully liquid, it is added to the molten portion of the axial cell which contains it. Axial mesh structure is thus preserved in the molten fuel cavity, although radial mesh structure is eliminated in the molten region of each axial cell.

The molten fuel cavity may thus have a shape such as that shown in Fig. 1 at the point of pin failure when the EPIC calculation begins. If the fuel has been irradiated, it is assumed that a known amount of fission gas is entrained in the solid fuel. The gaseous fission products are released when the solid fuel melts into the molten fuel cavity during the transient and are added to the fission gas already present in the cavity.

The liquid fuel and fission gas are considered to exist as a froth in the molten fuel cavity. The two components of the froth are always treated as having the same temperature. Flow of the froth is treated as homogeneous.

Two equations are written to describe the instantaneous composition of the froth, one for the fission gas and the other for the liquid fuel. The continuity equation for the fission gas in the molten region of any axial cell i is

$$\frac{\partial}{\partial t}\left(V_p(t,z)\cdot\rho_{fg,p}(t,z)\right) + \frac{\partial}{\partial z}\left(V_p(t,z)\cdot\rho_{fg,p}(t,z)\cdot U_{fr,p}(t,z)\right)$$

$$= S_{fu,melt}(t,z)\cdot X(z) - S_{fg,ej}(t,z), \qquad (2.1.1)$$

t = time

z = axial coordinate

V_p = volume of fuel pin cavity in axial cell to which equation is applied

$\rho_{fg,p}$ = smear density (total mass in cell divided by volume of cell) of fission gas in cell to which equation is applied ($V_p\cdot\rho_{fg,p}$ is therefore the mass of fission gas in the cell)

$U_{fr,p}$ = velocity of froth

$S_{fu,melt}$ = fuel melt-in rate (mass per unit time) source term during the time step

X = ratio of the mass of fission gas to the mass of fuel in the material melting into the cavity

$S_{fg,ej}$ = rate of fission gas mass ejection during the time step if the cell to which the equation is applied is an ejection cell (this is removed instantaneously at the end of each time step)

p = pin

fg = fission gas

fr = froth

$melt$ = melt-in

ej = ejection

The finite difference form of Eq. (2.1.1) is

$$\frac{1}{\Delta t}\left(V_p^{i,n+1}\cdot\rho_{fg,p}^{i,n+1} - V_p^{i,n}\cdot\rho_{fg,p}^{i,n}\right) + \frac{1}{\Delta z}\cdot(\text{TOP-BOT})$$

$$= S_{fu,melt}^{i}\cdot X^{i} - S_{fg,ej}^{i}, \qquad (2.1.2)$$

$$\text{TOP} = \begin{cases} \overline{V_p^{i} \cdot \rho_{fg,p}^{i} \cdot U_{fr,p}^{i+1/2}} & \text{if } \overline{U_{fr,p}^{i+1/2}} > 0 \\ \overline{V_p^{i+1} \cdot \rho_{fg,p}^{i+1} \cdot U_{fr,p}^{i+1/2}} & \text{if } \overline{U_{fr,p}^{i+1/2}} < 0 \end{cases}$$

$$\text{BOT} = \begin{cases} \overline{V_p^{i-1} \cdot \rho_{fg,p}^{i-1} \cdot U_{fr,p}^{i-1/2}} & \text{if } \overline{U_{fr,p}^{i-1/2}} > 0 \\ \overline{V_p^{i} \cdot \rho_{fg,p}^{i} \cdot U_{fr,p}^{i-1/2}} & \text{if } \overline{U_{fr,p}^{i-1/2}} < 0 \end{cases}$$

n = time point n

Δt = time step

Δz = Eulerian cell length

where the bars indicate time averages; i.e., $\overline{Z} = (Z^{n+1}+Z^{n})\cdot 1/2$ and for products, $\overline{W\cdot Z} = (W^{n+1}\cdot Z^{n+1} + W^{n}\cdot Z^{n})\cdot 1/2$, where the n values are at the beginning of the time step and the n+1 values are at the end. All quantities are cell centered except the velocities, which are at the cell edge, $U^{i+1/2}$ being at the top of cell i, $U^{i-1/2}$ being the velocity of the lower boundary of cell i. The spatial differencing is a varient of the full donor-cell technique made compatible with semi-implicit differencing in time.[7] Semi-implicit differencing means that initially a strictly explicit calculation is done, i.e. the t^{n+1} values are set equal to the t^{n} values. Then the values at t^{n+1} that were generated explicitly are used to form average values over the time step as above. New values are then generated for t^{n+1} and the process ends, although it could be continued.

The continuity equation for molten fuel in the cavity is

$$\frac{\partial}{\partial t}\left(V_p(t,z)\cdot\rho_{fu,p}(t,z)\right) + \frac{\partial}{\partial z}\left(V_p(t,z)\cdot\rho_{fu,p}(t,z)\cdot U_{fr,p}(t,z)\right) \cdot Y$$

$$= S_{fu,melt}(t,z) - S_{fu,ej}(t,z), \qquad (2.1.3)$$

$\rho_{fu,p}$ = fuel smear density (i.e., the mass of fuel in a cell divided by the volume of the cell)

Y = user-specified function which models fuel-fission gas slip during convection. Y is the ratio of the volume of fuel to the volume of fission gas convected across the boundaries of the cell

$S_{fu,ej}$ = the amount of fuel ejected during the time step

The finite difference form of Eq. (2.1.3) is

$$\frac{1}{\Delta t}\left(V_p^{i,n+1}\cdot\rho_{fu,p}^{i,n+1}-V_p^{i,n}\cdot\rho_{fu,p}^{i,n}\right)+\frac{1}{\Delta z}\,(TOP-BOT)\cdot Y$$

$$= S_{fu,melt}^{i} - S_{fu,ej}^{i}, \qquad (2.1.4)$$

$$TOP = \begin{cases} \overline{V_p^{i}\cdot\rho_{fu,p}^{i}\cdot U_{fr,p}^{i+1/2}} & \text{if } \overline{U_{fr,p}^{i+1/2}} > 0 \\ \overline{V_p^{i+1}\cdot\rho_{fu,p}^{i+1}\cdot U_{fr,p}^{i+1/2}} & \text{if } \overline{U_{fr,p}^{i+1/2}} < 0 \end{cases}$$

$$BOT = \begin{cases} \overline{V_p^{i-1}\cdot\rho_{fu,p}^{i-1}\cdot U_{fr,p}^{i-1/2}} & \text{if } \overline{U_{fr,p}^{i-1/2}} > 0 \\ \overline{V_p^{i}\cdot\rho_{fu,p}^{i}\cdot U_{fr,p}^{i-1/2}} & \text{if } \overline{U_{fr,p}^{i-1/2}} < 0 \end{cases}$$

The numerical values of the variables in Eqs. 2.1.2 and 2.1.4 must be adjusted at the end of each time step to provide input for the succeeding calculation. The source term $S_{fu,melt}$ represents the amount of liquid fuel to be added to the molten region of each axial cell as a result of melting of solid fuel during the time step. Whenever this occurs, the volume of the molten region of the axial cell i is also increased. Because of the placement of the radial subcell boundaries (so as to maintain constant subcell volume), the increments of mass and volume are always integral multiples of the unit subcell, i.e.

$$V_p^{i,n+1} = V_p^{i,n} + \frac{1}{\ell_{max}}\cdot\pi\cdot(r_{fu}^{i})^2\cdot\Delta z \qquad (2.1.5)$$

ℓ_{MAX} = number of radial subcells in fuel at axial cell i

r_{fu}^{i} = outer radius of the solid fuel at axial cell i

The addition of volume as well as mass of fuel and fission gas to the molten fuel cavity is treated as follows. The temperatures of the radial subcells of residual solid fuel as well as the fractions of the heat of fusion satisfied in each subcell are continually updated during the calculation. The amount of fission energy added to each radial subcell is calculated. This additional energy changes the temperature and/or the fraction of the heat of fusion satisfied. When any radial subcell of solid fuel has become completely molten, it is added to the liquid portion of the axial cell. This means that an amount of energy equal to the total heat of fusion of the material in the radial subcell must be added after the solidus temperature is reached. Heat conduction in the solid fuel is disregarded, and only fission heating causes an addition of energy. Whenever a radial subcell of liquid fuel is added to the molten portion of an axial cell, the material is homogenized in the molten cavity, and the previous radial boundaries in the liquid region are disregarded from then on.

Note: In the general case, where mixed oxide fuel might be considered, the "heat of fusion" would be a function of the mixture ratio, as would be the solidus and liquidus temperatures. Average values for the specific heats of the solid and liquid fuels as well as a latent-heat function across the solidus-liquidus region would have to be provided. Under these conditions, the criterion for addition of liquid fuel to the cavity would be attainment of the liquidus temperature in the particular radial subcell. At present, EPIC considers the fuel to be a pure substance with a unique melting point and latent heat of fusion. For a mixed-oxide fuel, average values for these quantities would have to be determined to describe the phase-change region.

The amount of energy (per unit mass) deposited by fission in any radial subcell of axial cell i during a time step is given by

$$Q^{i,\ell} = W^{i} \cdot \Phi^{n} \cdot \Delta t \qquad (2.1.6)$$

$Q_i^{i,\ell}$ = energy per unit mass at axial cell i, radial subcell ℓ over time step

W^{i} = nominal power per unit mass at axial cell i

Φ^{n} = normalized power level at t^{n} (a user-specified function of time)

In the solid fuel, $Q^{i,\ell}/C_{p,fu}$ ($C_{p,fu}$ is the specific heat of solid fuel which is a function of temperature) therefore gives the temperature rise over Δt if the particular radial subcell has not reached the solidus temperature and $Q^{i,\ell}/H_{sf,fu}$ is the fraction of the heat of fusion, $H_{sf,fu}$, that is satisfied over Δt if the cell is above the solidus temperature. After the heat of fusion has been satisfied, the mass of fuel in the radial subcell becomes part or all of the source term $S_{fu,melt}$ in Eqs. (2.1.1) and (2.1.3).

Define

$$Q_{ex}^{i,\ell} = Q^{i,\ell} - H_{sf,fu} \cdot (1-F), \qquad (2.1.7)$$

F = fraction of heat of fusion satisfied at the beginning of the time step.

During successive time steps, the temperature of each radial subcell continues to rise as fission energy is deposited until the melting point (solidus temperature) is reached. Eventually, during some time step if enough energy is added, addition of increment $Q^{i,\ell}$ will carry the fuel in radial subcell ℓ up to the melting point and begin melting the solid fuel. The factor F is the ratio of the energy in excess of the heat required to reach the melting point to the heat of fusion. If, during the next time step, the energy increment $Q^{i,\ell}$ is not sufficient to melt the remaining solid fuel in radial subcell ℓ, Q_{ex} will be negative and the factor F is recomputed. When Q_{ex} becomes non-negative, all of the fuel in the radial subcell is melted and the residual energy Q_{ex} raises the temperature of the liquid above the melting point. When the entire radial subcell becomes liquid, the subcell is added to the already liquid region of the axial cell and homogenized with it.

The cell temperature in the cavity is calculated as follows. There are three stages in the calculation of $T_{fu,p}^{i,n+1}$ from $T_{fu,p}^{i,n}$. Define $T'_{fu,p}$ and $T''_{fu,p}$ as the results of the first and second stages, respectively.

$$T'_{fu,p} = T_{fu,p}^{i,n} + \frac{Q_{ex}^{i} \cdot S_{fu,melt}^{i} \cdot \Delta t + W^{i} \cdot \phi^{n} \cdot \Delta t \cdot V_{p}^{i,n} \cdot \rho_{fu,p}^{i,n}}{V_{p}^{i,n} \cdot \rho_{fu,p}^{i,n} \cdot C_{P,fu}} \qquad (2.1.8)$$

$T_{fu,p}^{i,n}$ = temperature of cavity cell i at time point n

Q_{ex}^{i} = sum over radial subcells ℓ which have melted into the cavity in Δt

$S_{fu,melt}^{i}$ = sum of fuel mass over radial subcells ℓ which have melted into the cavity in Δt

Thus, $T'_{fu,p}$ is the temperature of the cavity cell adjusted to take into account the remainder of the heat of fusion to be satisfied, or the excess heat that is represented by the radial subcell or subcells of solid fuel melting in; $T'_{fu,p}$ also includes the fission heating of the cell over the time step.

$$T''_{fu,p} = \frac{T'_{fu,p} \cdot V_{p}^{i,n} \cdot \rho_{fu,p}^{i,n} + T_{melt} \cdot S_{fu,melt}^{i} \cdot \Delta t}{V_{p}^{i,n} \cdot \rho_{fu,p}^{i,n} + S_{fu,melt}^{i} \cdot \Delta t}. \qquad (2.1.9)$$

T_{melt} = fuel melting temperature

$T''_{fu,p}$ is the equilibrated temperature of cell i after $S_{fu,melt}^{i} \cdot \Delta t$ of fuel melt-in.

$$T^{i,n+1}_{fu,p} = [M^{n+1} \cdot T''_{fu,p} + Y \cdot \Delta t \cdot (\overline{V^k_p \cdot \rho^k_{fu,p} \cdot T^k_{fu,p} \cdot U^{i-1/2}_{fr,p}} - \overline{V^j_p \cdot \rho^j_{fu,p} \cdot T^j_{fu,p} \cdot U^{i+1/2}_{fr,p}})]$$

$$\div [M^{n+1} + Y \cdot \Delta t \cdot (\overline{V^k_p \cdot \rho^k_{fu,p} \cdot U^{i-1/2}_{fr,p}} - \overline{V^j_p \cdot \rho^j_{fu,p} \cdot U^{i+1/2}_{fr,p}})] \qquad (2.1.10)$$

where the bars are defined as for Eq. (2.1.2)

$M^{n+1} = V^{i,n+1}_p \cdot \rho^{i,n+1}_{fu,p}$

Y = ratio of volume of fuel to volume of fission gas during convection

$V^k \cdot \rho^k_{fu,p} \cdot U^{i-1/2}_{fr,p}$ = gains or losses from convection across the lower boundary

$V^j \cdot \rho^j_{fu,p} \cdot U^{i+1/2}_{fr,p}$ = gains or losses from convection across the upper boundary

$k = i$ if $\overline{U^{i-1/2}_{fr,p}} < 0$ and $k = i-1$ if $\overline{U^{i-1/2}_{fr,p}} > 0$

$j = i$ if $\overline{U^{i+1/2}_{fr,p}} > 0$ and $j = i+1$ if $\overline{U^{i+1/2}_{fr,p}} < 0$

Thus, $T^{i,n+1}_{fu,p}$ is the final temperature at t^{n+1}, accounting for all convection including melt-in and all fission heating. The value of $T^i_{fu,p}$ has been computed in semi-implicit fashion, since the values of V_p, $\rho_{fu,p}$, and $U_{fr,p}$ at t^{n+1} are set equal to those at t^n for the first pass and then updated as discussed above. When temperatures are time-averaged at cell i, the average is formed with $T^{i,n}_{fu,p}$ and $T''_{fu,p}$. One final adjustment is made to $T^{i,n+1}_{fu,p}$. This is due to the energy loss to the fuel which results from the vaporization of liquid fuel to keep the fuel vapor pressure at saturation.

The primary justification for this two-step technique, that allows the convenient use of algebraic expressions, is that the fuel temperature in the pin (as well as the sodium temperature in the channel) varies slowly with respect to time step size and is a stable function of time. In addition the errors implicit in this procedure are small compared to the errors in the treatment of other aspects of the energy balance, e.g., the discretized radial temperature shape in the fuel pin, the neglect of heat conduction in the pin and the approximate treatment of sodium-fuel heat transfer, and condensation in the channel.

The momentum conservation equation for the fuel in the molten fuel cavity is

$$\frac{\partial}{\partial t}\left(V_p(t,z)\cdot\rho_{fu,p}(t,z)\cdot U_{fr,p}(t,z)\right) + V_p(t,z)\cdot\rho_{fu,p}(t,z)\cdot U_{fr,p}(t,z)\cdot\frac{\partial}{\partial z}U_{fr,p}(t,z)$$

$$= -V_p(t,z)\cdot\frac{\partial}{\partial z}P_p(t,z) - V_p(t,z)\cdot\rho_{fu,p}(t,z)\cdot g - S_{fu,ej}\cdot U_{fr,p}(t,z)$$

$$-\frac{1}{2D_c}f(Re)\cdot\rho_{fu,p}(t,z)\cdot V_p(t,z)\cdot U_{fr,p}(t,z)\cdot\left|U_{fr,p}(t,z)\right| \qquad (2.1.11)$$

where the last term on the right hand side of the expression represents a viscous drag force.

P_p = total pressure

g = gravitational acceleration

D_c = $2\cdot[V_p(t,z)/(\Delta z\cdot\pi)]^{1/2}$

$f(Re)$ = $a\ Re^b$

Re = $D_c\cdot\left|U_{fr,p}(t,z)\right|\rho_{fu,p}(t,z)/\mu_{fu}$

a,b = constants (appropriate for the flow regime)

μ_{fu} = absolute viscosity of molten fuel

The finite-difference form of Eq. (2.1.11) is for $U_{fr,p}$ at the upper cell edge i+1/2:

$$\frac{1}{\Delta t}\left(V_p^{i+1/2,n+1}\cdot\rho_{fu,p}^{i+1/2,n+1}\cdot U_{fr,p}^{i+1/2,n+1} - V_p^{i+1/2,n}\cdot\rho_{fu,p}^{i+1/2,n}\cdot U_{fu,p}^{i+1/2,n}\right)$$

$$+\overline{V_p^{i+1/2}\cdot\rho_{fu,p}^{i+1/2}}\cdot\overline{U_{fr,p}^{i+1/2}}\cdot\frac{1}{\Delta z}\cdot\left(U_{fr,p}^{j+1/2,n+1} - U_{fr,p}^{j-1/2,n+1}\right)$$

$$= -\overline{V_p^{i+1/2}}\cdot\frac{1}{\Delta z}\cdot\left(P_p^{i+1}-P_p^{i}\right)$$

$$-\overline{V_p^{i+1/2}\cdot\rho_{fu,p}^{i+1/2}}\cdot g - S_{fu,ej}^{i+1/2}\cdot\overline{U_{fr,p}^{i+1/2}}$$

$$-\frac{1}{2D_c^{i+1/2}}\cdot a\cdot\left(\frac{1}{\mu_{fu}}\cdot D_c^{i+1/2}\cdot\left|\overline{U_{fr,p}^{i+1/2}}\right|\cdot\overline{\rho_{fu,p}^{i+1/2}}\right)^b$$

$$\times \overline{V_p^{i+1/2} \cdot \rho_{fu,p}^{i+1/2}} \cdot \overline{U_{fr,p}^{i+1/2}} \cdot \left| \overline{U_{fr,p}^{i+1/2}} \right| \qquad (2.1.12)$$

The values of the quantities defined at the cell edge ($\rho^{i+1/2}$, $S_{fu,ej}^{i+1/2}$, etc.) are obtained by averaging the cell-centered values of the two cells adjacent to the interface, e.g., $\rho^{i+1/2} = 1/2(\rho^{i+1} + \rho^{i})$,

$$D_c^{i+1/2} = 2 \cdot \left(\frac{1}{\pi \cdot \Delta z} \cdot \overline{V_p^{i+1/2}} \right)^{1/2},$$

and $j = i$ if $\overline{U_{fr,p}^{i+1/2}} > 0$ and $j = i + 1$ if $\overline{U_{fr,p}^{i+1/2}} < 0$. The V_p^{n+1} and $\rho_{fu,p}^{n+1}$ used in the time averages are from the solution of Eqs. (2.1.3) and (2.1.7). The right side can be treated as a constant. Equation (2.1.12) thus becomes a linear equation in $U_{fr,p}^{i+1/2,n+1}$, $U_{fr,p}^{j+1/2,n+1}$, and $U_{fr,p}^{j-1/2,n+1}$ (i.e. when the alternative values of j are considered, Eq. (2.1.12) is linear in $U_{fr,p}^{i+3/2,n+1}$, $U_{fr,p}^{i+1/2,n+1}$, and $U_{fr,p}^{i-1/2,n+1}$). When Eq. (2.1.12) is written for all cavity cells, a system of linear equations in velocity results. The coefficient matrix is tri-diagonal and is solved by Gaussian elimination. The momentum equation is solved implicitly as above on each of the two semi-implicit passes for the continuity and temperature equations.

Molten fuel is modeled as incompressible. In analyses of fresh fuel pins, there is nothing to prevent a cell from receiving more fuel from convection during a time step than can physically fit within the cell volume. (This overcompaction does not usually occur when modeling irradiated fuel pins since the fission gas partial pressure rapidly adjusts as mass moves from cell to cell, thus preventing too much fuel from moving into a cell.) When overcompaction occurs, cell boundary velocities are adjusted (conserving momentum wherever possible) to prevent further net mass flow into the cell. This adjustment prevents an initial overcompaction from worsening and will clear the overcompacted conditions in many cases.

The equation-of-state in the cavity is assumed to be the sum of the fuel vapor partial pressure and the fission-gas partial pressure computed in ideal gas fashion:

$$P_p(t,z) = P_{fu,sat}(T_{fu,p}(t,z)) + \frac{R_{fg} \cdot T_{fu,p}(t,z) \cdot \rho_{fg,p}(t,z)}{1 - \rho_{fu,p}(t,z)/\rho_{fu}^{p}}, \qquad (2.1.13)$$

$P_{fu,sat}(T_{fu,p})$ = saturation pressure of fuel corresponding to $T_{fu,p}$

R_{fg} = gas constant for fission gas

$\rho^{p}_{fu,p}$ = theoretical density of fuel (assumed to be constant, not a function of temperature, in the code).

The fuel is always assumed to follow its saturation curve and no nonequilibrium boiling is treated. The fission gas is assumed to be at the fuel temperature. The expression $(1 - \rho_{fu,p}/\rho^{p}_{fu,p})$ gives the volume fraction available for pressurization in the molten fuel cavity.

2.2 The Coolant Channel

In the one-dimensional model of the coolant channel, there are from one to three regions which can include two-phase sodium treated with homogeneous flow in an Eulerian mesh (see Fig. 1). However, only the region which includes the ejection cells may contain fission gas and fuel particles. In this region the two-phase sodium and fission gas move together without slip in a homogeneous flow treatment; the fuel motion is treated as particulate flow. This region will be called the interaction zone and can include part or all of the coolant channel so long as it includes all the ejection cells. The interaction zone extends as far as a region of single-phase liquid sodium (if there is any) which may bound it at either or both ends. The bounding single-phase regions extend either to the end of the coolant channel mesh or to a region of two-phase sodium which may intervene. There may also be a single-phase region between the intervening two-phase region and the end of the coolant channel mesh. There is no discrimination, however, between the intervening two-phase region and any single-phase regions between it and the end of the channel mesh since all the cells beginning with the intervening two-phase region and extending to the end of the mesh are treated in a homogeneous flow mode regardless of void fraction. The single-phase region or regions bounding the interaction zone are treated incompressibly.

The continuity equation (homogeneous flow is assumed) for fission gas in the interaction zone is

$$\frac{\partial}{\partial t}\left(V_c(t,z)\cdot\rho_{fg,c}(t,z)\right) + \frac{\partial}{\partial z}\left(V_c(t,z)\cdot\rho_{fg,c}(t,z)\cdot U_{m,c}(t,z)\right)$$

$$= S_{fg,ej} \qquad (2.2.1)$$

V_c = volume of coolant channel cell to which equation is applied

$\rho_{fg,c}$ = smear density (i.e., total mass in cell divided by volume of cell) of fission gas in cell to which equation is applied

$U_{m,c}$ = velocity of the mixture of fission gas and two-phase sodium

$S_{fg,ej}$ = rate of fission gas mass ejection during the time step if the cell to which the equation is applied is an ejection cell (this is added instantaneously at the end of each time step)

The motion of the fission gas is tracked by means of an interface location beyond which the gas is not allowed to convect. The velocity of the interface is determined by linear interpolation between the upper and lower cell-boundary values. In an initially unvoided channel, the fission gas interface will tend to move with the liquid slug interfaces as the slugs are expelled. In an initially voided channel, however, if an interface for the fission gas was not tracked, the fission gas would artificially convect one cell per time step (being instantly smeared across the entire cell as soon as any moved into a cell). Finally, fission gas is not allowed to penetrate the sodium liquid slug interfaces (although fuel particles are allowed).

The finite difference form of Eq. (2.2.1) is exactly analogous to Eq. (2.1.2). The velocity of the two-phase sodium and fission gas mixture is computed at the cell edge; all other quantities are cell-centered:

$$\frac{1}{\Delta t}\left(V_c^{i,n+1}\cdot\rho_{fg,c}^{i,n+1}-V_c^{i,n}\cdot\rho_{fg,c}^{i,n}\right)+\frac{1}{\Delta z}\left(\text{TOP}-\text{BOT}\right)=S_{fg,ej}^{i} \qquad (2.2.2)$$

$$\text{TOP}=\begin{cases}\overline{V_c^{i}\cdot\rho_{fg,c}^{i}\cdot U_{m,c}^{i+1/2}} & \text{if } U_{m,c}^{i+1/2}>0\\ \overline{V_c^{i+1}\cdot\rho_{fg,c}^{i+1}\cdot U_{m,c}^{i+1/2}} & \text{if } U_{m,c}^{i+1/2}<0\end{cases}$$

$$\text{BOT}=\begin{cases}\overline{V_c^{i-1}\cdot\rho_{fg.c}^{i-1}\cdot U_{m,c}^{i-1/2}} & \text{if } U_{m,c}^{i-1/2}>0\\ \overline{V_c^{i}\cdot\rho_{fg,c}^{i}\cdot U_{m,c}^{i-1/2}} & \text{if } U_{m,c}^{i-1/2}<0\end{cases}$$

The continuity equation for the liquid sodium (homogeneous flow is assumed) in the interaction zone and two-phase regions is

$$\frac{\partial}{\partial t}\left(V_c(t,z)\cdot\rho_{Na,c}(t,z)\right)+\frac{\partial}{\partial z}\left(V_c(t,z)\cdot\rho_{Na,c}(t,z)\cdot U_{m,c}(t,z)\right)=0 \qquad (2.2.3)$$

$\rho_{na,c}$ = smear density (mass in cell divided by volume of cell) of sodium in the cell to which the equation is applied.

There are no sources or sinks for the sodium; the mass balance for a cell is determined solely be convection. Condensation is included as a heat loss term in the sodium temperature calculation, but no corresponding mass loss is considered. There is no treatment of a sodium film. Mass loss from the liquid phase due to evaporation or mass gain due to condensation during phase change is included as an adjustment to the sodium liquid density resulting from convection. The finite difference form of Eq. (2.2.3) is analogous to Eq. (2.1.2):

$$\frac{1}{\Delta t}\left(V_c^{i,n+1} \cdot {}^{i,n+1}_{\rho_{Na,c}} - V_c^{i,n} \cdot {}^{i,n}_{\rho_{Na,c}}\right) + \frac{1}{\Delta z}\,(\text{TOP}-\text{BOT}) = 0 \qquad (2.2.4)$$

$$\text{TOP} = \begin{cases} \overline{V_c^{i} \cdot {}^{i}_{\rho_{Na,c}} \cdot U_{m,c}^{i+1/2}} & \text{if } \overline{U_{m,c}^{i+1/2}} > 0 \\ \overline{V_c^{i+1} \cdot {}^{i+1}_{\rho_{Na,c}} \cdot U_{m,c}^{i+1/2}} & \text{if } \overline{U_{m,c}^{i+1/2}} < 0 \end{cases}$$

$$\text{BOT} = \begin{cases} \overline{V_c^{i-1} \cdot {}^{i-1}_{\rho_{Na,c}} \cdot U_{m,c}^{i-1/2}} & \text{if } \overline{U_{m,c}^{i-1/2}} > 0 \\ \overline{V_c^{i} \cdot {}^{i}_{\rho_{Na,c}} \cdot U_{m,c}^{i-1/2}} & \text{if } \overline{U_{m,c}^{i-1/2}} < 0 \end{cases}$$

The temperature of the fission gas is computed as the volume-weighted average of the fuel temperature and the sodium temperature in a cell as follows:

$$T_{fg,c} = \frac{T_{fu,c} \cdot \rho_{fu,c}/\rho_{fu}^{p} + T_{Na,c} \cdot \rho_{Na,c}/\rho_{Na}^{p}}{\rho_{fu,c}/\rho_{fu}^{p} + \rho_{Na,c}/\rho_{Na}^{p}}, \qquad (2.2.5)$$

$T_{fg,c}$ = fission gas temperature in channel cell to which equation is applied

$T_{fu,c}$ = average fuel particle temperature in channel cell to which equation is applied

$\rho_{fu,c}$ = smear density (total mass of fuel particles in cell divided by volume of the cell) of fuel in cell to which the equation is applied

$\rho_{fu}^{p,1/2}$ = theoretical density of fuel (assumed constant)

$T_{Na,c}$ = temperature of two-phase sodium in cell

$\rho_{Na,c}$ = smear density of sodium in cell

$\rho_{Na}^{p,1/2}$ = theoretical density of liquid sodium (which is a function of $T_{Na,c}$)

This assumption about the fission gas temperature is made in lieu of an accounting of the energy exchange between the fission gas and the other materials. This energy exchange process is thought to be too complicated and too poorly understood to be modeled adequately.

Liquid sodium is assumed to be in thermodynamic phase equilibrium with the sodium vapor, and the vapor pressure is assumed to be the saturation pressure corresponding to the two-phase temperature. The above assumption is made because of the difficulty of treating non-equilibrium boiling, and because geometry and flow regime are unknown. As heat is exchanged with the system, temperature changes and concomitant change of phase are treated using an algorithm that was developed to apportion the energy input into the two-phase system between boiling and heating the liquid phase (see Appendix A). The algorithm states that

$$\frac{\Delta E_{vap}}{\Delta E_{liq}} = \left[\frac{\frac{d}{dT} P_{Na,sat}(T^n_{Na,c})}{P_{Na,sat}(T^n_{Na,c})} - \frac{1}{T^n_{Na,c}} \right] \cdot T^n_{Na,c} \cdot \frac{d}{dT} P_{Na,sat}(T^n_{Na,c}) \cdot V^n_{vap} \div \left[\overline{\rho_{Na,c} \cdot V_c} \cdot C_{P,Na} \right] \qquad (2.2.6)$$

ΔE_{vap} = the part of the total energy input going into change of phase

ΔE_{liq} = the part of the total energy input heating the liquid phase

$P_{Na,sat}$ = sodium saturation vapor pressure as a function of temperature

n = superscript denoting beginning of the time step

V^n_{vap} = volume available for vapor in the coolant channel cell to which the equation is applied at the beginning of the time step

$C_{P,Na}$ = liquid sodium specific heat

Since the total energy going into the system is ΔE_{tot} ($\Delta E_{tot} = \Delta E_{vap} + \Delta E_{liq}$),

$$\Delta E_{liq} = \Delta E_{tot} \cdot \frac{1}{1+\Delta E_{vap}/\Delta E_{liq}} \qquad (2.2.7)$$

The heat capacity of the sodium vapor is also taken into account since this becomes significant as the quality approaches unity. It should be kept in mind, however, that the assumptions inherent in the thermodynamic equilibrium treatment of the two-phase sodium system begin to break down as the quality approaches unity since the energy of the vapor phase begins to be important relative to the energy of the liquid phase, and it can no longer be assumed that there will be enough liquid to produce enough vapor at saturation conditions for a given volume.

The total energy that is transferred within a cell containing two-phase sodium and possibly fission gas and fuel particles must be defined. Sodium vapor condensation on the cladding accounts for the first mode of heat transfer. The second means of transferring heat to or from the sodium is by means of the liquid phase contacting the cladding. Fuel particles are assumed to be spherical and of uniform radius. Heat transfer from the fuel particles to the liquid sodium is included, but heat transfer to the sodium vapor is disregarded since this is negligible by comparison to the former. The energy increment that is transferred within a cell containing fuel particles and two-phase sodium during a time step Δt can thus be expressed as

$$\Delta E^i_{tot} = -h_{c,con} \cdot A^i_{cl} \cdot (\overline{T^i_{Na,c}} - \overline{T^i_{cl}}) \cdot \Delta t \cdot \alpha^i$$

$$+ \overline{h^i_{c,cl}} \cdot \overline{A^i_{cl}} \cdot (T^i_{cl} - T_{Na,c}) \cdot \Delta t \cdot \frac{\overline{\rho^i_{Na,c}}}{\rho^p_{Na}} + \frac{\overline{\rho^i_{fu,c} \cdot V^i_c}}{m_{fp}} \cdot 4\pi r^2_{fp} \cdot FAC \cdot \frac{k_{fu}}{r_{fp}} \cdot \frac{\overline{\rho^i_{Na,c}}}{\rho^p_{Na}}$$

$$\times (\overline{T^i_{fu,c}} - \overline{T^i_{Na,c}}) \cdot \Delta t \quad , \qquad (2.2.8)$$

ΔE^i_{tot} = total energy change for the two-phase sodium for cell i

$h_{c,con}$ = condensation heat transfer coefficient (a constant set by the user)

A^i_{cl} = area of cladding available for condensation of sodium vapor

T^i_{cl} = temperature of cladding for cell i

α^i = void fraction in cell i

$h_{c,cl}$ = cladding to liquid sodium heat transfer coefficient (a constant set by the user)

m_{fp} = mass of one fuel particle of radius r_{fp}

r_{fp} = radius of a fuel particle

FAC = user-specified parameter

k_{fu} = fuel thermal conductivity

The first term (sodium vapor condensation) is zero when $\overline{T^i_{Na,c}} < \overline{T^i_{cl}}$. The bars again indicate time averages. The first term models condensation, the second models heat transfer between cladding and liquid sodium, and the third treats the fuel to sodium heat transfer. In the third term, k_{fu}/r_p is the Cho-Wright steady-state heat transfer coefficient,[9] $\overline{V^i_c \cdot \rho^i_{fu,c}}/m_{fp}$ gives the number of particles in the cell (total fuel mass/mass per particle) and $4\pi r^2_{fp}$ is the surface area of one particle. The ratio, $\rho^i_{Na,c}/\rho^p_{Na}$, is the sodium liquid volume fraction in the cell. Multiplication by this ratio indicates that only this fraction of the surface area of the fuel particles[10] (in the third term) or of the cladding (in the second term) on the average is in intimate contact with the liquid sodium. The Cho-Wright (steady-state) model is followed in also assuming: 1) there is perfect mixing of fuel particles and sodium in the cell; 2) no interference occurs in heat transfer from the fuel to sodium as from vapor blanketing; 3) the resistance to heat transfer is solely in the fuel with its low thermal conductivity (more than an order of magnitude less than that of sodium); and 4) the temperature distribution in the particle is linear. The user-specified parameter, FAC, can be used to control the heat transfer between fuel and liquid sodium. It can be modified without changing the rest of the calculation. In this way variations could be accounted for in such things as surface and convective effects which the above equation does not model explicitly. The $\rho \cdot \Delta V$ energy change is included as a final adjustment to the two-phase sodium temperature.

We can thus obtain ΔE^i_{liq} from Eq. (2.2.7). The temperature of the sodium liquid (the heat capacity of the sodium vapor is also included since it is important as the quality approaches unity) is calculated in two steps. In the first step, the temperature of the liquid in the cell is computed without regard for convection; and in the second, the liquid temperature is adjusted for convective mixing.

Let $T'_{Na,c}$ be the result of the first step,

$$T'_{Na,c} = \frac{\Delta E^i_{liq}}{V^{i,n+1}_c \cdot \rho^{i,n+1}_{Na,c} \cdot C_{p,Na}} + T^{i,n}_{Na,c} \; ; \qquad (2.2.9)$$

then,

$$T^{i,n+1}_{Na,c} = \frac{V^{i,n}_c \cdot \rho^{i,n}_{Na,c} \cdot T'_{Na,c} + Z \cdot \frac{\Delta t}{\Delta z}}{V^{i,n}_c \cdot \rho^{i,n}_{Na,c} + \overline{V^k_c \cdot \rho^k_{Na,c}} \cdot \overline{U^{i-1/2}_{m,c}} \cdot \frac{\Delta t}{\Delta z} - \overline{V^j_c \cdot \rho^j_{Na,c}} \cdot \overline{U^{i+1/2}_{m,c}} \cdot \frac{\Delta t}{\Delta z}} \; , \qquad (2.2.10)$$

where

$$Z = \overline{V_c^{i-1} \cdot \rho_{Na,c}^{i-1}} \cdot \overline{U_{m,c}^{i-1/2}} \cdot \overline{T_{Na,c}^{i-1}} - \overline{V_c^{i} \cdot \rho_{Na,c}^{i}} \cdot \overline{U_{m,c}^{i+1/2}} \cdot T'_{Na,c}$$

$$\text{if } \overline{U_{m,c}^{i+1/2}} > 0, \text{ and } \overline{U_{m,c}^{i-1/2}} > 0$$

$$Z = \overline{V_c^{i} \cdot \rho_{Na,c}^{i}} \cdot \overline{U_{m,c}^{i-1/2}} \cdot T'_{Na,c} - \overline{V_c^{i+1} \cdot \rho_{Na,c}^{i+1}} \cdot \overline{U_{m,c}^{i+1/2}} \cdot T_{Na,c}^{i+1}$$

$$\text{if } \overline{U_{m,c}^{i+1/2}} < 0, \text{ and } \overline{U_{m,c}^{i-1/2}} < 0$$

$$Z = \overline{V_c^{i-1} \cdot \rho_{Na,c}^{i-1}} \cdot \overline{U_{m,c}^{i-1/2}} \cdot \overline{T_{Na,c}^{i-1}} - \overline{V_c^{i+1} \cdot \rho_{Na,c}^{i+1}} \cdot \overline{U_{m,c}^{i+1/2}} \cdot \overline{T_{Na,c}^{i+1}}$$

$$\text{if } \overline{U_{m,c}^{i+1/2}} < 0, \text{ and } \overline{U_{m,c}^{i-1/2}} > 0$$

and

$$T_{Na,c}^{i,n+1} = T'_{Na,c} \text{ , if } \overline{U_{m,c}^{i+1/2}} > 0 \text{ , and } \overline{U_{m,c}^{i-1/2}} < 0 \text{ ,}$$

where

$$k = i \text{ if } \overline{U_{m,c}^{i-1/2}} < 0$$

$$k = i - 1 \text{ if } \overline{U_{m,c}^{i-1/2}} > 0$$

$$j = i \text{ if } \overline{U_{m,c}^{i+1/2}} > 0$$

$$j = i+1 \text{ if } \overline{U_{m,c}^{i+1/2}} < 0.$$

The change in the cladding temperature with time is treated according to the following equation:

$$T_{cl}^{i,n+1} = T_{cl}^{i,n} + \frac{\Delta t}{C_{p,cl} \cdot M_{cl}^{i}} \cdot \left[h_{c,con} \cdot A_{cl}^{i} \cdot (\overline{T_{Na,c}^{i}} - \overline{T_{cl}^{i}}) \cdot \alpha \right.$$

$$- h_{c,cl} \cdot A_{cl}^{i} \cdot (\overline{T_{cl}^{i}} - \overline{T_{Na,c}^{i}}) \cdot \frac{\overline{\rho_{Na,c}^{i}}}{\rho_{Na}^{p}} + h_{b} \cdot A_{cl,in}^{i} \cdot (\overline{T_{fu,ps}^{i}} - \overline{T_{cl}^{i}})$$

$$\left. + h_{c,fu} \cdot A_{cl}^{i} \cdot (\overline{T_{fu,c}^{i}} - \overline{T_{cl}^{i}}) \cdot \alpha \right] \qquad (2.2.11)$$

$c_{p,cl}$ = specific heat of cladding

M_{cl}^{i} = mass of cladding in cell i

h_{b} = gap conductance (between fuel and cladding)

$A_{cl,in}^{i}$ = area of inner cladding wall exposed to fuel

$T_{fu,ps}^{i}$ = temperature of fuel in fuel pin at fuel-cladding interface

$h_{c,fu}$ = fuel vapor condensation heat transfer coefficient

The first term in the brackets represents heat transferred by sodium vapor condensation on the cladding, which is zero when $\overline{T_{Na,c}^{i}} < \overline{T_{cl}^{i}}$. The second term represents the heat transfer between the cladding and liquid sodium. The third term represents the heat transfer between fuel and the cladding across the gap within the pin. The last term represents heat transferred by fuel vapor condensation on the cladding, which is zero when T_{fu} is below 3800°K.

The conservation of momentum equation for the fission gas and sodium mixture (homogeneous flow is assumed) in the interaction zone and the two-phase regions is

$$\frac{\partial}{\partial t} [V_{c}(t,z) \cdot (\rho_{Na,c}(t,z) + \rho_{fg,c}(t,z)) \cdot U_{m,c}(t,z)] + V_{c}(t,z) \cdot (\rho_{Na,c}(t,z)$$

$$+ \rho_{fg,c}(t,z)) \cdot U_{m,c}(t,z) \cdot \frac{\partial}{\partial z} U_{m,c}(t,z)$$

$$= -V_m(t,z)\cdot\frac{\partial}{\partial z}P_c(t,z) - V_c(t,z)\cdot(\rho_{Na,c}(t,z) + \rho_{fg,c}(t,z))\cdot g$$

$$-V_c(t,z)\cdot(\rho_{Na,c}(t,z) + \rho_{fg,c}(t,z))\cdot U_{m,c}(t,z)\cdot\left|U_{m,c}(t,z)\right| \cdot \frac{f(Re)}{2\cdot D_c}$$

$$-h_{c,con}\cdot A_{cl}\cdot(T_{Na,c}(t,z) - T_{cl}(t,z))\cdot\alpha\cdot\frac{U_{m,c}(t,z)}{H_{fg,Na}} - \rho_{fu,c}\frac{1}{m_{fp}}$$

$$\times(U_{m,c}(t,z) - U_{fu,c}(t,z))\cdot\left|U_{m,c}(t,z) - U_{fu,c}(t,z)\right|\cdot V_c(t,z)$$

$$\times(\rho_{Na,c}(t,z) + \rho_{fg,c}(t,z))\cdot r_{fp}^2\cdot\frac{\pi}{2}\cdot C_D(Re_{fp})\cdot\varepsilon^{-2.7} \qquad (2.2.12)$$

V_m = V_c - volume of fuel particles in cell to which equation is applied (defined at cell edge)

P_c = total pressure in coolant channel in cell

$U_{fu,c}$ = average velocity of all fuel particles one-half cell on either side of cell edge where $U_{m,c}$ is defined, so that $U_{fu,c}$ also becomes the approximation to a cell-edge velocity

$H_{fg,Na}$ = heat of vaporization for sodium

D_c = hydraulic diameter of coolant channel (defined at cell edge)

$f(Re)$ = aRe^b

Re = $(1/\mu_m)\cdot D_c\cdot(\rho_{Na,c} + \rho_{fg,c})\cdot\left|U_{m,c}\right|\cdot V_c/V_m$

μ_m = effective viscosity of the mixture

a,b = constants appropriate for the flow regime

$$C_D(Re_{fp}) = \begin{cases} \dfrac{18.5}{Re_{fp}^{0.6}} & \text{if } Re_{fp} < 500 \\ 0.44 & \text{if } Re_{fp} > 500 \text{ (Ref. 11)} \end{cases}$$

Re_{fp} = $2\cdot r_{fp}\cdot\left|U_{m,c} - U_{fu,c}\right|\cdot(\rho_{Na,c} + \rho_{fg,c})/\mu_m$

ε = V_m/V_c

The third term on the right side of Eq. (2.2.12) represents the mixture/wall drag and the last term represents the fuel/sodium drag. $V_m/\Delta z$ is the area on which the cell pressure acts to accelerate the mixture.

The finite difference form of Eq. (2.2.12) for $U_c^{i+1/2}$ is

$$\frac{1}{\Delta t} \cdot [V_c^{i+1/2,n+1} \cdot (\rho_{Na,c}^{i+1/2,n+1} + \rho_{fg,c}^{i+1/2,n+1}) \cdot U_{m,c}^{i+1/2,n+1}$$

$$- V_c^{i+1/2,n} \cdot (\rho_{Na,c}^{i+1/2,n} + \rho_{fg,c}^{i+1/2,n}) \cdot U_{m,c}^{i+1/2,n}]$$

$$+ \overline{V_c^{i+1/2} \cdot (\rho_{Na,c}^{i+1/2} + \rho_{fg,c}^{i+1/2})} \cdot \overline{U_{m,c}^{i+1/2}} \cdot \frac{1}{\Delta z} \cdot (U_{m,c}^{j+1/2,n+1} - U_{m,c}^{j-1/2,n+1})$$

$$= - \overline{V_m^{i+1/2}} \cdot \frac{1}{\Delta z} \cdot (\overline{P_c^{i+1}} - \overline{P_c^{i}}) - \overline{V_c^{i+1/2} \cdot (\rho_{Na,c}^{i+1/2} + \rho_{fg,c}^{i+1/2})} \cdot g$$

$$- \overline{V_c^{i+1/2} \cdot (\rho_{Na,c}^{i+1/2} + \rho_{fg,c}^{i+1/2})} \cdot \frac{1}{2} \cdot (U_{m,c}^{i+1/2,n+1} + U_{m,c}^{i+1/2,n}) \cdot \left| \overline{U_{m,c}^{i+1/2}} \right|$$

$$\times \frac{1}{2} \cdot \frac{1}{D_c^{i+1/2}} \cdot a \cdot \left[\frac{1}{\mu_m} \cdot D_c^{i+1/2} \cdot (\overline{\rho_{Na,c}^{i+1/2}} + \overline{\rho_{fg,c}^{i+1/2}}) \cdot \left| \overline{U_{m,c}^{i+1/2}} \right| \cdot \overline{V_c^{i+1/2}} / \overline{V_m^{i+1/2}} \right]^b$$

$$- h_{c,con} \cdot A_{cl}^{i+1/2} \cdot (\overline{T_{Na,c}^{i+1/2}} - \overline{T_{cl}^{i+1/2}}) \cdot \frac{\alpha^{i+1/2}}{H_{fg,Na}} \cdot \overline{U_{m,c}^{i+1/2}} - \overline{\rho_{fu,c}^{i+1/2}}$$

$$\times \frac{1}{m_{fp}} \left(\frac{1}{2} U_{m,c}^{i+1/2,n+1} + \frac{1}{2} U_{m,c}^{i+1/2,n} - \overline{U_{fu,c}^{i+1/2}} \right) \cdot \left| \overline{U_{m,c}^{i+1/2}} - \overline{U_{fu,c}^{i+1/2}} \right|$$

$$\times \overline{V_c^{i+1/2}} \, (\overline{\rho_{Na,c}^{i+1/2}} + \overline{\rho_{fu,c}^{i+1/2}}) \cdot r_{fp}^2 \cdot \pi/2 \cdot C_D(Re_{fp}^{i+1/2}) \cdot (\overline{\varepsilon^{i+1/2}})^{-2.7} \qquad (2.2.13)$$

$$D_c^{i+1/2} = 4 \cdot V_c^{i+1/2} \cdot \frac{1}{\Delta z} \cdot \frac{1}{\pi \cdot 2 r_{cl}^{i+1/2}}$$

$$Re_{fp}^{i+1/2} = 2 \cdot r_{fp} \cdot \left| \overline{U_{m,c}^{i+1/2}} - \overline{U_{fu,c}^{i+1/2}} \right| \cdot \left(\overline{\rho_{Na,c}^{i+1/2}} + \overline{\rho_{fg,c}^{i+1/2}} \right) \cdot \frac{1}{\mu_m} ,$$

where the bars indicate time averages using the t^n values and the V_c and ρ at t^{n+1} from the previous solution of Eqs. (2.2.1) and (2.2.3); also,

$$j = i \text{ if } \overline{U_{m,c}^{i+1/2}} > 0 \text{ and } j = i + 1 \text{ if } \overline{U_{m,c}^{i+1/2}} < 0 .$$

Pairs of adjacent cell-centered quantities are averaged as in the pin cavity momentum equation to form cell-edge values: Eq. (2.2.13) is thus a linear equation in $U_{m,c}^{i+1/2,n+1}$, $U_{m,c}^{j+1/2,n+1}$, and $U_{m,c}^{j-1/2,n+1}$ (i.e., when the alternative values of j are considered, Eq. (2.2.13) is linear in $U_{m,c}^{i+3/2,n+1}$, $U_{m,c}^{i+1/2,n+1}$, and $U_{m,c}^{i-1/2,n+1}$). The velocity values are obtained implicitly by solving the resultant tridiagonal matrix as with the pin cavity momentum equation.

A variant of the particle-in-cell[12] (PIC) approach, called distributed particle-in-cell[13] (DPIC) is used to treat fuel motion in the interaction zone in the coolant channel. In the PIC technique, the properties (temperature, mass, etc.) of a fuel particle group are associated with a point, i.e., the mass centroid of the group. When the centroid crosses a mesh cell boundary, the properties of the entire group become associated with the receiving cell in a single time step. The DPIC formulation associates the particle-group quantities with a characteristic length (rather than a point as in the PIC approach), whose center is the centroid of the particle group. In DPIC, as a particle group moves across a cell boundary, the properties of the group gradually become associated with the receiving cell and disassociated from the donor cell and are apportioned according to the relative fractions of the characteristic length within each cell. The DPIC technique thus makes the motion of fuel from cell to cell occur smoothly over several time steps rather than one abrupt change that occurs in a single time step with the PIC technique.

The amount of fuel ejected into the coolant channel at the end of a time step is determined by the pressure equilibration technique (discussed below). The ejected fuel is assumed to fragment immediately into a number of particles of equal size. Groups of these particles are then tracked independently. The particle groups are assigned random locations in front of the cladding rupture. (The number of particles per group at ejection is a user option. Particle groups are combined in the channel when the number of groups exceeds a user-specified maximum. The combined particle group is located at the center of mass of the original particle groups and moves at the mass-averaged velocity.)

Each particle group begins with zero velocity if the fuel volume fraction in the channel cell into which the particle group is ejected is below a certain value (currently set at 0.3). If the volume fraction is above a certain value (currently set at 0.7), infinite drag is assumed between the newly ejected particle group and the existing particle groups in the ejection cell. Therefore the velocity, U, of the newly ejected particle group of mass M would be

$$U = \frac{\sum_i m^i u_o^i}{\sum_i m^i + M} \qquad (2.2.14)$$

where the summation is over the particle groups (of mass m^i and velocity u_o^i) in the cell into which the new particle group is ejected. The momentum added is thus $U \cdot M$, and the total momentum of the pre-existing particle groups must be reduced by this amount. Therefore, the new velocities of the other particle groups are reduced from u_o^i to u^i,

$$u^i = u_o^i - \frac{U \cdot M}{\sum_i m^i} \cdot \qquad (2.2.15)$$

If the volume fraction of fuel in the channel ejection cell is between the two threshold values stated above, assignment of the initial velocity is based on the assumption that velocity varies linearly between zero and the velocity which results from assuming infinite drag (as a function of fuel volume fraction).

The fuel particles are accelerated by both drag from the medium and the axial pressure gradient along the channel. The position and velocity of each group are then tracked separately. The cell average mass of any cell is the sum of the masses of the portions of particle groups in that cell. The average fuel-particle velocity at the cell-edge is the mass weighted average of the particle velocities on either side of the cell edge up to one-half cell length away from the cell edge.

The velocity equation for a particle group is

$$N \cdot m_{fp} \frac{\partial}{\partial t} U_{fp,c}(t) = -N \cdot \left(\frac{4}{3} \cdot \pi \cdot r_{fp}^3\right) \cdot \frac{\partial P_c(t,z)}{\partial z} + N \cdot (U_{m,c}(t,z) - U_{fp,c}(t))$$

$$\times \left|U_{m,c}(t,z) - U_{fp,c}(t)\right| \cdot (\rho_{Na,c}(t,z) + \rho_{fg,c}(t,z)) \cdot r_{fp}^2 \cdot \frac{\pi}{2} \cdot C_D(Re_{fp}) \cdot \varepsilon^{-2.7}$$

$$-N \cdot m_{fp} \cdot g - N \cdot m_{fp} \frac{\pi}{4D_c} \cdot U_{fp,c}(t) \cdot \left|U_{m,c}(t,z)\right|$$

$$\times \left(\frac{\rho_{fu,c}(t,z)}{\rho_{Na,c}(t,z) + \rho_{fg,c}(t,z)}\right)^{0.5} \cdot \psi \,, \qquad (2.2.16)$$

N = number of fuel particles in the particle group

$U_{fp,c}$ = velocity of the particle group

ψ = constant set to a value of $1.56 \cdot 10^{-5}$

The factors $C_D(Re_{fp})$ and Re_{fp} were defined following Eq. (2.2.12) except $U_{fp,c}$ replaces $U_{fu,c}$. The first term on the right hand side represents the force on a particle surface (for all the particles in a group) in a pressure field with a linear gradient.[14,15] The second term is the drag on the particles from the medium. The last term is the wall friction experienced by the particle group based on a correlation for pressure drops for particles suspended in a pipe.[16,17]

The finite difference form of Eq. (2.2.16) is

$$N^m \cdot m_{fp} \cdot \frac{1}{\Delta t} \cdot (U^{m,n+1}_{fp,c} - U^{m,n}_{fp,c})$$

$$= - N^m \cdot \left(\frac{4}{3} \cdot \pi r^3_{fp}\right) \cdot \frac{1}{\Delta z} \cdot (\overline{P^k_c} - \overline{P^{k-1}_c})$$

$$+ N^m \cdot (\overline{U_{m,c}} - U^{m,n}_{fp,c}) \cdot \left| \overline{U_{m,c}} - \overline{U^{m,n}_{fp,c}} \right|$$

$$\times (\overline{\rho^j_{Na,c}} + \overline{\rho^j_{fg,c}}) \cdot r^2_{fp} \cdot \frac{\pi}{2} \cdot C_D(Re^j_{fp}) \cdot \left(\frac{\overline{V^j_m}}{\overline{V^j_c}} \right)^{-2.7}$$

$$- N^m \cdot m_{fp} \cdot g - N^m \cdot m_{fp} \cdot \frac{\pi}{4 D^j_c} \cdot U^{m,n}_{fp,c} \cdot \left| \overline{U}_{m,c} \right|$$

$$\times \left(\frac{\overline{\rho^j_{fu,c}}}{\overline{\rho^j_{Na,c}} + \overline{\rho^j_{fg,c}}} \right)^{0.5} \cdot \psi \,, \qquad (2.2.17)$$

where the index m indicates particle group m; k is the cell such that the initial location of the centroid of the particle group is between the middle of cell k and the middle of cell k - 1; j is the cell (either k or k-1) in which the centroid of the particle group is located; and $\overline{U}_{m,c}$ is interpolated between cell edges at the particle location. The bars indicate time averages as before.

The temperature of each particle group is calculated by,

$$\frac{1}{\Delta t} N^m \cdot m_{fp} \cdot C_{P,fu} (T^{m,n+1}_{fp,c} - T^{m,n}_{fp,c})$$

$$= -N^m \cdot 4 \cdot \pi \cdot r^2_{fp} \cdot FAC \cdot \frac{k_{fu}}{r_{fp}} \cdot \frac{\rho^j_{Na,c}}{\rho^p_{Na}} \cdot (T^{m,n}_{fp,c} - \overline{T^j_{Na}})$$

$$+ N^m_p \cdot m_{fp} \cdot W^j \cdot \phi - N^m \cdot h_{c,fu} \cdot A^j_c \cdot (T^{m,n}_{fp,c} - \overline{T^j_{cl}}) \cdot m_{fp} / (\overline{\rho^j_{fu,c}} \cdot V^j_c) \qquad (2.2.18)$$

$T^m_{fp,c}$ = temperature of fuel particle group m

The first term on the right hand side represents the heat loss to the sodium in the cell from the particle group, the second term is the fission heating of the particle group, and the third term is used to represent a fuel vapor condensation heat loss.

The number of particle groups is limited by a specified maximum. When this maximum is exceeded, the particle groups are combined according to their location within subdivisions of cells. That is, all the particles whose centers are in a given subdivision of a coolant channel cell are combined.

In the coolant channel, the motion of single-phase liquid sodium slugs above and below the partially voided interaction zone (see Fig. 1) is treated as incompressible (with the exception of one set of conditions as explained below). The motion of the sodium slugs is determined by three effects; 1) the pressure difference from the last cell in the interaction zone at the slug interface and the pressure at the opposite end of the slug; 2) the frictional resistance; and 3) gravity. The pressure at the opposite end of the slug away from the interaction zone is either the plenum pressure (held constant) or the channel pressure at the two-phase cell forming the boundary of the single-phase liquid slug. No need has been seen for a compressible treatment of the liquid slugs except as it affects the interaction zone pressure in an unvoided channel case (see below). In such a case, where the void in front of the failure in the channel is caused by the compression of the sodium, EPIC computes an effective displacement of the liquid slugs because of the interaction zone pressure. This can alter the ejection cell pressure dramatically for a short time until a significant void has been produced in the channel.

This incompressible (and pseudo-compressible) treatment appears to predict the same results as a compressible one (for example, see the EPIC and revised PLUTO curves in (Fig. 2, Reference 1) where PLUTO uses a fully compressible treatment). Also, the incompressible treatment allows much larger time steps for the calculation, since the compressible treatment is limited by the Courant condition on sound speed.

The change in the momentum over the time step of the single-phase sodium liquid slugs above and below the interaction zone is given by the following expression.

$$MU_s^{n+1} = MU_s^n - \Delta t \cdot [P_c^j A_c^j - P_{END} \cdot A_{END} + g \cdot M_s$$

$$+ a \cdot \left(\rho_{Na,s} \cdot \left| \overline{U_s} \right| \cdot D_{c,s} \cdot \frac{1}{\mu_{Na}} \right)^b \cdot \overline{U_s} \cdot \left| \overline{U_s} \right| \cdot M_s \cdot \frac{1}{D_{c,s}} \cdot \frac{1}{2}] \qquad (2.2.19)$$

MU_s = momentum of the slug

A_c = area of coolant channel

M_s = mass of the slug

a, b = constants appropriate for slug flow

$\rho_{Na,s}$ = density of liquid sodium in the slug

$\overline{U_s}$ = average velocity of the slug

$D_{c,s}$ = hydraulic diameter over the length of the slug

μ_{Na} = viscosity of liquid sodium

j = index of interaction zone cell at the slug interface.

The bars indicate time averages as before. The subscript END denotes the conditions at the end of the slug opposite the interaction zone whether this is within the coolant channel or at the plenum. The second term on the right hand side of the equation, the pressure gradient across the slug, is written for the lower slug; the sign of the term is reversed for the upper slug. The third term is from gravity and the last term is a drag term.

The slug interface position is tracked precisely from its initial position. Within the interface cell, the single-phase liquid part of the cell is separate and not homogenized with the two-phase part of the cell. The interaction zone portion of the interface cell contains two-phase sodium, fission gas and fuel which convect in or out of the adjacent cell in the interaction zone. This material has a separate density and pressure from the single-phase liquid

portion of the cell where the sodium is at full density and is at its original temperature. The interface moves with the velocity of the slug. The pseudo-compressible treatment displaces the interface to take into account the interaction zone pressure compressing the slug (see below). The amount of this displacement, D, for one time step is

$$D = (\overline{P_c^j} - P_{END}) \cdot \beta_{Na} \cdot \Delta t \cdot c_{Na} (1 - t \cdot c_{Na}/L_s), \qquad (2.2.20)$$

β_{Na} = compressiblity of liquid sodium

c_{Na} = speed of sound in liquid sodium

t = time after pin failure

L_s = length of slug

$D = 0$ if $t \cdot c_{Na} > L_s$; and $\Delta t \cdot c_{Na}$ is the distance that the compression wave travels in Δt. At every time step this displacement is added to the normal slug displacement due to its gross velocity until the first compression wave reaches the end of the slug (i.e., until $t \cdot c_{Na} > L_s$) after which time the effect of the displacements on the interaction zone pressure is small. The $(P_c^j - P_{END}) \cdot \beta_{Na}$ is the fraction of the length $\Delta t \cdot c_{Na}$ that is actually compressed. The $c_{Na} \cdot (1 - t \cdot c_{Na}/L_s)$ term reduces the effect linearly to zero as the compression wave reaches the end of the slug so that no discontinuities result. The slug motions resulting from this approximate technique compare well with those calculated using a fully compressible treatment.

In the event that pin failure occurs in an unvoided channel, initially all and later (up to a 0.5 to 1 ms in cases studied) much of the void produced in the coolant channel is caused by compression of the sodium by the interaction zone pressure. The small void fraction produced by compressing the sodium directly in front of the pin failure can be drastically increased by including the effect of compression after a pressure pulse has passed through it.

The approximation to this compressible effect in EPIC is made by compressing all the sodium in the portion of the liquid slug through which the pressure pulse would have passed in a compressible treatment using a pressure equal to the interaction zone pressure. The slug interface is then artifically displaced to generate a volume that would have been generated by the compression. This represents the maximum contribution that this phenomenon can make and can double the void in some cases (and reduce the fission gas partial pressure to half) in the interaction zone in the initial portion of the transient. As the transient progresses, the effect will be less and less significant as more void is developed in front of the clad failure. Thus, no significant error is introduced by the approximation that the additional compression falls linearly to zero by the time the pressure pulse reaches the end of the slug.

The equation-of-state in the coolant channel is

$$P_c(t,z) = P_{fu,sat}(T_{fu,c}(t,z)) + P_{Na,sat}(T_{Na,c}(t,z))$$

$$+ \frac{R_{fg} \cdot T_{fg,c}(t,z) \cdot \rho_{fg,c}(t,z)}{V} \qquad (2.2.21)$$

where

$$V = 1 - \frac{\rho_{fu,c}(t,z)}{\rho^{p}_{fu}} - \frac{\rho_{Na,c}(t,z)}{\rho^{p}_{Na}} \cdot (1 - \beta_{Na} \cdot P_{c}(t,z)).$$

$P_{Na,sat}(T_{Na,c}(t,z))$ = saturation pressure corresponding to sodium temperature $T_{Na,c}(t,z)$.

The partial pressure due to fuel vapor is always assumed to be the saturation pressure corresponding to the liquid fuel temperature and likewise with sodium. In non-ejection cells, the P_c channel pressure used to compute the sodium compression is taken from the last time step (or the last semi-implicit pass), because it does not vary rapidly with the time. V is the fraction of the total volume of the coolant channel cell not taken up by the liquid fuel and sodium (including the volume generated by compressing the liquid sodium).

2.3 The Pressure-Equilibration Ejection Model

There are two models in the code for pressure equilibration, and the user must select one of the models via input. The first model assumes that the dominant term affecting pressure equilibration is the change in fission gas partial pressure in the pin and channel; all temperatures are assumed to remain constant during ejection. The second model is more general and allows fuel temperature to change during ejection; this model is best suited for the situation where changes in fuel vapor partial pressure dominate the ejection, although it may be used for all situations (it is, however, less efficient than the first model). The fission-gas driven ejection model will be described first followed by the additional equation needed to describe the general model.

In the first model, fuel/fission gas ejection is driven primarily by fission gas. At the end of every time step, the pressure in each fuel pin cell is equilibrated with the pressure in the adjacent coolant channel cell (for all of the cells that delimit the clad rip). This calculation results in determination of the amounts of fuel and fission gas ejected from the pin cavity into the coolant channel during a time step. Orifice effects are assumed to not significantly inhibit fuel motion into the channel for the typical EPIC time step size. (If an orifice coefficient is used to compute the ejection velocity of the material with such large initial pressure gradients as are common in pin failure conditions, extremely small time steps are necessary, so that the computation is impractical.) In the pressure equilibration model, details of the pressure history are ignored. It is believed that the area under the pressure-time curve is more important than its precise shape (over a small segment of the transient), and that the area under the pressure-time curve is determined largely by the amount of fission

gas initially available. It is also felt that the fuel temperature and the precise mechanism of the dissipation of the fission gas thermal energy is not important. The equilibration procedure is performed at the end of each pass for a time step and determines the quantities $S_{fu,ej}$ and $S_{fg,ej}$ needed to complete the solution of Eqs. 2.1.1, 2.1.3, 2.1.11 and 2.2.1. The equilibration calculation provides an explicit coupling between the pin and channel equations.

In the case of ejection driven primarily by fission gas partial pressure, an amount of fuel $\Delta V \cdot \rho_{fu,p} \cdot Y$ and fission gas $\Delta V \cdot \rho_{fg,p}$ is ejected from the pin cavity into the channel. This amount is subtracted from the original amount of fuel and fission gas in the pin cell and added to the original amount in the channel. The function Y is the ratio of the volume of fuel to the volume of fission gas ejected and is specified by the user. It describes slip between fuel and fission gas during ejection. The expressions for the post-ejection pressures in the pin cell i and the channel volume in front of it, P_p [Eq. (2.1.13] and P_c [Eq. (2.2.21)] are set equal:

$$P_p = P_{fu,sat}(T^{i,n+1}_{fu,p}) + \frac{R_{fg} \cdot T^{i,n+1}_{fu,p} \cdot \rho^{i,o}_{fg,p} \cdot [V^{i,n+1}_p - \Delta V \cdot Y]}{V^{i,n+1}_p - \frac{\rho^{i,o}_{fu,p}}{\rho^p_{fu}} \cdot (V^{i,n+1}_p - \Delta V \cdot Y)}$$

$$= P_{fu,sat}(T^{n+1}_{fu,c}) + P_{Na,sat}(T^{n+1}_{Na,c})$$

$$+ \frac{R_{fg} \cdot T^{n+1}_{fg,c} \cdot (\rho^{n+1}_{fg,c} \cdot V^{n+1}_c + \rho^{i,o}_{fg,p} \cdot \Delta V \cdot Y)}{V} = P_c \,, \qquad (2.3.1)$$

$$V = V^{n+1}_c - \frac{1}{\rho^p_{fu}} \cdot (\rho^{n+1}_{fu,c} \cdot V^{n+1}_c + \rho^{i,o}_{fu,p} \cdot \Delta V \cdot Y)$$

$$- \frac{1}{\rho^p_{Na}} \cdot \rho^{n+1}_{Na,c} \cdot V^{n+1}_c + \beta_{Na} \cdot \left[P_p \cdot \frac{1}{\rho^p_{Na}} \cdot \rho^{n+1}_{Na,c} \cdot V^{n+1}_c \right.$$

$$\left. + (P_p - P^U_{END}) \cdot \left(1 - t \cdot c_{Na} \cdot \frac{1}{L^U_{END}} \right) \cdot A^U_{END} \cdot c_{Na} \cdot \Delta t \right.$$

$$+(P_p - P^L_{END}) \cdot \left(1 - t \cdot c_{Na} \cdot \frac{1}{L^L_{END}}\right) \cdot A^L_{END} \cdot c_{Na} \cdot \Delta t \Bigg] .$$

P^U_{END} = pressure at end of upper sodium liquid slug opposite interaction zone

L^U_{END} = length of upper sodium liquid slug

A^U_{END} = area of upper sodium liquid slug

P^L_{END} = pressure at end of lower sodium liquid slug opposite interaction zone

L^L_{END} = length of lower sodium liquid slug

A^L_{END} = area of lower sodium liquid slug

Here P_p, which is the left side of the equation, is substituted for the equilibrated pressure on the right side for the sake of the compression terms. The volume in the coolant channel which is equilibrated with the pin ejection cell i is not necessarily that of channel cell i alone. It may include up to one cell additional volume on either side of cell i, but it is added only if the cell above or below is not an ejection cell. The volume is delimited by the slug interfaces, and the volume expands as the slug interfaces move away from the failure. The purpose of this pseudo-Lagrangian expanded cell for equilibration purposes is to avoid the large pressure gradients that would otherwise occur across the boundaries of ejection cells in an initially unvoided channel before enough material (fuel and fission gas) has moved into the adjacent cell to raise its pressure. These extremely high pressure gradients would require very small time steps to prevent numerical problems. For a coolant channel voided in front of the ejection cell, the interfaces are far enough removed from the ejection cell so this treatment is not necessary. All values in Eq. (2.3.1) are at t^{n+1}, and the t^{n+1} values in the channel do not have a cell index because they are for the expanded cell under the above conditions. The temperatures in the channel volume are the mass weighted average of those of the cells within the volume V at t^{n+1}, and the ρ's are averaged over V. The $\rho^{i,o}$ values are values at t^{n+1} prior to the ejection. The last two compression terms go to zero as described above at $t > (L_s/c_{Na})$. These two terms must be included in an unvoided channel case, as discussed above, since, initially, they can drastically affect the ejection zone pressure for a short time. When the expression for P_p from the left side of Eq. (2.3.1) is substituted into the right side of Eq. (2.3.1) in the compression terms, Eq. (2.3.1) becomes a cubic equation in the unknown ΔV. The three roots of the equation are found using the closed-form analytical solution. The smallest positive root is used. If there is no real, positive root, then the ejection is zero. This can happen when the channel pressure has become greater than the pin pressure [e.g., from a fuel-coolant interaction (FCI)]. No injection of channel material into the pin [a negative root of Eq. (2.3.1)] is allowed.

In addition to the case of predominantly fission gas driven ejection, for which the model above was developed, another model was created to deal with fresh fuel pins as well. The second model is totally general and can treat fuel ejection from pins with any amount of burnup (including zero burnup). In the case of zero burnup, the only non-condensible gas present would be fill gas. The ejection of molten fuel and gas is then driven by the pressure of the fuel vapor and any fill gas present. Since this generalized model takes more computer time, however,the more limited model described above should be used at the option of the user for the case of predominantly fission gas-driven ejection. Also, the user-specified function for fuel fission gas slip described above is not available in the general model.

In the generalized ejection model, the fuel temperature within the pin changes during the ejection as the material remaining in the pin expands to fill the available volume. The local fuel temperature within the channel changes due to the addition of the newly ejected fuel. The new total pressure in the pin after ejection consists of the linear superposition of fuel vapor pressure at the post-expansion fuel temperature plus the fission-gas pressure in the expanded fuel pin volume. The new pin pressure is then equalized with the channel pressure; the latter is a summation of the fuel vapor, fission-gas, and sodium vapor partial pressures at the post-ejection conditions.

The equations describing the additional features of the ejection are as follows. The fuel remaining in the pin is cooled by expansion (and vapor generation) into the volume freed by ejection of material during the time step:

$$\left\{\rho_{fu,p}^{i,o}\cdot V_{p}^{i,n+1} - \frac{1}{2}\cdot\Delta V\left[\rho_{fu,p}^{i,o} + \frac{P_{fu,sat}(T_{fu,p}^{i,n+1})}{R_{fu}\cdot T_{fu,p}^{i,n+1}}\right]\right\}\cdot C_{P,fu}\cdot(T_{fu,p}^{i,n+1} - T_{fu,p}^{i,o})$$

$$= \frac{\Delta V\cdot P_{fu,sat}(T_{fu,p}^{i,n+1})}{R_{fu}\cdot T_{fu,p}^{i,n+1}}\cdot H_{fg,fu}\cdot \qquad (2.3.2)$$

where most terms are defined as for Eq. (2.3.1). ΔV is the volume of material (fuel plus fission gas) ejected between time t^n and t^{n+1}, R_{fu} is the gas constant for fuel, and $H_{fg,fu}$ is the latent heat of vaporization of fuel; the superscript o denotes values at time n+1 but prior to ejection. The fuel vapor is treated as an ideal gas. This type of temperature calculation is also performed for the volume changes associated with melt-in and intra-pin convection of material from one mesh cell to another.

The newly ejected fuel enters the adjacent channel cell at a temperature

$$(T_{fu,p}^{i,o} + T_{fu,p}^{i,n+1})/2$$

and is mixed with the fuel in that cell to obtain the post-ejection fuel temperature in the channel:

$$\rho_{fu,c}^{n+1} \cdot V_c^{n+1} \cdot E_{fu,sat}(T_{fu,c}^{n+1}) = \rho_{fu,c}^{o} \cdot V_c^{n+1} \cdot E_{fu,sat}(T_{fu,c}^{o})$$

$$+ \rho_{fu,p}^{i,o} \cdot \Delta V \cdot E_{fu,sat}[\tfrac{1}{2} \cdot (T_{fu,p}^{i,o} + T_{fu,p}^{i,n+1})]. \qquad (2.3.3)$$

The mass-weighted energy balance allows the correct energy to be associated with solidified fuel in the coolant channel. $E_{fu,sat}(T)$ is the energy function.

Since the final pin and channel fuel temperatures appear implicitly (via $P_{fu,sat}$) in the equations, an iterative technique must be used to find the post-ejection conditions. For this purpose, the equations describing the ejection may be written using $T_{fu,p}^{i,n+1}$ as the primary unknown.

The number and location of ejection cells at pin failure where the EPIC model starts is specified in the input. There can be from one to as many cells as are necessary to encompass the extent of the molten fuel cavity. The failure cells need not be contiguous. The number and location of failure cells may remain constant during the whole transient if specified, or, at the option of the user, additional failure cells may be added during the transient. One way to add additional failure cells is for the user to program an arbitrary function into the code. There is a specific subroutine (RIPEXT) available for this purpose. There is another option presently available in the code for specifying the addition of failure cells. Ejection from any given axial pin cell can be triggered when a particular radial subcell (specified by the user) becomes fully molten.

3. PROGRAMMING CONSIDERATIONS

3.1 Description of Subroutines and Functions

The following is a brief general description of the purpose of each subroutine and function in the program.

CHAMOM

This routine solves the momentum equation (implicitly) for from 1 to 3 two-phase regions in the coolant channel.

CHINIT

This routine initializes certain terms for use in CHAMOM and CHMAST. The terms are sodium vapor condensation, FCI and the energy division between boiling and heating the liquid phase for sodium.

CHMAST

This routine solves the continuity equations for fission gas and two-phase sodium in the coolant channel. Also the temperatures of fission gas and sodium and the convection of the fissions gas interface are calculated here.

CPSLF

This function is for the specific heat of liquid sodium.

CPSVF

This function is for the specific heat of sodium vapor.

CUBRT

This routine solves a cubic equation which is necessary for the computation of fuel ejection.

DPFDT

This entry in the PFSAT routine provides the derivative of P_{sat} for fuel with respect to temperature.

DPSDT

This entry in the PSSAT routine provides the derivative of P_{sat} for sodium with respect to temperature.

EQUILN

This routine calculates the ejection of fuel and fission gas from all ejection nodes for all time steps after t = 0, adjusting densities, temperatures

and pressures accordingly. Also the pin and channel pressure calculations for non-ejection nodes is done here.

EQUILP

This routine calculates the ejection of fuel and fission gas by means of the generalized ejection model.

EQUIL1

This routine calculates the ejection of fuel and fission gas from all ejection nodes at t = 0.

ETOT

This function converts an energy per unit mass to a temperature for fuel.

FUPART

This routine calculates the convection, velocity and temperature of the fuel particle groups.

INPUT

This routine reads all data and initializes most variables and prints out their values in edited form.

MAIN

This program makes all the primary subroutine calls. There are some initializations, the time step is set, the current semi-implicit pass is determined and the results of the calculations on each semi-implicit pass are switched to the proper storage location, clad rip extension is calculated under one option and particle recombination is calculated.

MISC

This routine adjusts FCI zone boundaries as well as the velocities, pressures, temperatures and densities at the FCI zone boundaries. There is an adjustment to the temperature in the pin cavity due to fuel vaporization. There is a calculation to alleviate overcompaction in both pin and channel cells.

PFSAT

This function provides the saturation pressure of fuel as a function of temperature.

PHIT

This is a user-supplied function to provide normalized power as a function of time.

PIN

This routine solves the following equations in the fuel pin: continuity and momentum equations for fuel and fission gas, and energy for fuel. The momentum equation is solved implicitly. The temperature of each solid fuel cell is also calculated as a function of fission heating and the melt-in source term is computed.

PLOTER

This routine writes out data to be used by a separate program to generate plots.

PRINT

This routine prints results at specified intervals. The reactivity calculation is done here.

PSSAT

This function provides the saturation pressure of sodium as a function of temperature.

RANDU

This provides a "random number" for use by EQUILN in placing fuel particle groups in front of the ejection cells. The subroutine is specifically designed for IBM computers and can't be used except on IBM.

RIPEXT

This is an arbitrary user-supplied function to specify the extension of the clad failure as a function of time.

SIMQ

This routine solves a system of linear equations. It is used in the implicit solution of the momentum equations in the pin and channel.

SLDENS

This function provides the density of liquid sodium as a function of temperature.

SLGVEL

This routine calculates the motion of the single-phase regions above and below the interaction zone.

TTOE

This function converts temperature to energy per unit mass for fuel.

YFACF

This is an arbitrary user-supplied function which specifies the amount of slip between fuel and fission gas during convection in the pin cavity and during ejection.

3.2 Sequence of Execution

The MAIN program calls these subroutines in the following order:

INPUT (once to start problem)
EQUIL1 (once at time zero)
PLOTER (when specified according to time interval and by option)
PRINT (when specified according to time interval)
PIN
CHINIT
CHMAST
CHAMOM
SLGVEL
FUPART
RIPEXT (when specified according to option)
EQUILN
MISC

In addition, aside from function calls,

EQUIL1 calls YFACF, EQUILP, CUBRT
PIN calls YFACF, PHIT, SIMQ
CHAMOM calls SIMQ
EQUILN calls YFACF, EQUILP, CUBRT, RANDU
MISC calls YFACF.

3.3 Facility Requirements and General Operational Information

EPIC requires 400 K bytes of storage on the IBM 370/195 computer. There is one input file. There are three output files, two of which are optional. Besides the printer, there is an optional abreviated form of the output written on unit 10 and plotting information is written on an arbitrary unit number.

Certain subroutines must be supplied by the user. If the amount or form of the plotting information is not adequate as supplied by the version of PLOTER provided to the user, changes must be made to make this routine compatible with the plotting program used. PLOTER is only called if the plotting option is indicated, of course. YFACF as supplied to the user will specify a no slip condition between fuel and fission gas. The user must alter the routine to change this. The subroutine RIPEXT as supplied to the user has a particular arbitrary scheme for extending the cladding failure. Should the user wish RIPEXT to be called, he will undoubtedly want to change the scheme,

in which case the scheme provided will serve as a paradigm to show him what must be done. The PHIT routine must be specified by the user for the transient power function. The rountines PLOTER and RIPEXT are not called unless the appropriate input option is set; however, YFACF and PHIT are always called by the code.

Certain features of EPIC are specific to the IBM 370/195 system. They may have to be changed when bringing the code up on an incompatible system. The input unit is rewound after it is read and the input records are listed as read. This may not be allowed on other computer systems. The user may just eliminate this section of coding and the only effect will be to lose the listing of the input but the edited form of the input will still appear. RANDU generates a sequence of so-called "random numbers" using features that are peculiar to the IBM hardware. This routine will probably have to be replaced by a user if another system is used. RANDU is only called from EQUILN and it does nothing more than to provide a different number between 0.0 and 1.0 every time it is called. It can be replaced very easily.

All the floating point variables in the program are in IBM double precision (i.e., REAL*8) and all integers are full precision (INTEGER*4) except the following: YFL and some temporary variables in PLOTER are REAL*4 and LBUGPR is logical (*4).

4. INPUT AND OUTPUT DESCRIPTION

4.1 Input Description

The following is a description of the input to EPIC.

Card Group	No. of Cards in Group	Format	Variable Name	Units	Description
1	2	72A1	JOBID	-	Two cards of alphanumeric case identification.
2	1	10I6	NPL	-	Bottom cell of molten fuel cavity in pin (≤99).
			NPU	-	Top cell of molten fuel cavity in pin (≤99).
			NPLC	-	Bottom cell of fuel mesh (≤99).
			NPUC	-	Top cell of fuel mesh (≤99).
			NPRAD	-	Number of radial subcells at each axial cell in fuel mesh (≤10).
			NCL	-	Bottom cell of channel mesh (≤99).
			NCU	-	Top node of channel mesh (≤99).
			MPPART	-	Number of fuel particles per particle group at ejection (~50-200 suggested).
			MAXPRT	-	Maximum number of fuel particle groups allowed in channel before recombining particle groups (≤1000).
			NDIV	-	Number of divisions in each cell for the purpose of particle group recombination (~10-20 suggested).
3	1	10I6	INTPO	-	Number of time steps between print-outs.

Card Group	No. of Cards in Group	Format	Variable Name	Units	Description
3 (contd)	1	10I6	INTPO1	-	If 0, print both passes for all time steps; if 1, ignore option.
			IPR10	-	If nonzero, write short form of output on unit 10.
			IPLOT	-	If nonzero, unit number for plot data set.
			IPCYCL	-	Number of time steps between write-outs of plot data.
			IOPT1	-	If -1, the pin cavity area for each axial cell is calculated from the geometry of the molten portion of the r-z fuel mesh. If 0, read in values for pin cavity areas.
			IOPT2	-	If -1, the pin cavity temperatures are calculated as mass averages over the molten portion of the r-z fuel mesh. If 0, read in values for pin cavity temperatures.
			IOPT3	-	If -1, the fuel smear densities in the pin cavity nodes are calculated from masses in the molten portion of the r-z fuel mesh. If 0, the fuel smear density is calculated from radii of a central void space read in for each axial pin cavity cell. If +1, one void fraction is read in for all axial pin cavity cells.
			IOPT4	-	If -1, the fission gas smear density is calculated from the masses and fission gas/fuel mass ratios in the r-z mesh.

Card Group	No. of Cards in Group	Format	Variable Name	Units	Description
3 (contd)	1		IOPT4 (contd)		If 0, the fission gas smear density is calculated from fission gas/fuel mass ratios read in for each axial cell which are constant radially. If +1, only one value of fission gas/fuel mass ratio is read for all r-z cells.
			IOPT5	-	If 0, fuel ejection is driven predominantly by fuel vapor (generalized ejection model is used). If 1, fuel ejection is driven predominantly by fission gas.
4	1	10I6	IOPT6	-	If -1, a user supplied subroutine called RIPEXT is called to determine expansion of the clad failure during the transient. If 0, no extension of clad failure during transient. If >0, clad failure will occur at any axial cell when radial subcell IOPT6 is fully molten.
			IOPT7	-	If 0, initial pressures in coolant channel cells are read in. If 1, initial coolant channel pressures are assumed to be $P_{sat}(T_{Na})$.
			IOPT8	-	If 0, no reactivity worths are read. If >0, IOPT8 is lowest cell of reactivity worth mesh.
			IOPT9	-	If >0, and IOPT8 >0, highest cell of reactivity worth mesh.

Card Group	No. of Cards in Group	Format	Variable Name	Units	Description
5	I{(IIFAIL+1)/10}*	10I6	IIFAIL	-	Number of failure cells.
			IFAIL(I)	-	Failure cell numbers in increasing order from 1 to IIFAIL. Failure cells need not be contiguous.
6	1	6E12.5	DELZ	cm	Eulerian cell height
			ZPART	-	Fraction of DELZ for DPIC particle length (0.0 < ZPART < 0.9) (Normally ~0.5 works quite well; if PIC is to be approximated with DPIC, then set ZPART to some very small number greater than zero.)
			HLPLEN	cm	Location of lower free surface-probably the end of the subassembly (bottom of channel mesh is 0).
			HUPLEN	cm	Location of upper free surface-probably the end of the subassembly (bottom of channel mesh is 0).
			FCIL2	cm	Location of lower liquid slug interface. In a totally unvoided channel, set to any value higher than the clad rip.
			FCIU2	cm	Location of upper liquid slug interface. In a totally unvoided channel, set to any value lower than the clad rip.
7	1	6E12.5	DELT1	s	Initial time step (from t=0 to TIME01).

*The notation I{X} means round up to the next integer. For example, I {6/10} = 1, I {9/6} = 2, etc.

Card Group	No. of Cards in Group	Format	Variable Name	Units	Description
7 (contd)	1		DELT2	s	Second time step (from TIME01 to TIME02, Δt is varied linearly from DELT1 to DELT2; between TIME02 and TIME03, Δt = DELT2).
			DELT3	s	Third time step (from TIME03 to TIME04, Δt is varied linearly from DELT2 to DELT3; after TIME04, Δt = DELT3).
			TIME01	s	See DELT1 and DELT2 above.
			TIME02	s	See DELT2 above.
			TIME03	s	See DELT2 and DELT3 above. (If TIME03=0, it is set to 100.)
8	1	6E12.5	TIME04	s	See DELT3 above. (If TIME04=0, it is set to 100)
			TIMAX	s	Maximum problem time.
			EXTIME	s	Time after which differencing is explicit in time.
			PTIME1	s	Between PTIME1 and PTIME2, results are printed for all time steps and for each semi-implicit pass each step. (If PTIME1=0, it is set to 100.)
			PTIME2	s	See PTIME1 above.
			POINT	s	Time interval between prints.
9	1	6E12.5	PLINT	s	Time interval between data writes for fuel density plots.
			TMELT	K	Fuel melting temperature

Card Group	No. of Cards in Group	Format	Variable Name	Units	Description
9 (contd)	1		FDEN	K	Temperature at which the (constant) physical density of fuel is evaluated by a function in the code.
			HFGFU	ergs/g	Heat of vaporization of fuel
			HSFFU	ergs/g	Heat of fusion of fuel
			RFU	ergs/g·K	Gas constant for fuel vapor
10	1	6E12.5	CPFU	ergs/g·K	Specific heat of liquid fuel
			FUCOND	ergs/cm·s·K	Liquid fuel thermal conductivity
			VISCF	g/s·cm	Absolute fuel viscosity
			HCFV	ergs/cm^2·s·K	Fuel vapor condensation coefficient
			RPART	cm	Fragmented fuel particle radius
			FFCI	-	Multiplier for FCI heat transfer
11	1	6E12.5	HCSL	ergs/cm^2·s·K	Heat transfer coefficient between cladding and liquid sodium
			SCOMP	cm^2/dyne	Sodium compressibility
			CSNDNA	cm/s	Speed of sound in sodium liquid
			HCSV	ergs/cm^2·s·K	Sodium vapor condensation coefficient
			VISCSL	g/s.cm	Absolute viscosity of sodium liquid
			VISCM	g/s.cm	Absolute viscosity of two-phase sodium and fission gas mixture.

Card Group	No. of Cards in Group	Format	Variable Name	Units	Description
12	1	6E12.5	DCHANL	cm	Hydraulic diameter of lower sodium liquid slug from end of coolant mesh to HLPLEN.
			DCHANU	cm	Hydraulic diameter of upper sodium liquid slug from end of coolant mesh to HUPLEN.
			RAF	-	Coefficient in $RAF(Re)^{RBF}$ for sodium liquid and pin cavity friction factor.
			RBF	-	Exponent in $RAF(Re)^{RBF}$ for sodium liquid and pin cavity friction factor.
			RAM	-	Coefficient in $RAM(Re)^{RBM}$ for two-phase sodium friction factor.
			RBM	-	Exponent in $RAM(Re)^{RBM}$ for two-phase sodium friction factor.
13	1	6E12.5	PLPLEN	dynes/cm2	Pressure at lower free surface
			PUPLEN	dynes/cm2	Pressure at upper free surface
			TLPLEN	K	Temperature at lower free surface
			TUPLEN	K	Temperature at upper free surface
			ACLEND	cm^2	Area of coolant channel between end of coolant mesh and HLPLEN.
			ACUEND	cm^2	Area of coolant channel between end of coolant mesh and HUPLEN.
14	1	6E12.5	HSFCL	ergs/gm	Heat of fussion of cladding.

Card Group	No. of Cards in Group	Format	Variable Name	Units	Description
14 (contd)	1		CLDEN	gm/cm^3	Density of cladding.
			CPCL	ergs/gm·K	Specific heat of cladding.
			CLMELT	K	Cladding melting temperature.
			HBOND	$ergs/cm^2 \cdot s \cdot K$	Bond conductance between solid fuel and cladding at cladding inner surface.
			HBONDM	$ergs/cm^2 \cdot s \cdot K$	Bond conductance between molten fuel and cladding a cladding inner surface.
15	1	6E12.5	RFG	ergs/g·K	Gas constant for fission gas
			VFC	-	Volume fraction of coolant (used with card group 30 below; coolant flow area = VFC/(1-VFC) × $\pi \times r_{cl}^2$, where r_{cl} is outer clad radius)
16	I{(NPUC-NPLC+1)/6}	6E12.5	RFOUT(I)	cm	Read only if NPRAD>0. Outer radius of solid fuel for cells NPLC to NPUC.
17	(NPUC-NPLC+1)× I{NPRAD/6}	6E12.5	TFUPRZ(J,I)	K	Read only if NPRAD>0. Temperature of each r-z cell. For each axial cell, NPLC to NPUC, NPRAD numbers are read from I{NPRAD/6} cards and skip to the next card for the next axial cell.
18	(NPUC-NPLC+1) ×I{NPRAD/6}	6E12.5	HFPRZ(J,I)	-	Read only if NPRAD>0. Fraction of heat of fusion satisfied at each r-z cell. Read like card group 17.
19	(NPUC-NPLC+1) ×I{NPRAD/6}	6E12.5	GMPN(J,I)	g	Read only if NPRAD>0. Mass of fuel in each r-z cell. Read like card group 17.

Card Group	No. of Cards in Group	Format	Variable Name	Units	Description
20	(NPUC-NPLC+1) ×I{NPRAD/6}	6E12.5	FGFUF(J,I)	-	Read only if NPRAD>0 and IOPT4=-1. Ratio of fission gas mass to fuel mass in each r-z cell. Read like card group 17.
21	I{(NPU-NPL+1)/6}	6E12.5	TFUP2(I)	K	Read only if IOPT2=0. Temperature of each axial cell in the pin cavity, from NPL to NPU.
22	I{(NPU-NPL+1)/6}	6E12.5	AF2(I)	cm^2	Read only if IOPT1=0, cross-sectional area of each axial cell in the pin cavity. From NPL to NPU.
23	1	6E12.5	FGFUF(J,I)	-	Read only if IOPT4=1. Ratio of fission gas mass to fuel mass in all r-z cells, one value.
24	I{(NPUC-NPLC+1)/6}	6E12.5	FGFUF(J,I)	-	Read only if IOPT4=0. Ratio of fission gas mass to fuel mass in each axial cell (the same value is used in all radial sub-cells), NPLC to NPUC.
25	1	6E12.5	TEMP	-	Read only if IOPT3=1. Value of void fraction in all pin cavity cells. Fuel smear density = FDEN × (1-TEMP).
26	I{(NPU-NPL+1)/6}	6E12.5	RVOID(I)	cm	Read only if IOPT3=0. Radius of central void in each pin cavity cell which defines total void fraction in each cell in order to compute smear density, from NPL to NPU.
27	I{(NCU-NCL+1)/6}	6E12.5	RCL(I)	cm	Cladding outer radius, NCL to NCU.

Card Group	No. of Cards in Group	Format	Variable Name	Units	Description
28	I{(NCU-NCL+1)/6}	6E12.5	RCIN(I)	cm	Cladding inner radius, NCL to NCU.
29	I{(NCU-NCL+1)/6}	6E12.5	TCL2(I)	K	Cladding temperature, NCL to NCU.
30	I{(NCU-NCL+1)/6}	6E12.5	AC2(I)	cm^2	Coolant channel flow area, NCL to NCU. If a zero value for AC2 is read at any axial cell I, the flow area will be calculated by the formula: AC2(I) = VFC ×π·RCL(I)·RCL(I)/(1.0-VFC).
				-	If a negative value for AC2 is read at any axial cell I, the flow area will be calculated by the formula: AC2(I) = -AC2(I)·π·RCL(I)·RCL(I)/(1.0+AC2(I)).
31	I{(NCU-NCL+1)/6}	6E12.5	TNA2(I)	K	Sodium temperature, NCL to NCU
32	I{(NCU-NCL+1)/6}	6E12.5	VPFRO(I)	-	Void fraction in coolant channel, NCL to NCU.
				(g/cm^3)	(Liquid sodium densities may be input for any or all of these locations instead of void fractions by simply inserting the negative of the denisty in the appropriate cell location.)
33	I{(NCU-NCL+1)/6}	6E12.5	PM2(I)	$dynes/cm^3$	Read only if IOPT7=0. Channel pressure, NCL to NCU.
34	I{(NCU-NCL+2)/6}	6E12.5	UM2(I)	cm/s	Velocity of each cell bottom from NCL to NCU+1.
35	I{(NCU-NCL+1)/6}	6E12.5	WPGM(I)	W/g	Watts per gram of fuel NCL to NCU.

Card Group	No. of Cards in Group	Format	Variable Name	Units	Description
36	I{(IOPT9-IOPT8+1)/6}	6E12.5	TNASS(I)	K	Read only if IOPT8>0. Steady-state sodium temperature for sodium void reactivity calculation, cells IOPT8 to IOPT9.
37	I{(IOPT9-IOPT8+1)/6}	6E12.5	WFUEL(I)	$\frac{dk}{kg\ Na} \times 10^5$	Read only if IOPT8>0. Fuel worths, IOPT8 to IOPT9.
38	I{(IOPT9-IOPT8+1)/6}	6E12.5	WCOOL(I)	$\frac{dk}{kg\ Na} \times 10^5$	Read only if IOPT8>0. Coolant worths, IOPT8 to IOPT9.

4.2 Output Description

Initial Print-out

1) Listing of card input as read by the program.

2) Listing and explanation of fixed point data (e.g. indices describing the mesh structure) and options chosen for the case.

3) Listing and explanation of floating point data which describes geometry, material properties, etc.

4) Listing of various floating point arrays which store data by axial cell including reactivity worths, initial power and geometry data.

5) A description of the initial conditions in the r-z fuel mesh including the the outer radius of each radial subcell in every axial cell, the total cross-sectional area from the center of the fuel out to and including the radial subcell, and the temperature, melt fraction, mass and fission gas to fuel mass ratio for each subcell.

Time-dependent Print Out

1) Time (sec) since problem initiation and current time step (sec).

2) Normalized power level relative to the power per unit mass as input (WPGM), the multiplicative factor applied to WPGM at the current time.

3) Locations (cm) of the interaction zone boundaries (FCIL and FCIU) and the axial cells in which the boundaries lie. (Heights are relative to the bottom of the channel mesh which is zero cm.)

4) Indicies of the highest and lowest failure cells.

5) Total amount (gm) of fuel ejected into the coolant channel and the current number of particle groups into which this amount is subdivided.

6) The highest and lowest axial positions (cm) of the fuel particles in the coolant channel (XMAX and XMIN). (Heights are relative to the bottom of the channel mesh which is zero cm.)

7) Sodium reactivity change (Δk). The sodium reactivity change is zero at steady-state conditions so that the reactivity change due to the density difference could be non-zero at pin failure even with a full channel.

8) Fuel reactivity change (Δk). The fuel reactivity change is normalized to zero at pin failure.

9) Total reactivity change (Δk). Simply the sum of (7) and (8).

10) Pin fuel reactivity change (Δk). This is the current total worth of all pin fuel minus the worth at t=0.

11) Channel fuel reactivity change (Δk). This is the current total worth of all channel fuel minus the worth at t=0, which is zero, since there is initially no fuel in the channel. (10) and (11) add up to (8).

Note: The user specifies the reactivity worth for each axial cell in the reactivity mesh. The worths may correspond to any number of pins at the user's option but this number must be included in the worth as input. Although reactivity changes are calculated and printed, these changes have no feedback to the rest of the calculation. The power continues to be given by the user-suppied function PHIT.

The following are given for each axial cell:

12) Position (cm) of cell bottom. This is relative to the bottom of the channel mesh which is zero.

13) Fuel temperature (K) in the pin molten fuel cavity. This is the temperature of the homogenized cell fuel in radial subcells composing the cavity.

14) Pressure (dynes/cm^2) in the pin molten fuel cavity. This includes both the fission gas and fuel vapor partial pressure.

15) Smear density (gm/cm^3) of fuel in the pin molten fuel cavity. This is the mass of fuel in the cavity cell divided by the cavity cell (sum of radial subcells fully molten) volume.

16) Smear density (gm/cm^3) of fission gas in the pin molten fuel cavity. This is the mass of fission gas in the cavity cell divided by the cavity cell volume.

17) Area (cm^2) of the pin molten fuel cavity cell. This is computed from the ter radius of the outermost fully molten radial subcell. This area may change during the calculationfrom melt-in.

18) Velocity (cm/sec) of both fuel and fission gas in the molten fuel cavity. The velocity printed out for the cell is at the bottom edge of the cell.

19) Cladding temperature (K). Since there is a one radial node treatment of the cladding, this is the average temperature.

20) Pin fuel reactivity change (Δk). This is the current worth of the fuel (molten and solid) in an axial pin cell minus the worth at t=0. The sum of these cell worths gives (10).

21) Channel fuel reactivity change (Δk). This is the current worth of the fuel in an axial channel cell. The initial worth is zero since there is no fuel in the channel at t=0. The sum of these cell worths gives (11).

22) Total reactivity change (Δk). This is simply the sum of (20) and (21) for each cell.

23) Sodium temperature (K). This is the homogenized temperature of two-phase sodium in a channel cell. The temperature of sodium printed out for interface cells in the channel is only for the two-phase sodium in the partial cell and does not include the liquid sodium from the end of the sodium slug in the cell.

24) Fission gas temperature (K). This is for the homogenized cell fission gas in the channel.

25) Fuel temperature (K). This is the mass-weighted average of the temperature of all the sections of particle groups lying within the channel cell.

26) Total pressure (dynes/cm^2). This is the sum of the fission gas, sodium vapor and fuel vapor partial pressures within a channel cell. The channel pressure in front of the ejection cells, however, may be influenced by the creation of an expanded cell in an initially unvoided channel (as explained in the text) since the sodium and fuel and fission gas partial pressures are averaged for the entire expanded cell. The interface cell pressure in the coolant channel is always interpolated between the cells on either side of it when the interface cell is not an ejection cell. The pressure in the single-phase sodium liquid slugs in the coolant channel is interpolated between the interaction zone and the ends of the slugs (which may be in the coolant channel or at the free surfaces).

27) Density (gm/cm^3) of liquid sodium. This is the mass of sodium in the channel cell divided by the cell volume. The densities printed for the interface cells which are not ejection cells are the mass of liquid sodium in the part of the cell which is not part of the slug divided by the total cell volume (not the partial cell volume).

28) Density (gm/cm^3) of fission gas. This is the mass of fission gas in the channel cell divided by the cell volume. The densities in interface cells are as for liquid sodium (27).

29) Density (gm/cm^3) of fuel. This is the mass of all the sections of particle groups lying within the channel cell divided by the cell volume. The densities in interface cells are as for liquid sodium (27).

30) Density (gm/cm^3) of two-phase sodium plus fission gas. This is (27) plus (28) plus the density of sodium vapor in the channel cell. The sodium vapor density is computed from the two-phase sodium temperature and is not book-kept.

31) Fuel velocity (cm/sec). This is the mass weighted average of the velocities of the sections of particle group which lie within the range of one-half cell below the bottom of the channel cell to one-half cell above the channel cell.

32) Velocity (cm/sec) for the mixture of two-phase sodium and fission gas. The velocity printed out for the cell is at the bottom edge of the cell.

Note: 1) The two options which force an output edit after every pass (INTPO1 and PTIME1/PTIME2) also will give diagnostic output assoicated with ejection and over-compaction, 2) the code incorporates a 20% of Courant limitation (on local velocity not sound speed) and the time step size is decreased accordingly when necessary. This applies to all pin and channel velocities, including the individual particle group velocities. Also, the results of a time step will be discarded and the calculation repeated using a smaller time step size if the channel cells become severely overcompacted or if the pin pressure changes by more than 25% in one time step.

5. SAMPLE PROBLEM

The case chosen for the sample problem is for a mid-power-rated fuel pin which is experiencing burst failure conditions during a loss-of-flow transient. This situation, as explained in the introduction, is an important accident scenario to consider because of its generic nature and because it demonstrates one common type of problem which EPIC is intended to simulate.

5.1 Description of Input for Sample Problem

Figure 2 shows the cell structure and problem specifications at t=0. A description and explanation of the input follows. Refer to the description of the input variables in section 4.1 and to the listing of the sample problem input cards in this section.

The first two cards of card group 1 give a verbal description of the problem.

Referring to Fig. 2 for card group 2 one sees that the bottom cell of the molten fuel cavity in the fuel pin, NPL, is 22; and the top cell, NPU, is 31. The molten fuel cavity will be described later in the HFPRZ array which stores the fraction of the heat of fusion satisfied for every r-z cell in the fuel pin. The lowest axial cell which is fully molten (HFPRZ=1.0) in at least one radial subcell is 22 and the highest which satisfies this criterion is 31. The lowest axial cell in the fuel mesh, NPLC, is 19; and the highest, NPUC, is 32, which means that the molten fuel cavity could grow axially at most one cell upwards and three downwards with melt-in. Also there are 10 radial subcells specified in the r-z fuel mesh in the pin (NPRAD=10). The 10 radial subcells in each axial cell are of equal volume. The lowest cell in the coolant channel mesh, NCL, is 1. The highest cell, NCU, is 50. This extends the mesh structure almost from the subassembly inlet to the outlet, with less than a cell length to the inlet and outlet at each end. MPPART is the number of fuel particles with radius RPART (later in input) which constitute a particle group upon ejection. That is, when the fuel ejection model determines that a certain mass of fuel is to be ejected into the coolant channel, this mass is divided up into amounts equal to MPPART times the mass of one particle of radius RPART, with any remainder forming a separate group. Thus the purpose of MPPART is to provide a reasonable number of particle groups into which the ejected fuel is divided. MPPART should vary with the size of the particle and the product of MPPART and the mass of a single fuel particle should probably be in the range of 0.05 to 0.10 grams (in this case the product is about 0.1 grams). MAXPRT is the maximum number of fuel particle groups allowed in the coolant channel before recombination. The limit on this is 1000 but a maximum of the order of 500 to 1000 would be very expensive in computer time. A limit lower than 100-200 would, on the other hand, mean a less detailed calculation of the fuel behavior in the channel. A compromise must be made by considering how much fuel will be in the channel and how long the interaction zone will be; the user must make this decision. The number 200 was chosen for the sample problem. NDIV is the number of axial subdivisions in each axial cell for the purpose of combining fuel particle groups in the coolant channel when the number of groups exceeds MAXPRT. When recombination occurs, the centroids of each of the particle groups which are located in each of the NDIV axial subdivisions of each axial cell are combined into a single particle group. If NDIV times the

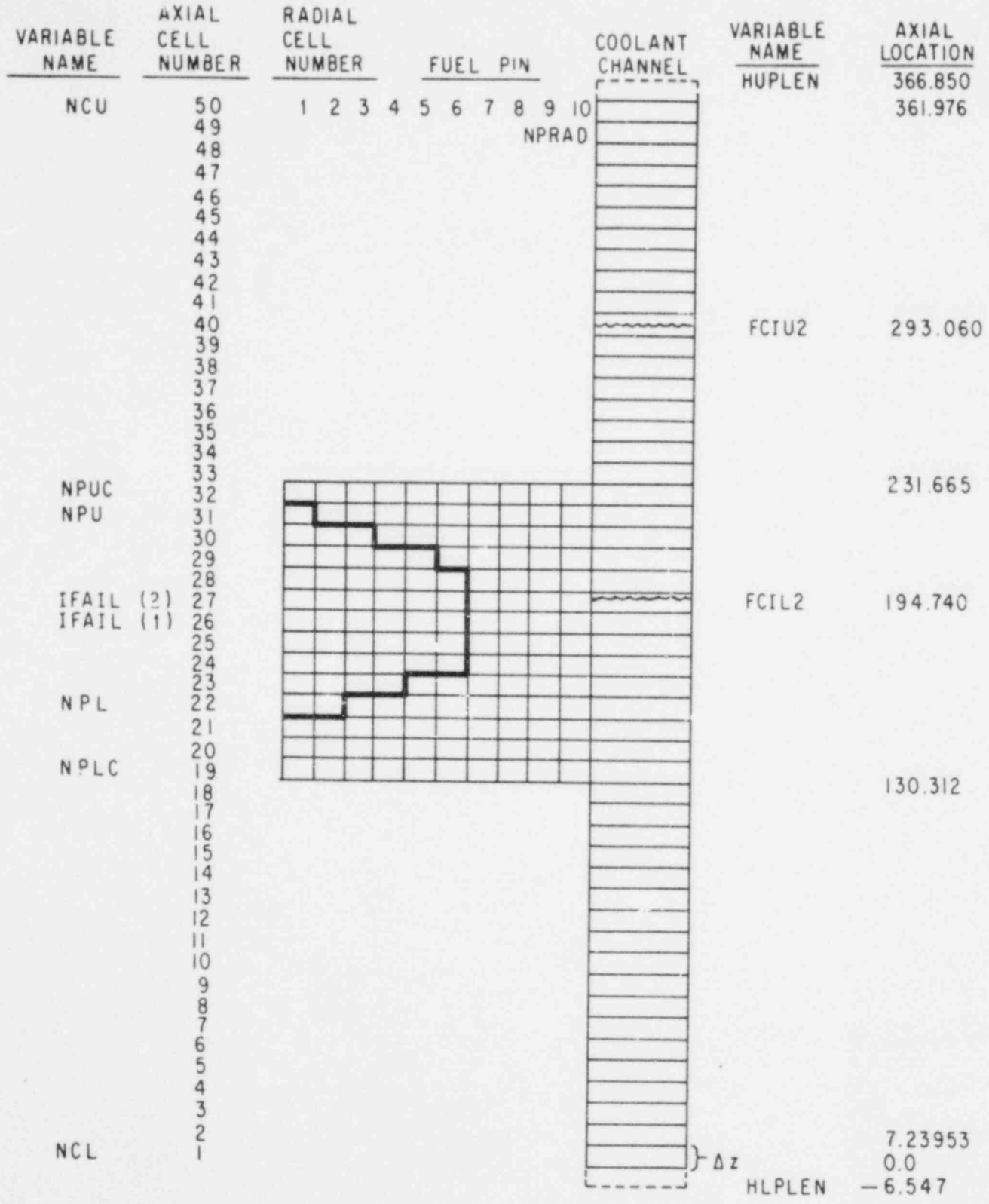

Fig. 2. Schematic Showing the Sample Problem Specifications.

```
CARD INPUT
SAMPLE PROBLEM FOR LOF-TOP CONDITIONS                                          00000010
INITIALLY 2 FAILURE CELLS, PARTIALLY VOIDED CHANNEL, NORM. POWER AT 439        00000020
    22     21     19     32     10      1     50    100    200     10          00000030
    10      1      0      0      0     -1     -1     -1     -1      1          00000040
     8      1      0                                                          00000050
     2     26     27                                                          00000060
7.23953  D0 0.5      D0 -6.547   D0 366.85   D0 194.74   D0 293.06  D000000070
0.00010  D0 0.0002   D0 0.0002   D0 0.020    D0 0.040    D0 1.0     D000000080
1.0      D0 0.05     D0 0.02     D0 1.0      D0 1.0      D0 1.0     D000000090
1.0      D0 3070.    D0 3536.8   D0 2.       D10 2.75    D9 3.079   D500000100
0.5032   D7 0.350    D6 0.040    D0 0.       D0 .03      D0 1.0     D000000110
7.0      D7 0.500  D-10 2.5      D5 6.       D7 0.002    D0 0.00020 D000000120
0.436    D0 0.436    D0 0.1875   D0 -0.2     D0 0.316    D0 -0.25   D000000130
2.867    D6 1.676    D6 643.1    D0 1209.0   D0 0.2      D0 0.2     D000000140
2.64     D9 7.4      D0 0.65     D7 1700.0   D0 1.0      D7 3.0     D700000150
0.659    D6 0.4271   D0                                             00000160
0.27168  D0 0.27168  D0 0.27168  D0 0.27168  D0 0.27168  D0 0.27168 D000000170
0.27168  D0 0.27168  D0 0.27168  D0 0.27168  D0 0.27168  D0 0.27168 D000000180
0.27168  D0 0.27168  D0                                             00000190
2751.       2696.       2648.       2600.       2548.       2488.   00000200
2410.       2291.       2053.       1663.                           00000210
3023.       2967.       2909.       2855.       2799.       2736.   00000220
2657.       2541.       2318.       1843.                           00000230
3070.       3070.       3070.       3070.       3018.       2953.   00000240
2874.       2762.       2557.       2074.                           00000250
3391.       3333.       3070.       3070.       3070.       3070.   00000260
3070.       2967.       2754.       2276.                           00000270
3587.       3597.       3490.       3187.       3070.       3070.   00000280
3070.       3070.       2896.       2459.                           00000290
3786.       3774.       3685.       3487.       3275.       3083.   00000300
3070.       3070.       2993.       2551.                           00000310
3891.       3873.       3798.       3639.       3415.       3225.   00000320
3070.       3070.       3061.       2626.                           00000330
3929.       3907.       3846.       3690.       3468.       3277.   00000340
3070.       3070.       3070.       2665.                           00000350
3879.       3871.       3810.       3658.       3431.       3235.   00000360
3070.       3070.       3070.       2656.                           00000370
3777.       3766.       3692.       3505.       3312.       3101.   00000380
3070.       3070.       3026.       2616.                           00000390
3567.       3596.       3481.       3220.       3100.       3070.   00000400
3070.       3070.       2947.       2555.                           00000410
3324.       3315.       3132.       3070.       3070.       3070.   00000420
3070.       3000.       2826.       2422.                           00000430
3070.       3070.       3070.       3070.       3070.       3020.   00000440
2950.       2857.       2672.       2240.                           00000450
3070.       3017.       2968.       2919.       2868.       2812.   00000460
2744.       2646.       2462.       2032.                           00000470
0.          0.          0.          0.          0.          0.      00000480
0.          0.          0.          0.                              00000490
0.          0.          0.          0.          0.          0.      00000500
0.          0.          0.          0.                              00000510
0.6356      0.4329      0.1934      0.0198      0.          0.      00000520
0.          0.          0.          0.                              00000530
1.          1.          0.9582      0.6159      0.4014      0.2137  00000540
0.0154      0.          0.          0.                              00000550
1.          1.          1.          1.          0.9707      0.6508  00000560
0.3744      0.0544      0.          0.                              00000570
1.          1.          1.          1.          1.          1.      00000580
0.6715      0.2995      0.          0.                              00000590
```

```
1.          1.          1.          1.          1.          1.          00000600
0.8857      0.4744      0.          0.                                  00000610
1.          1.          1.          1.          1.          1.          00000620
0.9711      0.5490      0.0513      0.                                  00000630
1.          1.          1.          1.          1.          1.          00000640
0.9048      0.4988      0.0162      0.                                  00000650
1.          1.          1.          1.          1.          1.          00000660
0.7225      0.3473      0.          0.                                  00000670
1.          1.          1.          1.          1.          0.7295      00000680
0.4412      0.1351      0.          0.                                  00000690
1.          1.          1.          0.7294      0.5084      0.3038      00000700
0.1005      0.          0.          0.                                  00000710
1.          0.5110      0.3315      0.1822      0.0254      0.          00000720
0.          0.          0.          0.                                  00000730
0.0492      0.          0.          0.          0.          0.          00000740
0.          0.          0.          0.                                  00000750
1.328       1.331       1.335       1.339       1.343       1.348       00000760
1.354       1.362       1.378       0.470                               00000770
1.300       1.305       1.312       1.318       1.323       1.328       00000780
1.334       1.344       1.360       0.614                               00000790
1.231       1.243       1.274       1.297       1.306       1.311       00000800
1.317       1.327       1.343       0.817                               00000810
0.438       1.437       1.474       1.523       1.394       1.273       00000820
1.296       1.311       1.328       1.010                               00000830
0.179       1.409       1.420       1.457       1.461       1.485       00000840
1.314       1.292       1.318       1.146                               00000850
0.094       1.390       1.398       1.420       1.445       1.470       00000860
1.462       1.263       1.305       1.221                               00000870
0.062       1.379       1.386       1.403       1.428       1.449       00000880
1.484       1.279       1.293       1.290                               00000890
0.046       1.376       1.381       1.398       1.422       1.443       00000900
1.475       1.294       1.288       1.325                               00000910
0.056       1.379       1.385       1.401       1.426       1.448       00000920
1.483       1.286       1.291       1.295                               00000930
0.039       1.390       1.398       1.418       1.440       1.468       00000940
1.448       1.273       1.302       1.235                               00000950
0.175       1.409       1.421       1.453       1.453       1.441       00000960
1.339       1.283       1.313       1.176                               00000970
0.466       1.426       1.433       1.474       1.433       1.262       00000980
1.287       1.310       1.325       1.049                               00000990
1.116       1.373       1.259       1.279       1.298       1.308       00001000
1.315       1.322       1.337       0.863                               00001010
1.295       1.309       1.313       1.317       1.321       1.326       00001020
1.331       1.339       1.354       0.625                               00001030
0.00228     0.00248     0.00248     0.00249     0.00249     0.00249     00001040
0.00249     0.00250     0.00250     0.00252                             00001050
0.00143     0.00232     0.00255     0.00260     0.00261     0.00262     00001060
0.00263     0.00264     0.00266     0.00268                             00001070
0.          0.          0.00219     0.00257     0.00259     0.00262     00001080
0.00264     0.00266     0.00271     0.00277                             00001090
0.01439     0.          0.          0.00133     0.00252     0.00253     00001100
0.00253     0.00255     0.00265     0.00281                             00001110
0.04369     0.          0.          0.          0.00154     0.00248     00001120
0.00246     0.00244     0.00252     0.00276                             00001130
0.08903     0.          0.          0.          0.          0.          00001140
0.00241     0.00234     0.00240     0.00270                             00001150
0.1408      0.          0.          0.          0.          0.          00001160
0.00204     0.00228     0.00231     0.00263                             00001170
0.1926      0.          0.          0.          0.          0.          00001180
0.00179     0.00226     0.00226     0.00258                             00001190
```

```
0.1567      0.          0.          0.          0.          0.          00001200
0.00191     0.00224     0.00225     0.00258                             00001210
0.09472     0.          0.          0.          0.          0.          00001220
0.00218     0.00225     0.00228     0.00259                             00001230
0.04491     0.          0.          0.          0.          0.00230     00001240
0.00231     0.00229     0.00234     0.00260                             00001250
0.01367     0.          0.          0.00070     0.00227     0.00232     00001260
0.00233     0.00234     0.00242     0.00263                             00001270
0.001967    0.          0.00131     0.00226     0.00231     0.00235     00001280
0.00238     0.00240     0.00246     0.00259                             00001290
0.00072     0.00223     0.00227     0.00230     0.00233     0.00234     00001300
0.00236     0.00237     0.00240     0.00245                             00001310
0.2921      0.2921      0.2921      0.2921      0.2921      0.2921      00001320
0.2921      0.2921      0.2921      0.2921      0.2921      0.2921      00001330
0.2921      0.2921      0.2921      0.2921      0.2921      0.2921      00001340
0.2921      0.2921      0.2921      0.2921      0.2921      0.2921      00001350
0.2921      0.2921      0.2921      0.2921      0.2921      0.2921      00001360
0.2921      0.2921      0.2921      0.2921      0.2921      0.2921      00001370
0.2921      0.2921      0.2921      0.2921      0.2921      0.2921      00001380
0.2921      0.2921      0.2921      0.2921      0.2921      0.2921      00001390
0.2921      0.2921                                                      00001400
0.254       0.254       0.254       0.254       0.254       0.254       00001410
0.254       0.254       0.254       0.254       0.254       0.254       00001420
0.254       0.254       0.254       0.254       0.254       0.254       00001430
0.254       0.254       0.254       0.254       0.254       0.254       00001440
0.254       0.254       0.254       0.254       0.254       0.254       00001450
0.254       0.254       0.254       0.254       0.254       0.254       00001460
0.254       0.254       0.254       0.254       0.254       0.254       00001470
0.254       0.254       0.254       0.254       0.254       0.254       00001480
0.254       0.254                                                       00001490
643.        643.        643.        643.        643.        643.        00001500
643.        643.        643.        643.        643.        643.        00001510
662.        662.        687.        687.        715.        763.        00001520
957.        1045.       1125.       1205.       1274.       1338.       00001530
1389.       1430.       1457.       1456.       1456.       1449.       00001540
1431.       1408.       1313.       1297.       1297.       1282.       00001550
1282.       1253.       1253.       1253.       1229.       1082.       00001560
1082.       1080.       1080.       1080.       1079.       1079.       00001570
1079.       1078.                                                       00001580
0.0         0.0         0.0         0.0         0.0         0.0         00001590
0.0         0.0         0.0         0.0         0.0         0.0         00001600
0.0         0.0         .0          0.0         0.0         0.0         00001610
0.0         0.0         0.0         0.0         .0          0.0         00001620
0.0         0.0         0.0         0.0         0.0         0.0         00001630
0.0         0.0         0.0         0.0         0.0         0.0         00001640
0.0         0.0         0.0         0.0         0.0         0.0         00001650
0.0         0.0         0.0         0.0         0.0         0.0         00001660
0.0         0.0                                                         00001670
643.        643.        643.        644.        644.        644.        00001680
644.        647.        647.        647.        647.        659.        00001690
659.        675.        675.        721.        775.        857.        00001700
973.        1052.       1125.       1195.       1257.       1312.       00001710
1356.       1389.       1407.       1432.       1430.       1424.       00001720
1410.       1377.       1315.       1297.       1287.       1278.       00001730
1268.       1296.       1249.       1240.       1254.       1256.       00001740
1230.       1230.       1230.       1216.       1216.       1216.       00001750
1209.       1209.                                                       00001760
0.          0.          0.          0.          0.          0.          00001770
0.          0.          0.          0.          0.          0.          00001780
0.          0.          0.          0.          0.          0.          00001790
```

```
0.          0.          0.          0.          0.          0.          00001800
0.          0.          -.624       -.1094      -.1064      -.1098      00001810
-.1129      -.1171      -.1234      -.1245      -.1245      -.1243      00001820
-.1235      -.1919      -.1298      -.1268      -.4313      0.          00001830
0.          0.          0.          0.          0.          0.          00001840
0.          0.                                                          00001850
-498.       -498.       -498.       -498.       -498.       -498.       00001860
-498.       -498.       -498.       -498.       -498.       -499.       00001870
-500.       -501.       -502.       -506.       -513.       -523.       00001880
-539.       -555.       -568.       -581.       -594.       -606.       00001890
-616.       -624.       -624.       -310.       0.          0.          00001900
0.          0.          0.          0.          0.          0.          00001910
0.          1291.       1291.       0.          338.        731.        00001920
782.        778.        778.        776.        775.        775.        00001930
774.        773.        773.                                            00001940
0.          0.          0.          0.          0.          0.          00001950
0.          0.          0.          0.          0.          2025.       00001960
2025.       2025.       2506.       3995.       5052.       18484.      00001970
50285.      58715.      66532.      73847.      78690.      81883.      00001980
83337.      83034.      80993.      77266.      71960.      65265.      00001990
57471.      48281.      7589.       2628.       2072.       1471.       00002000
1427.       0.          0.          0.          0.          0.          00002010
0.          0.          0.          0.          0.          0.          00002020
0.          0.                                                          00002030
```

number of cells in the interaction zone is greater than 1000, NDIV is automatically halved until the product is less than 1000. NDIV must therefore be appropriate for the number of cells anticipated in the interaction zone and for MAXPRT. In this case the number chosen was 10.

The third card group begins with instructions for printing the output. INTP0 is set to give print-outs at every 10 time steps. INTP01 is set so the option is ignored. IPR10 is 0 for no output on unit 10. IPLOT and IPCYCL are each 0 since no plot data is desired. IOPT1 is -1, indicating that the geometry of the pin molten fuel cavity is calculated from the fully molten cells indicated in the data. A search is made over the r-z mesh in the fuel pin and, at each axial cell, the number of radial subcells which have fully satisfied the heat of fusion is determined. This number of subcells divided by NPRAD is multiplied by the cross-sectional area of each axial cell to give the molten fuel area. A prototypical fast-reactor radial power profile which peaks in the center of the pin is assumed; there is no provision for other power shapes which may exist in certain experiments, e.g., those with thermal spectra. The other option for IOPT1 is simply to read in the molten fuel cavity areas for each axial cell. IOPT2 is set to -1 since the temperatures in each axial cell in the molten fuel cavity are computed from a mass-weighted average over the fully molten radial subcells and all the temperatures in the r-z mesh are provided. The other option for IOPT2 is simply to read in the cavity cell temperatures. IOPT3 is set to -1 since the mass of fuel in every r-z cell is specified. The smear density of each axial cell in the molten fuel cavity is formed by summing the masses in each radial cell and dividing by the volume of the cavity cell. Another option for IOPT3 is to specify the radius of a central void space for each axial cell in the cavity. This specifies the total void in the axial cavity cell, and the rest of the volume in the cavity cell is assumed to be filled by fuel at the density specified in the input. This amount of fuel is then spread over the whole cell volume to provide the smear density for the cavity cell. The last option for IOPT3 is to read in one void fraction for all molten fuel cavity cells. The smear density for all cavity cells is then simply 1 minus the void fraction times the full density specified later. IOPT4 is set to -1 since the mass ratios of fission gas to fuel are specified for all r-z cells as well as the fuel mass. The fission gas mass is merely summed over the fully molten radial subcells for each axial cell. Another option for IOPT4 is to read in fission gas to fuel mass ratios which are constant radially in the cavity for each axial cavity cell. These are merely multiplied by the smear densities calculated for the fuel to obtain the fission gas smear densities for each axial cell. The last option for IOPT4 is to read in only one value for the fission gas to fuel mass ratio and use this as in the preceeding option but for all axial cells. IOPT5 is set to 1 since irradiated fuel is modeled and fuel vapor pressure is expected to play a less important role in fuel ejection. IOPT5 would have been set to 0 for fresh fuel or if fuel vapor pressure was expected to become important in the course of the calculation. For example, a fuel pin could fail and expel fuel mainly on fission gas pressure and due to a power increase or simply to a dissipation of fission gas pressure, fuel vapor pressure could become relatively more important after the initial part of the calculation.

In card group 4, IOPT6 is set to 8 because the clad failure is intended to extend during the transient to axial cells which have at least 8 radial subcells fully molten (corresponding to a fuel melt fraction greater than 80% since NPRAD is 10 and since the remaining radial cells will be partially molten when

8 are fully molten). Another option for IOPT6 is to set it to -1 if a subroutine called RIPEXT is provided for determining the extension of the clad failure as a function of time. If IOPT6 is set to 0, no extension is allowed. IOPT7 is set to 1 since saturation pressure conditions (according to coolant channel temperatures) are assumed in the coolant channel cells prior to pin failure. The other option is to set IOPT7 to 0, and set all the coolant channel cell pressures in the input. IOPT8 is set to 0 since no reactivity worths are read in. If IOPT8 and IOPT9 were non-zero, worths would be read in for fuel and sodium and a reactivity calculation would be done. The interpretation of the reactivities is up to the user. The worths may correspond to a single pin, a subassembly, several subassemblies, etc. The cells for which the worths are input are entirely arbitrary and can be any set of cells in the mesh.

Card group 5 specifies the extent of the initial failure. IIFAIL specifies the number of failure cells. IFAIL is the array containing the failure cell numbers in increasing order. Note that the failure cells need not be contiguous and any cell may be a failure cell so long as the cell is part of the molten fuel cavity in the pin.

DELZ, the Eulerian cell height, begins card group 6. DELZ was chosen for this case so that an integral number of cells will exactly span the length of the molten fuel cavity in the fuel pin. Also DELZ should not be too long because the detail of the calculation would be lost or too short because the calculation run time will become excessive unless the latter is not important. ZPART is the DPIC particle length expressed as a fraction of DELZ. ZPART may be any number from 0 to 0.9 (the value zero reduces it to a simple particle-in-cell technique). It has been found in practice, however, that a value of about 0.5 gives the best results in most cases. HLPLEN is the height of the lower free surface which would typically be the subassembly inlet, where the 0.0 location is always set at the bottom of the channel mesh. Since the coolant channel mesh was chosen to reach almost from the subassembly inlet to the outlet, the location of the inlet from the bottom of the mesh is less than a cell length and HLPLEN is -6.55 cm. Likewise, the position of the upper free surface (which is typically the subassembly outlet), HUPLEN, is at 366.85 cm, only about 5 cm above the top of the coolant channel mesh at 361.98 cm. The location of the lower slug interface, FCIL2, is at 194.74 in cell 27 as can be seen from Fig. 2. The location of the upper slug interface, FCIU2, is at 293.06 in cell 40. The meaning of these interfaces is that above the upper interface and below the lower interface is single phase liquid at least until a two-phase region might intervene between the interface and the end of the channel. In this case there are no intervening two-phase regions and there is single-phase sodium from the upper interface to the subassembly outlet and from the subassembly inlet to the lower interface. In between the interfaces is a region of two-phase sodium which is treated with homogeneous flow. The liquid sodium in this region may originate from small slugs of liquid sodium, from sodium film (which is not treated at present in EPIC) or from liquid droplets suspended in the coolant channel; but whatever the original configuration of the liquid sodium may be in the two-phase region before the EPIC input is prepared, it is treated with homogeneous flow in EPIC and all the liquid sodium in a cell is homogenized and treated in the same way.

Card group 7 specifies the time step control DELT1 (in this case 0.0001 s) is the time step from t=0 to t=TIME01 (in this case 0.02 s). DELT2 (in this case 0.0002 s) is the time step between TIME02 and TIME03 (0.04 s and 1.0 s in

this case). Between TIME01 and TIME02, the time step is varied linearly from DELT1 to DELT2. DELT3 (in this case 0.0002 s) is the time step after TIME04 (next card group) and between TIME03 and TIME04, the time step is varied linearly from DELT2 to DELT3 (which are both the same in this case). These time step specifications are upper limits on the time step. The time step is set to these values by default but the time step calculated will be reduced according to the Courant condition (20% of local material velocities) and according to the necessity to repeat time steps (for example, when overcompacted cells force this).

In card group 8, after TIME04, the maximum problem time is specified (0.05 s in this case). EXTIME (0.02 s here) is the time into the transient after which the semi-implicit differencing in time is dispensed with and replaced with a strictly explicit scheme (which is equivalent to completing only the first step of the two-step semi-implicit method). PTIME1 and PTIME2 are used if detailed printout (every time step and twice every time step if the differencing in time is semi-implicit) is desired for a particular part of the calculation. POINT is an alternative method of specifying the frequency of print-outs so that not only a number of time steps can be specified between print-outs but a time interval can be specified (this option as well as the previous detailed print-out option were not used in this calculation and the times were set outside the time limits of the problem).

PLINT begins card group 9. This specifies a time interval such that at multiples of this interval (as well as at t=0) fuel density plot data for pin and channel will be included in the plot data written out. These data are to provide input for a plotting program to be run later (in this calculation the option isn't used). TMELT begins the specification of fuel material properties. No variation in temperature is allowed between the liquidus and the solidus. A function (specified in Appendix B) determines the physical density used for molten fuel which is held constant throughout the calculation. Input for the function is a temperature which the user selects as a reasonable average value over the transient. This constant density is not only used in the fuel pin cavity but for all channel fuel as well, even when the channel fuel freezes. The heats of vaporization and fusion as well as a gas constant for fuel vapor (used when calculating fuel vapor densities) are also specified on card group 9.

Card group 10 begins with the specific heat and thermal conductivity for liquid fuel (the latter is used in the FCI heat transfer). The fuel viscosity is used in the momentum equation in the pin cavity. The fuel vapor condensation coefficient is used in the coolant channel and must be understood as a lumped parameter. The value of this parameter can be varied over a very wide range given the uncertainty in characterizing the phenomenon. There is an automatic cutoff on fuel vapor condensation when the channel fuel temperature is below 3800°K, approximately the atmospheric boiling point of fuel. Since fuel vapor condensation was not expected to play a large a role in this calculation, the coefficient was set to zero. RPART is the constant fragmented fuel particle radius used for the fuel-coolant heat transfer as well as the drag formulation for the fuel particles throughout the calculation. It should be considered as a lumped parameter. FFCI is an arbitrary multiplier on the fuel-coolant heat transfer so that the fuel-coolant heat transfer term can be varied abitrarily without varying anything else (for example, if RPART were varied instead both the heat transfer and drag would be affected). This term can model such

phenomena as convective and surface (i.e., contact and vapor blanketing) effects on heat transfer.

The first thing specified on card group 11 is the heat transfer coefficient between cladding and liquid sodium. This is multified by the liquid volume fraction in the cell where it is used. The compressibility of liquid sodium and the speed of sound in liquid sodium, specified next, are constants throughout the calculation. The sodium vapor condensaton coefficient should be viewed as a lumped parameter like the fuel vapor condensation coefficient. The value used is derived from experimental data but may have significant uncertainty. The viscosity of sodium liquid is used in the drag formulation for the liquid slugs in the channel as well as for the effective viscosity of the two-phase sodium and fission gas mixture in the channel. On the average a number corresponding to relatively high void fraction two-phase sodium is most appropriate here.

The values of the hydraulic diameters of the lower and upper sodium slugs from the ends of the coolant mesh to the lower and upper free surfaces in the channel begin card group 12. RAF and RBF are the coefficient and exponent, respectively, of the Reynold's number appropriate for the single-phase sodium liquid slugs and the fuel/fission gas froth in the fuel pin cavity. RAM and RBM are for the homogeneous flow treatment of the two-phase sodium and fission gas mixture in the coolant channel.

Card group 13 begins with the pressures of the lower and upper free surfaces (typically the subassembly inlet and outlet) which serve as boundary values for the momentum equations in the coolant channel. These pressures are held constant throughout the calculation and therefore some average value may be appropriate. For instance, the inlet pressure may change over the transient and the effective orifice resistance (ΔP) to lower slug expulsion may change with the variation in lower slug velocity. The temperatures of the liquid sodium at the ends of the coolant channel mesh are specified next. Next the area ACLEND of the coolant channel between the lower end of the coolant mesh and the lower free surface (HLPLEN) and the area ACUEND of the coolant channel between the upper end of the coolant mesh and the upper free surface (HUPLEN) are specified.

Card group 14 concerns the cladding, whose heat of fusion, density, specific heat and melting temperature are specified. Next the gap conductance is specified between the fuel outer surface and the cladding inner surface. First a conductance is specified when the outermost radial subcell in the fuel is solid and secondly, the conductance is specified for the case when the molten fuel cavity has reached the cladding.

Card group 15 requires two pieces of data: the gas constant used in the ideal gas treatment of fission gas pressure and the volume fraction of coolant which is used below in card group 30 to calculate coolant flow areas.

Card group 16 specifies the fuel outer radius. RFOUT, in this case is the same for all axial cells. RFOUT determines the total fuel cross sectional area. The cross section is then divided into concentric annuli of equal area to form NPRAD equal volume radial subcells. Note how the values are read in. There are 14 axial fuel cells from NPLC (19) to NPUC (32) and since there are 6 values per card maximum, 3 cards are needed with 2 values on the last card.

Card group 17 specifies the temperature of all the r-z cells when NPRAD > 0. In each axial cell which contains any fully molten radial subcells, the temperature of the axial cell in the molten fuel cavity is the mass-weighted average of the temperatures specified in the TFUPRZ array for the fully molten radial subcells (only if IOPT2 = -1 as it is in this case). If IOPT2 = 0, the TFUPRZ values in the molten fuel cavity cells are not used and the radially homogenized molten fuel cavity cell temperatures are read in directly to the TFUP2 array below. Note how the TFUPRZ values are read in. Beginning with node NPLC (19), NPRAD (10) values are read on as many cards (6 per card) as necessary (in this case 2 cards per axial cell with 6 on the first card and 4 on the second). After each group of NPRAD temperatures are read for an axial cell, the values for the next axial cell begin on the next card. Therefore the total number of cards in this case needed to read in the TFUPRZ array is $14 \times 2 = 28$ cards (using the formula, $(NPUC-NPLC+1) \times I\{NPRAD/6\}$, $(32-19+1) \times I\{10/6\} = 14 \times 2 = 28$).

Card group 18 specifies the heat of fusion array, HFPRZ, for the r-z mesh. These values are read like the TFUPRZ array and only if NPRAD > 0. This array specifies the extent of the molten fuel cavity which is defined as the sum of all r-z cells having fully satisfied the heat of fusion (HFPRZ = 1.0). Thus, in this case, axial cell 22 has 2 fully molten radial subcells, 23 has 4, to the last molten fuel cavity cell, 31, which has only 1 fully molten radial subcell. From inspection of the HFPRZ array, it can be seen that many additional subcells have the potential of melting into the molten fuel cavity, thus extending the cavity radially as well as axially.

Card group 19 specifies the GMPN array which gives the mass of fuel in every r-z cell when NPRAD > 0. This group is read like the previous 2 groups. If IOPT3 = -1, (as in this case), the fuel smear densities of the axial cells in the molten fuel cavity are determined by summing the masses in the fully molten radial subcells.

Card group 20 is read only if NPRAD > 0 and if IOPT4 = -1, as they are in this case. It is read like the previous 3 groups. FGFUF is the ratio of fission gas mass to fuel mass in every r-z cell in the fuel mesh. This is used to specify not only the amount of fission gas in the molten fuel cavity, but also the amount in each solid fuel cell which instantly becomes available for pressurization when the solid fuel subcell melts into the cavity. The mass of fission gas in each r-z cell is the product of FGFUF and GMPN for each cell. In this case, it was not known at the time of pin failure how the fission gas in the molten fuel cavity was distributed radially, but only that a certain amount of fission gas was located in a certain axial cell in the cavity. In each axial cell in the cavity therefore, all the fission gas was put in the first radial subcell and the remaining radial subcells in the cavity have FGFUF = 0. Thus FGFUF can be used in this fashion to specify the amount of fission gas in the cavity as well as by a radial subcell by radial subcell specification.

Card group 21 is not used in this case because IOPT2 = -1. If IOPT2 = 0, the TFUP2 array specifying the radially homogenized temperatures in each axial cell in the molten fuel cavity are read directly.

Card group 22 is not read in this case since IOPT1 = -1 and the cross-sectional area of each axial cell in the molten fuel cavity is computed from

the number of radial subcells in the cavity and RFOUT as explained above. Card group 22 would be read if IOPT1 was 0, in which case the calculation of cross-sectional areas as with the IOPT1 = -1 option would not be done and the cross-sectional areas of each axial cell in the cavity would be read in directly. It would be up to the user, however, to make certain that these cross-sectional areas were compatable with the r-z mesh as computed from RFOUT in the case where NPRAD > 0.

Card group 23 is also not read since IOPT4 = -1. When IOPT4 = 1, one value of the ratio of fission gas mass to fuel mass is read and used for all r-z cells.

Likewise, card group 24 is not read, but when IOPT4 = 0, the mass ratio is read such that each axial cell has its own mass ratio which is the same in each radial subcell at that axial level.

Card group 25 is not read since IOPT3 = -1 and in the given case, the fuel smear density is calculated from the geometry of the r-z mesh and the sums of GMPN for each axial cell. If IOPT3 = 1, then a single void fraction is read here such that the fuel smear density in all axial molten fuel cavity cells is simply the theoretical density of the fuel times one minus this void fraction.

Card group 26 is also not read since IOPT3 = -1. If IOPT3 = 0, then a radius of a region assumed to be void is read in for each axial cell in the molten fuel cavity. The rest of the axial cell in the cavity is assumed to be full density fuel and the smear density is computed accordingly.

Card group 27 specifies the outer cladding radius, RCL, for each axial cell in the coolant channel. These are used to calculate the coolant flow area (see card group 30). RCL is also used to compute the area of the clad wall available for condensation.

Card group 28 specifies the cladding inner radius, RCIN, for each axial cell. RCIN is only used to calculate the cladding volume and the surface area available for heat transfer between fuel and cladding.

Card group 29 specifies the initial cladding temperature for each axial cell in the channel.

Card group 30 specifies the coolant flow areas, AC2, for cells NCL to NCL. When the value of AC2 is positive, then it is the flow area which is specified. When the value of AC2 is 0.0 (as it is for all the cells in this case), then the coolant flow area for that cell is $VFC \cdot \pi \cdot RCL \cdot RCL/(1.0-VFC)$. When the value of AC2 is negative for a cell, then the flow area is $-AC2 \cdot \pi \cdot RCL \times RCL/(1.0+AC2)$ for that cell. RCL is the value for the cell being calculated, of course.

Card group 31 specifies the sodium temperature in every axial cell. In cells with no void fraction, it is the liquid sodium temperature. In cells with two-phase sodium, since saturation conditions are always assumed, the temperature specified is for the liquid and vapor.

Card group 32 specifies the void fraction in each coolant channel cell so that the liquid smear density is the theoretical density of liquid sodium at

the temperature specified for a cell times one minus the void fraction specified. The vapor density is calculated from the void fraction at any given time during the calculation; an ideal gas formulation for the vapor pressure and saturation pressure conditions are assumed. As an alternative to specifying the void fraction for each axial cell, the density itself may be specified by putting in the negative of the density. This may be done in any or all axial cells. In the given case, this latter option is used in the cells with two-phase sodium. In the single-phase cells, the zero values are interpreted as void fractions since they are non-negative. It must be noted that in interface cells, the smear density of sodium is computed by dividing the mass of sodium in the two-phase portion of the cell only by the total volume of the cell, not by the partial cell volume.

Card group 33 is not read since IOPT7 = 1. This option sets the pressure in each coolant channel cell equal to the saturation pressure corresponding to the sodium temperature read in. If IOPT7 = 0, the pressure of each axial coolant channel cell will be read in.

Card group 34 specifies the cell-edge velocities for the coolant channel cells. The value specified at cell I is for the bottom of cell I and therefore (NCU-NCL+2) values must be given, since the last value specified will be for the top of cell NCU.

Card group 35 specifies the axial power shape for the fuel in terms of watts per gram of fuel at each axial cell for the whole coolant channel. This is simply the steady-state value (with fuel in the original configuration) times whatever normalization factor is desired. Note that the power function built into the code provides a factor by which WPGM is multiplied at any given point during the transient. This factor should be taken into account in the initial specification of WPGM. In the case given here, a normalization factor of 439 has been applied to the steady state values of watts per gram since this is the value of normalized power at pin failure.

Card groups 36, 37 and 38 are not specified since no reactivity calculation is requested (IOPT8 = 0). The data specification is self-explanatory but it should be noted that the worths are to be interpreted by the user in terms of how many pins the worths represent.

The function YFACF was programmed to model the no-slip condition between fission gas and fuel (YFAC = 1.0 and YFAC1 = 1.0). The function PHIT was programmed to give the following power function, (a normalized power level of 439 times nominal power at t = 0 was assumed); a linear increase to 775 times nominal at 0.0016 sec; a linear decrease to 1.0 at 0.005 sec; and a further linear decrease to 0.1 at 0.05 sec, the maximum problem time.

5.2 Description of Output of Sample Problem

There is first a simple listing of all card input. Next the input is displayed in edited form with a verbal description for each item. The first page of this edit gives the fixed point input including all options. The second page displays the floating point data, excluding arrays, including geometry data and material properties. Next, power, reactivity worths, etc.,

```
 SAMPLE PROBLEM FOR LOF-TOP CONDITIONS
INITIALLY 2 FAILURE CELLS, PARTIALLY VOIDED CHANNEL, NORM. POWER AT 439


NUMBER OF LOWEST CELL IN FUEL MESH     19
NUMBER OF LOWEST CELL IN PIN CAVITY    22
NUMBER OF HIGHEST CELL IN PIN CAVITY    31
NUMBER OF HIGHEST CELL IN FUEL MESH    32
NUMBER OF RADIAL CELLS IN FUEL PIN     10
NUMBER OF LOWEST CELL IN COOLANT CHANNEL      1
NUMBER OF HIGHEST CELL IN COOLANT CHANNEL    50

MAXIMUM NUMBER OF PARTICLE GROUPS   200
NUMBER OF FUEL PARTICLES PER PARTICLE GROUP   100
NUMBER OF CELL DIVISIONS FOR PARTICLE RECOMBINATION     10

NUMBER OF TIME STEPS BETWEEN PRINT OUTS     10
IF THIS NUMBER IS ZERO, PRINT TWICE EVERY TIME STEP      1
IF THIS NUMBER IS NONZERO, UNIT NUMBER FOR PLOTTING      0
NUMBER OF TIME STEPS BETWEEN PLOTTING DATA WRITEOUTS      0
IF THIS NUMBER IS NONZERO, WRITE RESULTS ON UNIT 10      0

IF THIS NUMBER IS 0, READ IN AREAS OF PIN CELLS
IF -1,AREAS ARE CALCULATED FROM R-Z MESH AS INPUT    -1

IF THIS NUMBER IS 0, READ IN PIN CELL TEMPERATURES
IF -1, TEMPERATURES ARE CALCULATED FROM R-Z MESH     -1

IF -1, FUEL SMEAR DENSITY IN PIN CALCULATED FROM GMPN
IF 0, READ RADIUS OF CENTRAL VOID IN PIN CELLS
IF 1, USE ONE VOID FRACTION IN ALL PIN CELLS    -1

IF -1, FISSION GAS DENSITY CALCULATED FROM R-Z MESH
IF 0, READ FISS. GAS MASS RATIO FOR ALL PIN CELLS
IF 1, READ ONE NUMBER FOR ALL CELLS     -1

IF 0, FUEL EJECTION DRIVEN MAINLY BY FUEL VAPOR
IF 1, FUEL EJECTION DRIVEN MAINLY BY FISSION GAS      1

IF 0, READ IN ALL CHANNEL PRESSURES
IF 1, CALCULATE CHANNEL PRESSURES FROM PSAT(TNA)      1

IF 0, NO CLAD RIP EXTENSION DURING TRANSIENT
IF -1, USE PROGRAMMED SCHEME IN CODE
IF NONZERO, NUMBER OF RADIAL CELL WHICH MUST BE FULLY
   MOLTEN TO FAIL CLAD AT ANY AXIAL CELL      8

IF ZERO, NO REACTIVITY WORTHS ARE READ IN
IF POSITIVE, NUMBER OF LOWER CELL FOR REACTIVITY MESH      0

IF NONZERO, UPPER CELL FOR REACTIVITY MESH      0
```

```
EULERIAN CELL WIDTH (CM)    7.23953D 00
COOLANT VOLUME FRACTION (CONSTANT)    4.27100D-01
HEIGHT OF UPPER FREE SURFACE (CM)    3.66850D 02
HEIGHT OF LOWER FREE SURFACE (CM)    -6.54700D 00
HEIGHT OF FCI ZONE - SLUG TOP INTERFACE (CM)    2.93060D 02
HEIGHT OF FCI ZONE-SLUG BOTTOM INTERFACE(CM)    1.94740D 02

INITIAL TIME STEP (SEC)    1.00000D-04
SECOND TIME STEP (SEC)    2.00000D-04
THIRD TIME STEP (SEC)    2.00000D-04
FIRST TIME STEP LIMIT (SEC)    2.00000D-02
SECOND TIME STEP LIMIT (SEC)    4.00000D-02
THIRD TIME STEP LIMIT (SEC)    1.00000D 00
FOURTH TIME STEP LIMIT (SEC)    1.00000D 00
MAXIMUM PROBLEM TIME (SEC)    5.00000D-02
TIME TO SWITCH TO EXPLICIT DIFFERENCING (SEC)    2.00000D-02
TIME TO INITIATE FULL PRINTOUTS (SEC)    1.00000D 00
TIME TO END FULL PRINTOUTS (SEC)    1.00000D 00
TIME INTERVAL FOR PRINTOUTS, IF NONZERO (SEC)    1.00000D 00
TIME INTERVAL FOR FUEL DENSITY PLOTS (SEC)    1.00000D 00

FUEL PARTICLE RADIUS (CM)    3.00000D-02
MOLTEN FUEL DENSITY COMPUTED AT TEMPERATURE (K)    3.53680D 03
MOLTEN FUEL DENSITY (GMS/CC)    8.49997D 00
HEAT OF FUSION FOR FUEL (ERGS/GM)    2.75000D 09
FUEL THERMAL CONDUCTIVITY (ERGS/CM-SEC-K)    3.50000D 05
FUEL SPECIFIC HEAT (ERGS/GM-K)    5.03200D 06
FUEL MELTING TEMPERATURE (K)    3.07000D 03
HEAT OF VAPORIZATION FOR FUEL (ERGS/GM)    2.00000D 10
GAS CONSTANT FOR FUEL VAPOR (ERGS/GM-K)    3.07900D 05
ABSOLUTE FUEL VISCOSITY (GMS/SEC-CM)    4.00000D-02

SODIUM COMPRESSIBILITY (CM**2/DYNE)    5.00000D-11
SPEED OF SOUND IN SODIUM LIQUID (CM/SEC)    2.50000D 05
ABSOLUTE VISCOSITY OF LIQUID SODIUM (GM/SEC-CM)    2.00000D-03

COEFFICIENT OF REYNOLDS NUMBER IN SODIUM LIQUID AND  PIN CAVITY    1.87500D-01
EXPONENT OF REYNOLDS NUMBER IN SODIUM LIQUID AND IN PIN CAVITY   -2.00000D-01
COEFFICIENT OF REYNOLDS NUMBER FOR 2-PHASE SODIUM    3.16000D-01
EXPONENT OF REYNOLDS NUMBER FOR 2-PHASE SODIUM   -2.50000D-01

MULTIPLICATIVE FACTOR ON FCI HEAT TRANSFER    1.00000D 00
SODIUM VAPOR CONDENSATION COEFFICIENT (ERGS/K-SEC-CM**2)    6.00000D 07
SODIUM LIQUID HEAT TRANSFER COEFFICIENT (ERGS/K-SEC-CM**2)    7.00000D 07

PRESSURE IN LOWER PLENUM (DYNES/CM**2)    2.86700D 06
PRESSURE IN UPPER PLENUM (DYNES/CM**2)    1.67600D 06
TEMPERATURE BELOW COOLANT MESH (K)    6.43100D 02
TEMPERATURE ABOVE COOLANT MESH (K)    1.20900D 03
HYDRAULIC DIAMETER BELOW COOLANT MESH (CM)    4.36000D-01
HYDRAULIC DIAMETER ABOVE COOLANT MESH (CM)    4.36000D-01
FLOW AREA BELOW COOLANT MESH (CM**2)    2.00000D-01
FLOW AREA ABOVE COOLANT MESH (CM**2)    2.00000D-01

HEAT OF FUSION FOR CLADDING (ERGS/GM)    2.64000D 09
CLADDING DENSITY (GM/CC)    7.40000D 00
CLADDING SPECIFIC HEAT (ERGS/GM-K)    6.50000D 06
CLADDING MELTING TEMPERATURE (K)    1.70000D 03
GAP CONDUCTANCE FROM SOLID FUEL (ERGS/K-SEC-CM**2)    1.00000D 07
GAP CONDUCTANCE FROM MOLTEN FUEL (ERGS/K-SEC-CM**2)    3.00000D 07
```

GAS CONSTANT FOR FISSION GAS (ERGS/GM-K) 6.59000D 05
LENGTH OF DPIC PARTICLE GROUP (CM) 3.61977D 00
ABSOLUTE VISCOSITY FOR 2-PHASE SODIUM/FISSION GAS (GM/SEC-CM) 2.00000D-04
FUEL VAPOR CONDENSATION COEFFICIENT(ERGS/K-SEC-CM**2) 0.0

AXIAL CELL	NODAL POWER W/GM FUEL	STEADY STATE NA TEMP.(K)	COOLANT WORTH DK/KG*10**5	FUEL WORTH DK/KG*10**5	INITIAL CHAN. VOID FRACTION	OUTER RADIUS OF CLADDING	INNER RADIUS OF CLADDING	NODAL AREA IN CHANNEL
50	0.0	0.0	0.0	0.0	0.0	2.92100D-01	2.54000D-01	1.99831D-01
49	0.0	0.0	0.0	0.0	0.0	2.92100D-01	2.54000D-01	1.99831D-01
48	0.0	0.0	0.0	0.0	0.0	2.92100D-01	2.54000D-01	1.99831D-01
47	0.0	0.0	0.0	0.0	0.0	2.92100D-01	2.54000D-01	1.99831D-01
46	0.0	0.0	0.0	0.0	0.0	2.92100D-01	2.54000D-01	1.99831D-01
45	0.0	0.0	0.0	0.0	0.0	2.92100D-01	2.54000D-01	1.99831D-01
44	0.0	0.0	0.0	0.0	0.0	2.92100D-01	2.54000D-01	1.99831D-01
43	0.0	0.0	0.0	0.0	0.0	2.92100D-01	2.54000D-01	1.99831D-01
42	0.0	0.0	0.0	0.0	0.0	2.92100D-01	2.54000D-01	1.99831D-01
41	0.0	0.0	0.0	0.0	3.91976D-01	2.92100D-01	2.54000D-01	1.99831D-01
40	0.0	0.0	0.0	0.0	8.21978D-01	2.92100D-01	2.54000D-01	1.99831D-01
39	0.0	0.0	0.0	0.0	8.17284D-01	2.92100D-01	2.54000D-01	1.99831D-01
38	0.0	0.0	0.0	0.0	7.26054D-01	2.92100D-01	2.54000D-01	1.99831D-01
37	1.42700D 03	0.0	0.0	0.0	8.25172D-01	2.92100D-01	2.54000D-01	1.99831D-01
36	1.47100D 03	0.0	0.0	0.0	8.23514D-01	2.92100D-01	2.54000D-01	1.99831D-01
35	2.07200D 03	0.0	0.0	0.0	8.22752D-01	2.92100D-01	2.54000D-01	1.99831D-01
34	2.62800D 03	0.0	0.0	0.0	8.22217D-01	2.92100D-01	2.54000D-01	1.99831D-01
33	7.58900D 03	0.0	0.0	0.0	8.22820D-01	2.92100D-01	2.54000D-01	1.99831D-01
32	4.82810D 04	0.0	0.0	0.0	8.28585D-01	2.92100D-01	2.54000D-01	1.99831D-01
31	5.74710D 04	0.0	0.0	0.0	8.32974D-01	2.92100D-01	2.54000D-01	1.99831D-01
30	6.52650D 04	0.0	0.0	0.0	8.36817D-01	2.92100D-01	2.54000D-01	1.99831D-01
29	7.19600D 04	0.0	0.0	0.0	8.41559D-01	2.92100D-01	2.54000D-01	1.99831D-01
28	7.72660D 04	0.0	0.0	0.0	8.36984D-01	2.92100D-01	2.54000D-01	1.99831D-01
27	8.09930D 04	0.0	0.0	0.0	7.77391D-02	2.92100D-01	2.54000D-01	1.99831D-01
26	8.30340D 04	0.0	0.0	0.0	0.0	2.92100D-01	2.54000D-01	1.99831D-01
25	8.33370D 04	0.0	0.0	0.0	0.0	2.92100D-01	2.54000D-01	1.99831D-01
24	8.18830D 04	0.0	0.0	0.0	0.0	2.92100D-01	2.54000D-01	1.99831D-01
23	7.86920D 04	0.0	0.0	0.0	0.0	2.92100D-01	2.54000D-01	1.99831D-01
22	7.38470D 04	0.0	0.0	0.0	0.0	2.92100D-01	2.54000D-01	1.99831D-01
21	6.65320D 04	0.0	0.0	0.0	0.0	2.92100D-01	2.54000D-01	1.99831D-01
20	5.87150D 04	0.0	0.0	0.0	0.0	2.92100D-01	2.54000D-01	1.99831D-01
19	5.02850D 04	0.0	0.0	0.0	0.0	2.92100D-01	2.54000D-01	1.99831D-01
18	1.84840D 04	0.0	0.0	0.0	0.0	2.92100D-01	2.54000D-01	1.99831D-01
17	5.05200D 03	0.0	0.0	0.0	0.0	2.92100D-01	2.54000D-01	1.99831D-01
16	3.99500D 03	0.0	0.0	0.0	0.0	2.92100D-01	2.54000D-01	1.99831D-01
15	2.50600D 03	0.0	0.0	0.0	0.0	2.92100D-01	2.54000D-01	1.99831D-01
14	2.02500D 03	0.0	0.0	0.0	0.0	2.92100D-01	2.54000D-01	1.99831D-01
13	2.02500D 03	0.0	0.0	0.0	0.0	2.92100D-01	2.54000D-01	1.99831D-01
12	2.02500D 03	0.0	0.0	0.0	0.0	2.92100D-01	2.54000D-01	1.99831D-01
11	0.0	0.0	0.0	0.0	0.0	2.92100D-01	2.54000D-01	1.99831D-01
10	0.0	0.0	0.0	0.0	0.0	2.92100D-01	2.54000D-01	1.99831D-01
9	0.0	0.0	0.0	0.0	0.0	2.92100D-01	2.54000D-01	1.99831D-01
8	0.0	0.0	0.0	0.0	0.0	2.92100D-01	2.54000D-01	1.99831D-01
7	0.0	0.0	0.0	0.0	0.0	2.92100D-01	2.54000D-01	1.99831D-01
6	0.0	0.0	0.0	0.0	0.0	2.92100D-01	2.54000D-01	1.99831D-01
5	0.0	0.0	0.0	0.0	0.0	2.92100D-01	2.54000D-01	1.99831D-01
4	0.0	0.0	0.0	0.0	0.0	2.92100D-01	2.54000D-01	1.99831D-01
3	0.0	0.0	0.0	0.0	0.0	2.92100D-01	2.54000D-01	1.99831D-01
2	0.0	0.0	0.0	0.0	0.0	2.92100D-01	2.54000D-01	1.99831D-01
1	0.0	0.0	0.0	0.0	0.0	2.92100D-01	2.54000D-01	1.99831D-01

FUEL MESH

RADIAL CELL	1	2	3	4	5	6	7	8	9	10

AXIAL CELL 32 OUTERMOST RADIAL CELL THAT IS FULLY MOLTEN 0 FUEL OUTER RADIUS (CM) 2.71680D-01

OUTER RADIUS	8.59128D-02	1.21499D-01	1.48805D-01	1.71826D-01	1.92107D-01	2.10442D-01	2.27304D-01	2.42998D-01	2.57738D-01	2.71680D-01
TOTAL AREA	2.31881D-02	4.63762D-02	6.95643D-02	9.27524D-02	1.15941D-01	1.39129D-01	1.62317D-01	1.85505D-01	2.08693D-01	2.31881D-01
TEMPERATURE	3.07000D 03	3.01700D 03	2.96800D 03	2.91900D 03	2.86800D 03	2.81200D 03	2.74400D 03	2.64600D 03	2.46200D 03	2.03200D 03
MELT FRACT.	4.92000D-02	0.0	0.0	0.0	0.0	0.0	0.0	0.0	0.0	0.0
MASS	1.29500D 00	1.30900D 00	1.31300D 00	1.31700D 00	1.32100D 00	1.32600D 00	1.33100D 00	1.33900D 00	1.35400D 00	6.25000D-01
F.G.MASS RAT	7.20000D-04	2.23000D-03	2.27000D-03	2.30000D-03	2.33000D-03	2.34000D-03	2.36000D-03	2.37000D-03	2.40000D-03	2.45000D-03

AXIAL CELL 31 OUTERMOST RADIAL CELL THAT IS FULLY MOLTEN 1 FUEL OUTER RADIUS (CM) 2.71680D-01

OUTER RADIUS	8.59128D-02	1.21499D-01	1.48805D-01	1.71826D-01	1.92107D-01	2.10442D-01	2.27304D-01	2.42998D-01	2.57738D-01	2.71680D-01
TOTAL AREA	2.31881D-02	4.63762D-02	6.95643D-02	9.27524D-02	1.15941D-01	1.39129D-01	1.62317D-01	1.85505D-01	2.08693D-01	2.31881D-01
TEMPERATURE	3.07000D 03	3.07000D 03	3.07000D 03	3.07000D 03	3.07000D 03	3.02000D 03	2.95000D 03	2.85700D 03	2.67200D 03	2.24000D 03
MELT FRACT.	1.00000D 00	5.11000D-01	3.31500D-01	1.82200D-01	2.54000D-02	0.0	0.0	0.0	0.0	0.0
MASS	1.11600D 00	1.37300D 00	1.25900D 00	1.27900D 00	1.29800D 00	1.30800D 00	1.31500D 00	1.32200D 00	1.33700D 00	8.63000D-01
F.G.MASS RAT	1.96700D-03	0.0	1.31000D-03	2.26000D-03	2.31000D-03	2.35000D-03	2.38000D-03	2.40000D-03	2.46000D-03	2.59000D-03

AXIAL CELL 30 OUTERMOST RADIAL CELL THAT IS FULLY MOLTEN 3 FUEL OUTER RADIUS (CM) 2.71680D-01

OUTER RADIUS	8.59128D-02	1.21499D-01	1.48805D-01	1.71826D-01	1.92107D-01	2.10442D-01	2.27304D-01	2.42998D-01	2.57738D-01	2.71680D-01
TOTAL AREA	2.31881D-02	4.63762D-02	6.95643D-02	9.27524D-02	1.15941D-01	1.39129D-01	1.62317D-01	1.85505D-01	2.08693D-01	2.31881D-01
TEMPERATURE	3.32400D 03	3.31500D 03	3.13200D 03	3.07000D 03	3.07000D 03	3.07000D 03	3.07000D 03	3.00000D 03	2.82600D 03	2.42200D 03
MELT FRACT.	1.00000D 00	1.00000D 00	1.00000D 00	7.29400D-01	5.08400D-01	3.03800D-01	1.00500D-01	0.0	0.0	0.0
MASS	4.66000D-01	1.42600D 00	1.43300D 00	1.47400D 00	1.43300D 00	1.26200D 00	1.28700D 00	1.31000D 00	1.32500D 00	1.04900D 00
F.G.MASS RAT	1.36700D-02	0.0	0.0	7.00000D-04	2.27000D-03	2.32000D-03	2.33000D-03	2.34000D-03	2.42000D-03	2.63000D-03

AXIAL CELL 29 OUTERMOST RADIAL CELL THAT IS FULLY MOLTEN 5 FUEL OUTER RADIUS (CM) 2.71680D-01

OUTER RADIUS	8.59128D-02	1.21499D-01	1.48805D-01	1.71826D-01	1.92107D-01	2.10442D-01	2.27304D-01	2.42998D-01	2.57738D-01	2.71680D-01
TOTAL AREA	2.31881D-02	4.63762D-02	6.95643D-02	9.27524D-02	1.15941D-01	1.39129D-01	1.62317D-01	1.85505D-01	2.08693D-01	2.31881D-01
TEMPERATURE	3.56700D 03	3.59600D 03	3.48100D 03	3.22000D 03	3.10000D 03	3.07000D 03	3.07000D 03	3.07000D 03	2.94700D 03	2.55500D 03
MELT FRACT.	1.00000D 00	1.00000D 00	1.00000D 00	1.00000D 00	1.00000D 00	7.29500D-01	4.41200D-01	1.35100D-01	0.0	0.0
MASS	1.75000D-01	1.40900D 00	1.42100D 00	1.45300D 00	1.45300D 00	1.44100D 00	1.33900D 00	1.28300D 00	1.31300D 00	1.17600D 00
F.G.MASS RAT	4.49100D-02	0.0	0.0	0.0	0.0	2.30000D-03	2.31000D-03	2.29000D-03	2.34000D-03	2.60000D-03

AXIAL CELL 28 OUTERMOST RADIAL CELL THAT IS FULLY MOLTEN 6 FUEL OUTER RADIUS (CM) 2.71680D-01

OUTER RADIUS	8.59128D-02	1.21499D-01	1.48805D-01	1.71826D-01	1.92107D-01	2.10442D-01	2.27304D-01	2.42998D-01	2.57738D-01	2.71680D-01
TOTAL AREA	2.31881D-02	4.63762D-02	6.95643D-02	9.27524D-02	1.15941D-01	1.39129D-01	1.62317D-01	1.85505D-01	2.08693D-01	2.31881D-01
TEMPERATURE	3.77700D 03	3.76600D 03	3.69200D 03	3.50500D 03	3.31200D 03	3.10100D 03	3.07000D 03	3.07000D 03	3.02600D 03	2.61600D 03
MELT FRACT.	1.00000D 00	1.00000D 00	1.00000D 00	1.00000D 00	1.00000D 00	1.00000D 00	7.22500D-01	3.47300D-01	0.0	0.0
MASS	8.90000D-02	1.39000D 00	1.39800D 00	1.41800D 00	1.44000D 00	1.46800D 00	1.44800D 00	1.27300D 00	1.30200D 00	1.23500D 00
F.G.MASS RAT	9.47200D-02	0.0	0.0	0.0	0.0	0.0	2.18000D-03	2.25000D-03	2.28000D-03	2.59000D-03

AXIAL CELL 27 OUTERMOST RADIAL CELL THAT IS FULLY MOLTEN 6 FUEL OUTER RADIUS (CM) 2.71680D-01

OUTER RADIUS	8.59128D-02	1.21499D-01	1.48805D-01	1.71826D-01	1.92107D-01	2.10442D-01	2.27304D-01	2.42998D-01	2.57738D-01	2.71680D-01
TOTAL AREA	2.31881D-02	4.63762D-02	6.95643D-02	9.27524D-02	1.15941D-01	1.39129D-01	1.62317D-01	1.85505D-01	2.08693D-01	2.31881D-01
TEMPERATURE	3.87900D 03	3.87100D 03	3.81000D 03	3.65800D 03	3.43100D 03	3.23500D 03	3.07000D 03	3.07000D 03	3.07000D 03	2.65600D 03
MELT FRACT.	1.00000D 00	1.00000D 00	1.00000D 00	1.00000D 00	1.00000D 00	1.00000D 00	9.04800D-01	4.98800D-01	1.62000D-02	0.0
MASS	5.60000D-02	1.37900D 00	1.38500D 00	1.40100D 00	1.42600D 00	1.44800D 00	1.48300D 00	1.28600D 00	1.29100D 00	1.29500D 00
F.G.MASS RAT	1.56700D-01	0.0	0.0	0.0	0.0	0.0	1.91000D-03	2.24000D-03	2.25000D-03	2.58000D-03

AXIAL CELL 26 OUTERMOST RADIAL CELL THAT IS FULLY MOLTEN 6 FUEL OUTER RADIUS (CM) 2.71680D-01

OUTER RADIUS	8.59128D-02	1.21499D-01	1.48805D-01	1.71826D-01	1.92107D-01	2.10442D-01	2.27304D-01	2.42998D-01	2.57738D-01	2.71680D-01
TOTAL AREA	2.31881D-02	4.63762D-02	6.95643D-02	9.27524D-02	1.15941D-01	1.39129D-01	1.62317D-01	1.85505D-01	2.08693D-01	2.31881D-01
TEMPERATURE	3.92900D 03	3.90700D 03	3.84600D 03	3.69000D 03	3.46800D 03	3.27700D 03	3.07000D 03	3.07000D 03	3.07000D 03	2.66500D 03
MELT FRACT.	1.00000D 00	1.00000D 00	1.00000D 00	1.00000D 00	1.00000D 00	1.00000D 00	9.71100D-01	5.49000D-01	5.13000D-02	0.0
MASS	4.60000D-02	1.37600D 00	1.38100D 00	1.39800D 00	1.42200D 00	1.44300D 00	1.47500D 00	1.29400D 00	1.28800D 00	1.32500D 00
F.G.MASS RAT	1.92600D-01	0.0	0.0	0.0	0.0	0.0	1.79000D-03	2.26000D-03	2.26000D-03	2.58000D-03

AXIAL CELL 25 OUTERMOST RADIAL CELL THAT IS FULLY MOLTEN 6 FUEL OUTER RADIUS (CM) 2.71680D-01

OUTER RADIUS	8.59128D-02	1.21499D-01	1.48805D-01	1.71826D-01	1.92107D-01	2.10442D-01	2.27304D-01	2.42998D-01	2.57738D-01	2.71680D-01
TOTAL AREA	2.31881D-02	4.63762D-02	6.95643D-02	9.27524D-02	1.15941D-01	1.39129D-01	1.62317D-01	1.85505D-01	2.08693D-01	2.31881D-01
TEMPERATURE	3.89100D 03	3.87300D 03	3.79800D 03	3.63900D 03	3.41500D 03	3.22500D 03	3.07000D 03	3.07000D 03	3.06100D 03	2.62600D 03
MELT FRACT.	1.00000D 00	1.00000D 00	1.00000D 00	1.00000D 00	1.00000D 00	1.00000D 00	8.85700D-01	4.74400D-01	0.0	0.0
MASS	6.20000D-02	1.37900D 00	1.38600D 00	1.40300D 00	1.42800D 00	1.44900D 00	1.48400D 00	1.27900D 00	1.29300D 00	1.29000D 00
F.G.MASS RAT	1.40800D-01	0.0	0.0	0.0	0.0	0.0	2.04000D-03	2.28000D-03	2.31000D-03	2.63000D-03

AXIAL CELL 24 OUTERMOST RADIAL CELL THAT IS FULLY MOLTEN 6 FUEL OUTER RADIUS (CM) 2.71680D-01

OUTER RADIUS	8.59128D-02	1.21499D-01	1.48805D-01	1.71826D-01	1.92107D-01	2.10442D-01	2.27304D-01	2.42998D-01	2.57738D-01	2.71680D-01
TOTAL AREA	2.31881D-02	4.63762D-02	6.95643D-02	9.27524D-02	1.15941D-01	1.39129D-01	1.62317D-01	1.85505D-01	2.08693D-01	2.31881D-01
TEMPERATURE	3.78600D 03	3.77400D 03	3.68500D 03	3.48700D 03	3.27500D 03	3.08300D 03	3.07000D 03	3.07000D 03	2.99300D 03	2.55100D 03
MELT FRACT.	1.00000D 00	1.00000D 00	1.00000D 00	1.00000D 00	1.00000D 00	1.00000D 00	6.71500D-01	2.99500D-01	0.0	0.0
MASS	9.40000D-02	1.39000D 00	1.39800D 00	1.42000D 00	1.44500D 00	1.47000D 00	1.46200D 00	1.26300D 00	1.30500D 00	1.22100D 00
F.G.MASS RAT	8.90300D-02	0.0	0.0	0.0	0.0	0.0	2.41000D-03	2.34000D-03	2.40000D-03	2.70000D-03

AXIAL CELL 23 OUTERMOST RADIAL CELL THAT IS FULLY MOLTEN 4 FUEL OUTER RADIUS (CM) 2.71680D-01

OUTER RADIUS	8.59128D-02	1.21499D-01	1.48805D-01	1.71826D-01	1.92107D-01	2.10442D-01	2.27304D-01	2.42998D-01	2.57738D-01	2.71680D-01
TOTAL AREA	2.31881D-02	4.63762D-02	6.95643D-02	9.27524D-02	1.15941D-01	1.39129D-01	1.62317D-01	1.85505D-01	2.08693D-01	2.31881D-01
TEMPERATURE	3.58700D 03	3.59700D 03	3.49000D 03	3.18700D 03	3.07000D 03	3.07000D 03	3.07000D 03	3.07000D 03	2.89600D 03	2.45900D 03
MELT FRACT.	1.00000D 00	1.00000D 00	1.00000D 00	1.00000D 00	9.70700D-01	6.50800D-01	3.74400D-01	5.44000D-02	0.0	0.0
MASS	1.79000D-01	1.40900D 00	1.42000D 00	1.45700D 00	1.46100D 00	1.48500D 00	1.31400D 00	1.29200D 00	1.31800D 00	1.14600D 00
F.G.MASS RAT	4.36900D-02	0.0	0.0	0.0	1.54000D-03	2.48000D-03	2.46000D-03	2.44000D-03	2.52000D-03	2.76000D-03

AXIAL CELL 22 OUTERMOST RADIAL CELL THAT IS FULLY MOLTEN 2 FUEL OUTER RADIUS (CM) 2.71680D-01

OUTER RADIUS	8.59128D-02	1.21499D-01	1.48805D-01	1.71826D-01	1.92107D-01	2.10442D-01	2.27304D-01	2.42998D-01	2.57738D-01	2.71680D-01
TOTAL AREA	2.31881D-02	4.63762D-02	6.95643D-02	9.27524D-02	1.15941D-01	1.39129D-01	1.62317D-01	1.85505D-01	2.08693D-01	2.31881D-01
TEMPERATURE	3.39100D 03	3.33300D 03	3.07000D 03	3.07000D 03	3.07000D 03	3.07000D 03	3.07000D 03	2.96700D 03	2.75400D 03	2.27600D 03
MELT FRACT.	1.00000D 00	1.00000D 00	9.58200D-01	6.15900D-01	4.01400D-01	2.13700D-01	1.54000D-02	0.0	0.0	0.0
MASS	4.38000D-01	1.43700D 00	1.47400D 00	1.52300D 00	1.39400D 00	1.27300D 00	1.29600D 00	1.31100D 00	1.32800D 00	1.01000D 00
F.G.MASS RAT	1.43900D-02	0.0	0.0	1.33000D-03	2.52000D-03	2.53000D-03	2.53000D-03	2.55000D-03	2.65000D-03	2.81000D-03

AXIAL CELL 21 OUTERMOST RADIAL CELL THAT IS FULLY MOLTEN 0 FUEL OUTER RADIUS (CM) 2.71680D-01

OUTER RADIUS	8.59128D-02	1.21499D-01	1.48805D-01	1.71826D-01	1.92107D-01	2.10442D-01	2.27304D-01	2.42998D-01	2.57738D-01	2.71680D-01
TOTAL AREA	2.31881D-02	4.63762D-02	6.95643D-02	9.27524D-02	1.15941D-01	1.39129D-01	1.62317D-01	1.85505D-01	2.08693D-01	2.31881D-01
TEMPERATURE	3.07000D 03	3.07000D 03	3.07000D 03	3.07000D 03	3.01800D 03	2.95300D 03	2.87400D 03	2.76200D 03	2.55700D 03	2.07400D 03
MELT FRACT.	6.35600D-01	4.32900D-01	1.93400D-01	1.98000D-02	0.0	0.0	0.0	0.0	0.0	0.0
MASS	1.23100D 00	1.24300D 00	1.27400D 00	1.29700D 00	1.30600D 00	1.31100D 00	1.31700D 00	1.32700D 00	1.34300D 00	8.17000D-01
F.G.MASS RAT	0.0	0.0	2.19000D-03	2.57000D-03	2.59000D-03	2.62000D-03	2.64000D-03	2.66000D-03	2.71000D-03	2.77000D-03

AXIAL CELL 20 OUTERMOST RADIAL CELL THAT IS FULLY MOLTEN 0 FUEL OUTER RADIUS (CM) 2.71680D-01

OUTER RADIUS	8.59128D-02	1.21499D-01	1.48805D-01	1.71826D-01	1.92107D-01	2.10442D-01	2.27304D-01	2.42998D-01	2.57738D-01	2.71680D-01
TOTAL AREA	2.31881D-02	4.63762D-02	6.95643D-02	9.27524D-02	1.15941D-01	1.39129D-01	1.62317D-01	1.85505D-01	2.08693D-01	2.31881D-01
TEMPERATURE	3.02300D 03	2.96700D 03	2.90900D 03	2.85500D 03	2.79900D 03	2.73600D 03	2.65700D 03	2.54100D 03	2.31800D 03	1.84300D 03
MELT FRACT.	0.0	0.0	0.0	0.0	0.0	0.0	0.0	0.0	0.0	0.0
MASS	1.30000D 00	1.30500D 00	1.31200D 00	1.31800D 00	1.32300D 00	1.32800D 00	1.33400D 00	1.34400D 00	1.36000D 00	6.14000D-01
F.G.MASS RAT	1.43000D-03	2.32000D-03	2.55000D-03	2.60000D-03	2.61000D-03	2.62000D-03	2.63000D-03	2.64000D-03	2.66000D-03	2.68000D-03

AXIAL CELL 19 OUTERMOST RADIAL CELL THAT IS FULLY MOLTEN 0 FUEL OUTER RADIUS (CM) 2.71680D-01

OUTER RADIUS	8.59128D-02	1.21499D-01	1.48805D-01	1.71826D-01	1.92107D-01	2.10442D-01	2.27304D-01	2.42998D-01	2.57738D-01	2.71680D-01
TOTAL AREA	2.31881D-02	4.63762D-02	6.95643D-02	9.27524D-02	1.15941D-01	1.39129D-01	1.62317D-01	1.85505D-01	2.08693D-01	2.31881D-01
TEMPERATURE	2.75100D 03	2.69600D 03	2.64800D 03	2.60000D 03	2.54800D 03	2.48800D 03	2.41000D 03	2.29100D 03	2.05300D 03	1.66300D 03
MELT FRACT.	0.0	0.0	0.0	0.0	0.0	0.0	0.0	0.0	0.0	0.0
MASS	1.32800D 00	1.33100D 00	1.33500D 00	1.33900D 00	1.34300D 00	1.34800D 00	1.35400D 00	1.36200D 00	1.37800D 00	4.70000D-01
F.G.MASS RAT	2.28000D-03	2.48000D-03	2.48000D-03	2.49000D-03	2.49000D-03	2.49000D-03	2.49000D-03	2.50000D-03	2.50000D-03	2.52000D-03

SAMPLE PROBLEM FOR LOF-TOP CONDITIONS
INITIALLY 2 FAILURE CELLS, PARTIALLY VOIDED CHANNEL, NORM. POWER AT 439

TIME= 0.0 DELT= 1.0000D-04 NORMALIZED POWER= 1.0000D 00
FCI BOUNDARIES IN CELLS 26 AND 41 FCIL= 1.8135D 02 FCIU= 2.9306D 02 HIGHEST FAILURE CELL IS 27
9.2111D-01 GRAMS FUEL IN 10 GROUPS XNIN= 1.8135D 02 XMAX= 1.9511D 02 LOWEST FAILURE CELL IS 26
REACTIVITY CHANGES-- SODIUM= 0.0 TOTAL FUEL= 0.0 TOTAL= 0.0 PIN FUEL= 0.0 CHANNEL FUEL= 0.0

*** FUEL PIN QUANTITIES ***

*** REACTIVITIES ***

J	POSITION OF CELL BOTTOM	FUEL TEMPRTURE TFUP	CAVITY PRESSURE PF	FUEL DENSITY ROFUP	FIS.GAS DENSITY ROGFP	CAVITY AREA AF	FUEL+FGAS VELOCITY UF	CLAD TEMPRTURE TCL	PIN FUEL REACTIVTY CHANGE	CHAN FUEL REACTIVTY CHANGE	TOTL FUEL REACTIVTY CHANGE
50	3.547D 02	0.0	0.0	0.0	0.0	0.0	0.0	1.078D 03	0.0	0.0	0.0
49	3.475D 02	0.0	0.0	0.0	0.0	0.0	0.0	1.079D 03	0.0	0.0	0.0
48	3.403D 02	0.0	0.0	0.0	0.0	0.0	0.0	1.079D 03	0.0	0.0	0.0
47	3.330D 02	0.0	0.0	0.0	0.0	0.0	0.0	1.079D 03	0.0	0.0	0.0
46	3.258D 02	0.0	0.0	0.0	0.0	0.0	0.0	1.080D 03	0.0	0.0	0.0
45	3.185D 02	0.0	0.0	0.0	0.0	0.0	0.0	1.080D 03	0.0	0.0	0.0
44	3.113D 02	0.0	0.0	0.0	0.0	0.0	0.0	1.080D 03	0.0	0.0	0.0
43	3.041D 02	0.0	0.0	0.0	0.0	0.0	0.0	1.082D 03	0.0	0.0	0.0
42	2.968D 02	0.0	0.0	0.0	0.0	0.0	0.0	1.082D 03	0.0	0.0	0.0
41	2.896D 02	0.0	0.0	0.0	0.0	0.0	0.0	1.229D 03	0.0	0.0	0.0
40	2.823D 02	0.0	0.0	0.0	0.0	0.0	0.0	1.253D 03	0.0	0.0	0.0
39	2.751D 02	0.0	0.0	0.0	0.0	0.0	0.0	1.253D 03	0.0	0.0	0.0
38	2.679D 02	0.0	0.0	0.0	0.0	0.0	0.0	1.253D 03	0.0	0.0	0.0
37	2.606D 02	0.0	0.0	0.0	0.0	0.0	0.0	1.282D 03	0.0	0.0	0.0
36	2.534D 02	0.0	0.0	0.0	0.0	0.0	0.0	1.282D 03	0.0	0.0	0.0
35	2.461D 02	0.0	0.0	0.0	0.0	0.0	0.0	1.297D 03	0.0	0.0	0.0
34	2.389D 02	0.0	0.0	0.0	0.0	0.0	0.0	1.297D 03	0.0	0.0	0.0
33	2.317D 02	0.0	0.0	0.0	0.0	0.0	0.0	1.313D 03	0.0	0.0	0.0
32	2.244D 02	0.0	0.0	0.0	0.0	0.0	0.0	1.408D 03	0.0	0.0	0.0
31	2.172D 02	3.070D 03	1.214D 08	6.648D 00	1.308D-02	2.319D-02	0.0	1.431D 03	0.0	0.0	0.0
30	2.099D 02	3.237D 03	1.209D 08	6.602D 00	1.265D-02	6.956D-02	0.0	1.449D 03	0.0	0.0	0.0
29	2.027D 02	3.353D 03	1.208D 08	7.042D 00	9.363D-03	1.159D-01	0.0	1.456D 03	0.0	0.0	0.0
28	1.955D 02	3.474D 03	1.210D 08	7.151D 00	8.370D-03	1.391D-01	0.0	1.456D 03	0.0	0.0	0.0
27	1.882D 02	3.599D 03	6.747D 07	6.194D 00	7.661D-03	1.391D-01	0.0	1.457D 03	0.0	0.0	0.0
26	1.810D 02	3.635D 03	1.151D 08	6.951D 00	8.715D-03	1.391D-01	0.0	1.430D 03	0.0	0.0	0.0
25	1.737D 02	3.588D 03	1.211D 08	7.056D 00	8.667D-03	1.391D-01	0.0	1.389D 03	0.0	0.0	0.0
24	1.665D 02	3.460D 03	1.209D 08	7.165D 00	8.309D-03	1.391D-01	0.0	1.338D 03	0.0	0.0	0.0
23	1.593D 02	3.429D 03	1.211D 08	6.649D 00	1.165D-02	9.275D-02	0.0	1.274D 03	0.0	0.0	0.0
22	1.520D 02	3.347D 03	1.208D 08	5.585D 00	1.877D-02	4.638D-02	0.0	1.205D 03	0.0	0.0	0.0
21	1.448D 02	0.0	0.0	0.0	0.0	0.0	0.0	1.125D 03	0.0	0.0	0.0
20	1.376D 02	0.0	0.0	0.0	0.0	0.0	0.0	1.045D 03	0.0	0.0	0.0
19	1.303D 02	0.0	0.0	0.0	0.0	0.0	0.0	9.570D 02	0.0	0.0	0.0
18	1.231D 02	0.0	0.0	0.0	0.0	0.0	0.0	7.630D 02	0.0	0.0	0.0
17	1.158D 02	0.0	0.0	0.0	0.0	0.0	0.0	7.150D 02	0.0	0.0	0.0
16	1.086D 02	0.0	0.0	0.0	0.0	0.0	0.0	6.870D 02	0.0	0.0	0.0
15	1.014D 02	0.0	0.0	0.0	0.0	0.0	0.0	6.870D 02	0.0	0.0	0.0
14	9.411D 01	0.0	0.0	0.0	0.0	0.0	0.0	6.620D 02	0.0	0.0	0.0
13	8.687D 01	0.0	0.0	0.0	0.0	0.0	0.0	6.620D 02	0.0	0.0	0.0
12	7.963D 01	0.0	0.0	0.0	0.0	0.0	0.0	6.430D 02	0.0	0.0	0.0
11	7.240D 01	0.0	0.0	0.0	0.0	0.0	0.0	6.430D 02	0.0	0.0	0.0
10	6.516D 01	0.0	0.0	0.0	0.0	0.0	0.0	6.430D 02	0.0	0.0	0.0
9	5.792D 01	0.0	0.0	0.0	0.0	0.0	0.0	6.430D 02	0.0	0.0	0.0
8	5.068D 01	0.0	0.0	0.0	0.0	0.0	0.0	6.430D 02	0.0	0.0	0.0
7	4.344D 01	0.0	0.0	0.0	0.0	0.0	0.0	6.430D 02	0.0	0.0	0.0
6	3.620D 01	0.0	0.0	0.0	0.0	0.0	0.0	6.430D 02	0.0	0.0	0.0
5	2.896D 01	0.0	0.0	0.0	0.0	0.0	0.0	6.430D 02	0.0	0.0	0.0
4	2.172D 01	0.0	0.0	0.0	0.0	0.0	0.0	6.430D 02	0.0	0.0	0.0

3	1.448D 01	0.0	0.0	0.0	0.0	0.0	0.0	6.430D 02	0.0	0.0	0.0
2	7.240D 00	0.0	0.0	0.0	0.0	0.0	0.0	6.430D 02	0.0	0.0	0.0
1	0.0	0.0	0.0	0.0	0.0	0.0	0.0	6.430D 02	0.0	0.0	0.0

*** CHANNEL QUANTITIES ***

J	POSITION OF CELL BOTTOM	SODIUM TEMPRTURE TNA	FIS.GAS TEMPRTURE TFG	FUEL TEMPRTURE TFU	TOTAL PRESSURE PM	LIQ. NA DENSITY ROSLC	FIS.GAS DENSITY ROFGC	FUEL DENSITY ROFPC	NA+FISGAS DENSITY ROMC	FUEL VELOCITY UP	NA+FISGAS VELOCITY UM
50	3.547D 02	1.209D 03	0.0	0.0	1.749D 06	7.187D-01	0.0	0.0	7.187D-01	0.0	7.730D 02
49	3.475D 02	1.209D 03	0.0	0.0	1.812D 06	7.187D-01	0.0	0.0	7.187D-01	0.0	7.740D 02
48	3.403D 02	1.216D 03	0.0	0.0	1.875D 06	7.173D-01	0.0	0.0	7.173D-01	0.0	7.750D 02
47	3.330D 02	1.216D 03	0.0	0.0	1.937D 06	7.173D-01	0.0	0.0	7.173D-01	0.0	7.750D 02
46	3.258D 02	1.216D 03	0.0	0.0	2.000D 06	7.173D-01	0.0	0.0	7.173D-01	0.0	7.760D 02
45	3.185D 02	1.230D 03	0.0	0.0	2.062D 06	7.144D-01	0.0	0.0	7.144D-01	0.0	7.780D 02
44	3.113D 02	1.230D 03	0.0	0.0	2.125D 06	7.144D-01	0.0	0.0	7.144D-01	0.0	7.780D 02
43	3.041D 02	1.230D 03	0.0	0.0	2.188D 06	7.144D-01	0.0	0.0	7.144D-01	0.0	7.820D 02
42	2.968D 02	1.256D 03	0.0	0.0	2.250D 06	7.089D-01	0.0	0.0	7.089D-01	0.0	7.310D 02
41	2.896D 02	1.254D 03	0.0	0.0	2.314D 06	4.313D-01	0.0	0.0	4.315D-01	0.0	3.380D 02
40	2.823D 02	1.240D 03	0.0	0.0	2.077D 06	1.268D-01	0.0	0.0	1.272D-01	0.0	0.0
39	2.751D 02	1.249D 03	0.0	0.0	2.227D 06	1.298D-01	0.0	0.0	1.303D-01	0.0	1.291D 03
38	2.679D 02	1.296D 03	0.0	0.0	3.154D 06	1.919D-01	0.0	0.0	1.925D-01	0.0	1.291D 03
37	2.606D 02	1.268D 03	0.0	0.0	2.572D 06	1.235D-01	0.0	0.0	1.240D-01	0.0	0.0
36	2.534D 02	1.278D 03	0.0	0.0	2.769D 06	1.243D-01	0.0	0.0	1.249D-01	0.0	0.0
35	2.461D 02	1.287D 03	0.0	0.0	2.957D 06	1.245D-01	0.0	0.0	1.251D-01	0.0	0.0
34	2.389D 02	1.297D 03	0.0	0.0	3.177D 06	1.245D-01	0.0	0.0	1.251D-01	0.0	0.0
33	2.317D 02	1.315D 03	0.0	0.0	3.604D 06	1.234D-01	0.0	0.0	1.241D-01	0.0	0.0
32	2.244D 02	1.377D 03	0.0	0.0	5.425D 06	1.171D-01	0.0	0.0	1.181D-01	0.0	0.0
31	2.172D 02	1.410D 03	0.0	0.0	6.643D 06	1.129D-01	0.0	0.0	1.142D-01	0.0	0.0
30	2.099D 02	1.424D 03	0.0	0.0	7.218D 06	1.098D-01	0.0	0.0	1.112D-01	0.0	0.0
29	2.027D 02	1.430D 03	0.0	0.0	7.475D 06	1.064D-01	0.0	0.0	1.078D-01	0.0	0.0
28	1.955D 02	1.432D 03	0.0	0.0	7.562D 06	1.094D-01	0.0	0.0	1.108D-01	0.0	-3.100D 02
27	1.882D 02	1.407D 03	1.561D 03	3.599D 03	6.747D 07	6.240D-01	7.319D-04	5.918D-01	6.247D-01	0.0	-6.240D 02
26	1.810D 02	1.389D 03	1.401D 03	3.635D 03	1.151D 08	6.805D-01	5.430D-05	4.480D-02	6.806D-01	0.0	-6.240D 02
25	1.737D 02	1.356D 03	0.0	0.0	1.128D 08	6.877D-01	0.0	0.0	6.877D-01	0.0	-6.160D 02
24	1.665D 02	1.312D 03	0.0	0.0	1.084D 08	6.971D-01	0.0	0.0	6.971D-01	0.0	-6.060D 02
23	1.593D 02	1.257D 03	0.0	0.0	1.041D 08	7.087D-01	0.0	0.0	7.087D-01	0.0	-5.940D 02
22	1.520D 02	1.195D 03	0.0	0.0	9.978D 07	7.216D-01	0.0	0.0	7.216D-01	0.0	-5.810D 02
21	1.448D 02	1.125D 03	0.0	0.0	9.546D 07	7.359D-01	0.0	0.0	7.359D-01	0.0	-5.680D 02
20	1.376D 02	1.052D 03	0.0	0.0	9.113D 07	7.505D-01	0.0	0.0	7.505D-01	0.0	-5.550D 02
19	1.303D 02	9.730D 02	0.0	0.0	8.680D 07	7.660D-01	0.0	0.0	7.660D-01	0.0	-5.390D 02
18	1.231D 02	8.570D 02	0.0	0.0	8.248D 07	7.883D-01	0.0	0.0	7.883D-01	0.0	-5.230D 02
17	1.158D 02	7.750D 02	0.0	0.0	7.815D 07	8.038D-01	0.0	0.0	8.038D-01	0.0	-5.130D 02
16	1.086D 02	7.210D 02	0.0	0.0	7.383D 07	8.138D-01	0.0	0.0	8.138D-01	0.0	-5.060D 02
15	1.014D 02	6.750D 02	0.0	0.0	6.950D 07	8.222D-01	0.0	0.0	8.222D-01	0.0	-5.020D 02
14	9.411D 01	6.750D 02	0.0	0.0	6.518D 07	8.222D-01	0.0	0.0	8.222D-01	0.0	-5.010D 02
13	8.687D 01	6.590D 02	0.0	0.0	6.085D 07	8.251D-01	0.0	0.0	8.251D-01	0.0	-5.000D 02
12	7.963D 01	6.590D 02	0.0	0.0	5.652D 07	8.251D-01	0.0	0.0	8.251D-01	0.0	-4.990D 02
11	7.240D 01	6.470D 02	0.0	0.0	5.220D 07	8.273D-01	0.0	0.0	8.273D-01	0.0	-4.980D 02
10	6.516D 01	6.470D 02	0.0	0.0	4.787D 07	8.273D-01	0.0	0.0	8.273D-01	0.0	-4.980D 02
9	5.792D 01	6.470D 02	0.0	0.0	4.355D 07	8.273D-01	0.0	0.0	8.273D-01	0.0	-4.980D 02
8	5.068D 01	6.470D 02	0.0	0.0	3.922D 07	8.273D-01	0.0	0.0	8.273D-01	0.0	-4.980D 02
7	4.344D 01	6.440D 02	0.0	0.0	3.490D 07	8.279D-01	0.0	0.0	8.279D-01	0.0	-4.980D 02
6	3.620D 01	6.440D 02	0.0	0.0	3.057D 07	8.279D-01	0.0	0.0	8.279D-01	0.0	-4.980D 02
5	2.896D 01	6.440D 02	0.0	0.0	2.624D 07	8.279D-01	0.0	0.0	8.279D-01	0.0	-4.980D 02
4	2.172D 01	6.440D 02	0.0	0.0	2.192D 07	8.279D-01	0.0	0.0	8.279D-01	0.0	-4.980D 02
3	1.448D 01	6.430D 02	0.0	0.0	1.759D 07	8.280D-01	0.0	0.0	8.280D-01	0.0	-4.980D 02
2	7.240D 00	6.430D 02	0.0	0.0	1.327D 07	8.280D-01	0.0	0.0	8.280D-01	0.0	-4.980D 02
1	0.0	6.430D 02	0.0	0.0	8.942D 06	8.280D-01	0.0	0.0	8.280D-01	0.0	-4.980D 02

SAMPLE PROBLEM FOR LOF-TOP CONDITIONS
INITIALLY 2 FAILURE CELLS, PARTIALLY VOIDED CHANNEL, NORM. POWER AT 439

TIME= 5.3987D-03 DELT= 1.0000D-04 NORMALIZED POWER= 2.4316D-01
FCI BOUNDARIES IN CELLS 21 AND 42 FCIL= 1.4651D 02 FCIU= 2.9731D 02 HIGHEST FAILURE CELL IS 30
3.7607D 01 GRAMS FUEL IN 70 GROUPS XMIN= 1.4974D 02 XMAX= 2.2422D 02 LOWEST FAILURE CELL IS 22
REACTIVITY CHANGES-- SODIUM= 0.0 TOTAL FUEL= 0.0 TOTAL= 0.0 PIN FUEL= 0.0 CHANNEL FUEL= 0.0

*** FUEL PIN QUANTITIES ***

*** REACTIVITIES ***

J	POSITION OF CELL BOTTOM	FUEL TEMPRTURE TFUP	CAVITY PRESSURE PF	FUEL DENSITY ROFUP	FIS.GAS DENSITY ROGFP	CAVITY AREA AF	FUEL+FGAS VELOCITY UF	CLAD TEMPRTURE TCL	PIN FUEL REACTIVTY CHANGE	CHAN FUEL REACTIVTY CHANGE	TOTL FUEL REACTIVTY CHANGE
50	3.547D 02	0.0	0.0	0.0	0.0	0.0	0.0	1.101D 03	0.0	0.0	0.0
49	3.475D 02	0.0	0.0	0.0	0.0	0.0	0.0	1.102D 03	0.0	0.0	0.0
48	3.403D 02	0.0	0.0	0.0	0.0	0.0	0.0	1.103D 03	0.0	0.0	0.0
47	3.330D 02	0.0	0.0	0.0	0.0	0.0	0.0	1.103D 03	0.0	0.0	0.0
46	3.258D 02	0.0	0.0	0.0	0.0	0.0	0.0	1.104D 03	0.0	0.0	0.0
45	3.185D 02	0.0	0.0	0.0	0.0	0.0	0.0	1.106D 03	0.0	0.0	0.0
44	3.113D 02	0.0	0.0	0.0	0.0	0.0	0.0	1.106D 03	0.0	0.0	0.0
43	3.041D 02	0.0	0.0	0.0	0.0	0.0	0.0	1.109D 03	0.0	0.0	0.0
42	2.968D 02	0.0	0.0	0.0	0.0	0.0	0.0	1.113D 03	0.0	0.0	0.0
41	2.896D 02	0.0	0.0	0.0	0.0	0.0	0.0	1.233D 03	0.0	0.0	0.0
40	2.823D 02	0.0	0.0	0.0	0.0	0.0	0.0	1.253D 03	0.0	0.0	0.0
39	2.751D 02	0.0	0.0	0.0	0.0	0.0	0.0	1.256D 03	0.0	0.0	0.0
38	2.679D 02	0.0	0.0	0.0	0.0	0.0	0.0	1.257D 03	0.0	0.0	0.0
37	2.606D 02	0.0	0.0	0.0	0.0	0.0	0.0	1.282D 03	0.0	0.0	0.0
36	2.534D 02	0.0	0.0	0.0	0.0	0.0	0.0	1.282D 03	0.0	0.0	0.0
35	2.461D 02	0.0	0.0	0.0	0.0	0.0	0.0	1.297D 03	0.0	0.0	0.0
34	2.389D 02	0.0	0.0	0.0	0.0	0.0	0.0	1.300D 03	0.0	0.0	0.0
33	2.317D 02	0.0	0.0	0.0	0.0	0.0	0.0	1.320D 03	0.0	0.0	0.0
32	2.244D 02	3.125D 03	5.772D 07	6.976D 00	5.023D-03	2.319D-02	-1.162D 03	1.438D 03	0.0	0.0	0.0
31	2.172D 02	3.367D 03	3.718D 07	4.557D 00	7.741D-03	1.391D-01	-2.013D 03	1.469D 03	0.0	0.0	0.0
30	2.099D 02	3.527D 03	4.506D 07	4.693D 00	8.616D-03	1.855D-01	-4.882D 02	1.493D 03	0.0	0.0	0.0
29	2.027D 02	3.742D 03	5.573D 07	4.951D 00	9.278D-03	2.087D-01	-6.810D 02	1.505D 03	0.0	0.0	0.0
28	1.955D 02	3.992D 03	6.295D 07	5.238D 00	8.811D-03	2.087D-01	-4.142D 02	1.509D 03	0.0	0.0	0.0
27	1.882D 02	4.160D 03	7.112D 07	5.415D 00	8.803D-03	2.087D-01	8.057D 02	1.513D 03	0.0	0.0	0.0
26	1.810D 02	4.233D 03	9.407D 07	5.902D 00	9.660D-03	2.087D-01	9.027D 02	1.488D 03	0.0	0.0	0.0
25	1.737D 02	4.136D 03	7.985D 07	5.579D 00	9.526D-03	2.087D-01	6.196D 02	1.449D 03	0.0	0.0	0.0
24	1.665D 02	3.999D 03	6.889D 07	5.214D 00	9.721D-03	2.087D-01	6.340D 02	1.397D 03	0.0	0.0	0.0
23	1.593D 02	3.786D 03	5.318D 07	4.597D 00	9.582D-03	2.087D-01	7.979D 02	1.336D 03	0.0	0.0	0.0
22	1.520D 02	3.583D 03	3.503D 07	3.980D 00	7.789D-03	1.855D-01	2.031D 03	1.265D 03	0.0	0.0	0.0
21	1.448D 02	3.318D 03	6.536D 07	5.458D 00	1.068D-02	1.623D-01	2.028D 03	1.176D 03	0.0	0.0	0.0
20	1.376D 02	3.123D 03	9.521D 07	6.298D 00	1.198D-02	4.638D-02	0.0	1.089D 03	0.0	0.0	0.0
19	1.303D 02	0.0	0.0	0.0	0.0	0.0	0.0	9.989D 02	0.0	0.0	0.0
18	1.231D 02	0.0	0.0	0.0	0.0	0.0	0.0	7.923D 02	0.0	0.0	0.0
17	1.158D 02	0.0	0.0	0.0	0.0	0.0	0.0	7.356D 02	0.0	0.0	0.0
16	1.086D 02	0.0	0.0	0.0	0.0	0.0	0.0	6.999D 02	0.0	0.0	0.0
15	1.014D 02	0.0	0.0	0.0	0.0	0.0	0.0	6.900D 02	0.0	0.0	0.0
14	9.411D 01	0.0	0.0	0.0	0.0	0.0	0.0	6.662D 02	0.0	0.0	0.0
13	8.687D 01	0.0	0.0	0.0	0.0	0.0	0.0	6.630D 02	0.0	0.0	0.0
12	7.963D 01	0.0	0.0	0.0	0.0	0.0	0.0	6.465D 02	0.0	0.0	0.0
11	7.240D 01	0.0	0.0	0.0	0.0	0.0	0.0	6.447D 02	0.0	0.0	0.0
10	6.516D 01	0.0	0.0	0.0	0.0	0.0	0.0	6.440D 02	0.0	0.0	0.0
9	5.792D 01	0.0	0.0	0.0	0.0	0.0	0.0	6.438D 02	0.0	0.0	0.0
8	5.068D 01	0.0	0.0	0.0	0.0	0.0	0.0	6.437D 02	0.0	0.0	0.0
7	4.344D 01	0.0	0.0	0.0	0.0	0.0	0.0	6.434D 02	0.0	0.0	0.0
6	3.620D 01	0.0	0.0	0.0	0.0	0.0	0.0	6.432D 02	0.0	0.0	0.0
5	2.896D 01	0.0	0.0	0.0	0.0	0.0	0.0	6.432D 02	0.0	0.0	0.0
4	2.172D 01	0.0	0.0	0.0	0.0	0.0	0.0	6.432D 02	0.0	0.0	0.0

3	1.448D 01	0.0	0.0	0.0	0.0	0.0	0.0	6.431D 02	0.0	0.0	0.0
2	7.240D 00	0.0	0.0	0.0	0.0	0.0	0.0	6.430D 02	0.0	0.0	0.0
1	0.0	0.0	0.0	0.0	0.0	0.0	0.0	6.430D 02	0.0	0.0	0.0

*** CHANNEL QUANTITIES ***

J	POSITION OF CELL BOTTOM	SODIUM TEMPRTURE TNA	FIS.GAS TEMPRTURE TFG	FUEL TEMPRTURE TFU	TOTAL PRESSURE PM	LIQ. NA DENSITY ROSLC	FIS.GAS DENSITY ROFGC	FUEL DENSITY ROFPC	NA+FISGAS DENSITY ROMC	FUEL VELOCITY UP	NA+FISGAS VELOCITY UM
50	3.547D 02	1.175D 03	0.0	0.0	1.738D 06	7.187D-01	0.0	0.0	7.187D-01	0.0	7.923D 02
49	3.475D 02	1.177D 03	0.0	0.0	1.790D 06	7.184D-01	0.0	0.0	7.184D-01	0.0	7.930D 02
48	3.403D 02	1.180D 03	0.0	0.0	1.843D 06	7.175D-01	0.0	0.0	7.175D-01	0.0	7.936D 02
47	3.330D 02	1.181D 03	0.0	0.0	1.895D 06	7.172D-01	0.0	0.0	7.172D-01	0.0	7.941D 02
46	3.258D 02	1.185D 03	0.0	0.0	1.948D 06	7.167D-01	0.0	0.0	7.167D-01	0.0	7.954D 02
45	3.185D 02	1.191D 03	0.0	0.0	2.000D 06	7.149D-01	0.0	0.0	7.149D-01	0.0	7.967D 02
44	3.113D 02	1.193D 03	0.0	0.0	2.053D 06	7.143D-01	0.0	0.0	7.143D-01	0.0	7.975D 02
43	3.041D 02	1.201D 03	0.0	0.0	2.105D 06	7.135D-01	0.0	0.0	7.135D-01	0.0	7.960D 02
42	2.968D 02	1.244D 03	0.0	0.0	2.157D 06	3.235D-02	0.0	0.0	3.236D-02	0.0	8.144D 02
41	2.896D 02	1.246D 03	0.0	0.0	2.180D 06	4.768D-01	0.0	0.0	4.770D-01	0.0	1.087D 03
40	2.823D 02	1.253D 03	0.0	0.0	2.297D 06	1.538D-01	0.0	0.0	1.543D-01	0.0	1.363D 03
39	2.751D 02	1.260D 03	0.0	0.0	2.428D 06	1.853D-01	0.0	0.0	1.857D-01	0.0	1.640D 03
38	2.679D 02	1.265D 03	0.0	0.0	2.510D 06	9.021D-02	0.0	0.0	9.075D-02	0.0	9.775D 02
37	2.606D 02	1.276D 03	0.0	0.0	2.723D 06	1.152D-01	0.0	0.0	1.158D-01	0.0	1.054D 03
36	2.534D 02	1.286D 03	0.0	0.0	2.944D 06	1.398D-01	0.0	0.0	1.404D-01	0.0	1.367D 03
35	2.461D 02	1.311D 03	0.0	0.0	3.507D 06	2.007D-01	0.0	0.0	2.013D-01	0.0	2.762D 03
34	2.389D 02	1.349D 03	0.0	0.0	4.520D 06	2.629D-01	0.0	0.0	2.636D-01	0.0	6.517D 03
33	2.317D 02	1.426D 03	0.0	0.0	7.301D 06	1.446D-01	0.0	0.0	1.459D-01	0.0	8.053D 03
32	2.244D 02	1.539D 03	0.0	0.0	1.347D 07	1.140D-01	0.0	0.0	1.164D-01	5.945D 03	6.685D 03
31	2.172D 02	1.625D 03	2.713D 03	3.679D 03	2.087D 07	2.027D-01	0.0	3.096D 00	2.040D-01	5.388D 03	7.349D 03
30	2.099D 02	1.678D 03	2.805D 03	3.898D 03	5.051D 07	1.263D-01	7.339D-03	1.797D 00	1.368D-01	2.598D 03	3.863D 03
29	2.027D 02	1.711D 03	2.973D 03	4.083D 03	5.729D 07	1.495D-01	5.969D-03	2.377D 00	1.583D-01	1.919D 03	2.623D 03
28	1.955D 02	1.759D 03	2.909D 03	4.256D 03	6.318D 07	2.112D-01	3.893D-03	2.571D 00	2.176D-01	1.073D 03	1.767D 03
27	1.882D 02	1.788D 03	2.972D 03	4.170D 03	7.112D 07	2.036D-01	4.325D-03	2.913D 00	2.104D-01	9.876D 02	2.165D 03
26	1.810D 02	1.786D 03	2.737D 03	4.279D 03	9.407D 07	3.224D-01	3.142D-03	2.863D 00	3.264D-01	4.842D 02	4.797D 02
25	1.737D 02	1.789D 03	2.977D 03	4.326D 03	1.098D 08	2.625D-01	5.191D-03	3.339D 00	2.690D-01	-8.721D 01	-8.562D 01
24	1.665D 02	1.620D 03	2.432D 03	4.051D 03	6.889D 07	3.645D-01	3.797D-03	2.462D 00	3.688D-01	-7.967D 02	-1.956D 03
23	1.593D 02	1.552D 03	2.134D 03	3.855D 03	5.318D 07	4.151D-01	3.715D-03	1.849D 00	4.192D-01	-1.483D 03	-2.648D 03
22	1.520D 02	1.523D 03	2.170D 03	3.612D 03	3.503D 07	4.033D-01	5.401D-03	2.361D 00	4.090D-01	-2.142D 03	-3.663D 03
21	1.448D 02	1.466D 03	1.637D 03	3.610D 03	3.499D 07	3.300D-01	0.0	3.680D-01	3.305D-01	0.0	-3.660D 03
20	1.376D 02	1.167D 03	0.0	0.0	3.391D 07	7.457D-01	0.0	0.0	7.457D-01	0.0	-3.538D 03
19	1.303D 02	1.090D 03	0.0	0.0	3.239D 07	7.669D-01	0.0	0.0	7.669D-01	0.0	-3.448D 03
18	1.231D 02	9.874D 02	0.0	0.0	3.087D 07	7.851D-01	0.0	0.0	7.851D-01	0.0	-3.376D 03
17	1.158D 02	8.893D 02	0.0	0.0	2.935D 07	8.001D-01	0.0	0.0	8.001D-01	0.0	-3.321D 03
16	1.086D 02	8.077D 02	0.0	0.0	2.783D 07	8.112D-01	0.0	0.0	8.112D-01	0.0	-3.284D 03
15	1.014D 02	7.471D 02	0.0	0.0	2.630D 07	8.184D-01	0.0	0.0	8.184D-01	0.0	-3.262D 03
14	9.411D 01	7.061D 02	0.0	0.0	2.478D 07	8.221D-01	0.0	0.0	8.221D-01	0.0	-3.250D 03
13	8.687D 01	6.821D 02	0.0	0.0	2.326D 07	8.242D-01	0.0	0.0	8.242D-01	0.0	-3.244D 03
12	7.963D 01	6.672D 02	0.0	0.0	2.174D 07	8.255D-01	0.0	0.0	8.255D-01	0.0	-3.239D 03
11	7.240D 01	6.576D 02	0.0	0.0	2.022D 07	8.266D-01	0.0	0.0	8.266D-01	0.0	-3.236D 03
10	6.516D 01	6.515D 02	0.0	0.0	1.870D 07	8.271D-01	0.0	0.0	8.271D-01	0.0	-3.234D 03
9	5.792D 01	6.482D 02	0.0	0.0	1.718D 07	8.273D-01	0.0	0.0	8.273D-01	0.0	-3.234D 03
8	5.068D 01	6.467D 02	0.0	0.0	1.565D 07	8.275D-01	0.0	0.0	8.275D-01	0.0	-3.233D 03
7	4.344D 01	6.457D 02	0.0	0.0	1.413D 07	8.277D-01	0.0	0.0	8.277D-01	0.0	-3.232D 03
6	3.620D 01	6.448D 02	0.0	0.0	1.261D 07	8.278D-01	0.0	0.0	8.278D-01	0.0	-3.232D 03
5	2.896D 01	6.442D 02	0.0	0.0	1.109D 07	8.279D-01	0.0	0.0	8.279D-01	0.0	-3.232D 03
4	2.172D 01	6.439D 02	0.0	0.0	9.568D 06	8.279D-01	0.0	0.0	8.279D-01	0.0	-3.231D 03
3	1.448D 01	6.436D 02	0.0	0.0	8.047D 06	8.280D-01	0.0	0.0	8.280D-01	0.0	-3.231D 03
2	7.240D 00	6.433D 02	0.0	0.0	6.525D 06	8.280D-01	0.0	0.0	8.280D-01	0.0	-3.231D 03
1	0.0	6.431D 02	0.0	0.0	5.004D 06	8.280D-01	0.0	0.0	8.280D-01	0.0	-3.231D 03

SAMPLE PROBLEM FOR LOF-TOP CONDITIONS
INITIALLY 2 FAILURE CELLS, PARTIALLY VOIDED CHANNEL, NORM. POWER AT 439

TIME= 1.0399D-02 DELT= 1.0000D-04 NORMALIZED POWER= 2.0730D-03
FCI BOUNDARIES IN CELLS 18 AND 42 FCIL= 1.2815D 02 FCIU= 3.0135D 02 HIGHEST FAILURE CELL IS 30
4.2694D 01 GRAMS FUEL IN 193 GROUPS XMIN= 1.3066D 02 XMAX= 2.5902D 02 LOWEST FAILURE CELL IS 22
REACTIVITY CHANGES-- SODIUM= 0.0 TOTAL FUEL= 0.0 TOTAL= 0.0 PIN FUEL= 0.0 CHANNEL FUEL= 0.0

*** FUEL PIN QUANTITIES ***

*** REACTIVITIES ***

J	POSITION OF CELL BOTTOM	FUEL TEMPRTURE TFUP	CAVITY PRESSURE PF	FUEL DENSITY ROFUP	FIS.GAS DENSITY ROGFP	CAVITY AREA AF	FUEL+FGAS VELOCITY UF	CLAD TEMPRTURE TCL	PIN FUEL REACTIVTY CHANGE	CHAN FUEL REACTIVTY CHANGE	TOTL FUEL REACTIVTY CHANGE
50	3.547D 02	0.0	0.0	0.0	0.0	0.0	0.0	1.113D 03	0.0	0.0	0.0
49	3.475D 02	0.0	0.0	0.0	0.0	0.0	0.0	1.114D 03	0.0	0.0	0.0
48	3.403D 02	0.0	0.0	0.0	0.0	0.0	0.0	1.115D 03	0.0	0.0	0.0
47	3.330D 02	0.0	0.0	0.0	0.0	0.0	0.0	1.115D 03	0.0	0.0	0.0
46	3.258D 02	0.0	0.0	0.0	0.0	0.0	0.0	1.117D 03	0.0	0.0	0.0
45	3.185D 02	0.0	0.0	0.0	0.0	0.0	0.0	1.120D 03	0.0	0.0	0.0
44	3.113D 02	0.0	0.0	0.0	0.0	0.0	0.0	1.120D 03	0.0	0.0	0.0
43	3.041D 02	0.0	0.0	0.0	0.0	0.0	0.0	1.124D 03	0.0	0.0	0.0
42	2.968D 02	0.0	0.0	0.0	0.0	0.0	0.0	1.130D 03	0.0	0.0	0.0
41	2.896D 02	0.0	0.0	0.0	0.0	0.0	0.0	1.235D 03	0.0	0.0	0.0
40	2.823D 02	0.0	0.0	0.0	0.0	0.0	0.0	1.253D 03	0.0	0.0	0.0
39	2.751D 02	0.0	0.0	0.0	0.0	0.0	0.0	1.255D 03	0.0	0.0	0.0
38	2.679D 02	0.0	0.0	0.0	0.0	0.0	0.0	1.260D 03	0.0	0.0	0.0
37	2.606D 02	0.0	0.0	0.0	0.0	0.0	0.0	1.286D 03	0.0	0.0	0.0
36	2.534D 02	0.0	0.0	0.0	0.0	0.0	0.0	1.294D 03	0.0	0.0	0.0
35	2.461D 02	0.0	0.0	0.0	0.0	0.0	0.0	1.316D 03	0.0	0.0	0.0
34	2.389D 02	0.0	0.0	0.0	0.0	0.0	0.0	1.332D 03	0.0	0.0	0.0
33	2.317D 02	0.0	0.0	0.0	0.0	0.0	0.0	1.362D 03	0.0	0.0	0.0
32	2.244D 02	3.182D 03	2.272D 07	4.968D 00	4.492D-03	2.319D-02	5.892D 02	1.503D 03	0.0	0.0	0.0
31	2.172D 02	3.401D 03	4.637D 07	5.060D 00	8.341D-03	1.391D-01	1.066D 03	1.540D 03	0.0	0.0	0.0
30	2.099D 02	3.563D 03	5.035D 07	4.933D 00	8.923D-03	1.855D-01	1.274D 03	1.569D 03	0.0	0.0	0.0
29	2.027D 02	3.792D 03	6.414D 07	5.261D 00	9.604D-03	2.087D-01	7.556D 02	1.585D 03	0.0	0.0	0.0
28	1.955D 02	4.021D 03	6.572D 07	5.301D 00	8.928D-03	2.087D-01	3.242D 02	1.591D 03	0.0	0.0	0.0
27	1.882D 02	4.181D 03	6.276D 07	5.116D 00	8.347D-03	2.087D-01	5.001D 00	1.596D 03	0.0	0.0	0.0
26	1.810D 02	4.227D 03	6.003D 07	4.940D 00	8.151D-03	2.087D-01-5.612D 02		1.580D 03	0.0	0.0	0.0
25	1.737D 02	4.142D 03	4.742D 07	4.415D 00	7.581D-03	2.087D-01-8.812D 01		1.534D 03	0.0	0.0	0.0
24	1.665D 02	4.006D 03	6.027D 07	4.920D 00	9.188D-03	2.087D-01	1.041D 02	1.485D 03	0.0	0.0	0.0
23	1.593D 02	3.762D 03	5.980D 07	4.899D 00	1.005D-02	2.087D-01-3.516D 02		1.424D 03	0.0	0.0	0.0
22	1.520D 02	3.466D 03	4.710D 07	4.554D 00	8.910D-03	1.855D-01-8.884D 02		1.358D 03	0.0	0.0	0.0
21	1.448D 02	3.301D 03	2.961D 07	3.831D 00	7.450D-03	1.623D-01	2.167D 02	1.275D 03	0.0	0.0	0.0
20	1.376D 02	3.132D 03	1.217D 07	2.267D 00	4.311D-03	4.638D-02	0.0	1.181D 03	0.0	0.0	0.0
19	1.303D 02	0.0	0.0	0.0	0.0	0.0	0.0	1.075D 03	0.0	0.0	0.0
18	1.231D 02	0.0	0.0	0.0	0.0	0.0	0.0	8.441D 02	0.0	0.0	0.0
17	1.158D 02	0.0	0.0	0.0	0.0	0.0	0.0	7.808D 02	0.0	0.0	0.0
16	1.086D 02	0.0	0.0	0.0	0.0	0.0	0.0	7.359D 02	0.0	0.0	0.0
15	1.014D 02	0.0	0.0	0.0	0.0	0.0	0.0	7.141D 02	0.0	0.0	0.0
14	9.411D 01	0.0	0.0	0.0	0.0	0.0	0.0	6.837D 02	0.0	0.0	0.0
13	8.687D 01	0.0	0.0	0.0	0.0	0.0	0.0	6.735D 02	0.0	0.0	0.0
12	7.963D 01	0.0	0.0	0.0	0.0	0.0	0.0	6.547D 02	0.0	0.0	0.0
11	7.240D 01	0.0	0.0	0.0	0.0	0.0	0.0	6.498D 02	0.0	0.0	0.0
10	6.516D 01	0.0	0.0	0.0	0.0	0.0	0.0	6.471D 02	0.0	0.0	0.0
9	5.792D 01	0.0	0.0	0.0	0.0	0.0	0.0	6.456D 02	0.0	0.0	0.0
8	5.068D 01	0.0	0.0	0.0	0.0	0.0	0.0	6.448D 02	0.0	0.0	0.0
7	4.344D 01	0.0	0.0	0.0	0.0	0.0	0.0	6.441D 02	0.0	0.0	0.0
6	3.620D 01	0.0	0.0	0.0	0.0	0.0	0.0	6.437D 02	0.0	0.0	0.0
5	2.896D 01	0.0	0.0	0.0	0.0	0.0	0.0	6.435D 02	0.0	0.0	0.0
4	2.172D 01	0.0	0.0	0.0	0.0	0.0	0.0	6.434D 02	0.0	0.0	0.0

3	1.448D 01	0.0	0.0	0.0	0.0	0.0	0.0	6.432D 02	0.0	0.0	0.0
2	7.240D 00	0.0	0.0	0.0	0.0	0.0	0.0	6.431D 02	0.0	0.0	0.0
1	0.0	0.0	0.0	0.0	0.0	0.0	0.0	6.431D 02	0.0	0.0	0.0

*** CHANNEL QUANTITIES ***

J	POSITION OF CELL BOTTOM	SODIUM TEMPRTURE TNA	FIS.GAS TEMPRTURE TFG	FUEL TEMPRTURE TFU	TOTAL PRESSURE PM	LIQ. NA DENSITY ROSLC	FIS.GAS DENSITY ROFGC	FUEL DENSITY ROFPC	NA+FISGAS DENSITY ROMC	FUEL VELOCITY UP	NA+FISGAS VELOCITY UM
50	3.547D 02	1.157D 03	0.0	0.0	1.738D 06	7.186D-01	0.0	0.0	7.186D-01	0.0	8.212D 02
49	3.475D 02	1.159D 03	0.0	0.0	1.791D 06	7.183D-01	0.0	0.0	7.183D-01	0.0	8.218D 02
48	3.403D 02	1.161D 03	0.0	0.0	1.844D 06	7.176D-01	0.0	0.0	7.176D-01	0.0	8.224D 02
47	3.330D 02	1.163D 03	0.0	0.0	1.897D 06	7.172D-01	0.0	0.0	7.172D-01	0.0	8.231D 02
46	3.258D 02	1.167D 03	0.0	0.0	1.950D 06	7.164D-01	0.0	0.0	7.164D-01	0.0	8.243D 02
45	3.185D 02	1.171D 03	0.0	0.0	2.003D 06	7.151D-01	0.0	0.0	7.151D-01	0.0	8.254D 02
44	3.113D 02	1.175D 03	0.0	0.0	2.056D 06	7.145D-01	0.0	0.0	7.145D-01	0.0	8.254D 02
43	3.041D 02	1.183D 03	0.0	0.0	2.110D 06	7.151D-01	0.0	0.0	7.152D-01	0.0	8.209D 02
42	2.968D 02	1.224D 03	0.0	0.0	2.152D 06	3.113D-01	0.0	0.0	3.114D-01	0.0	1.212D 03
41	2.896D 02	1.245D 03	0.0	0.0	2.156D 06	3.631D-01	0.0	0.0	3.633D-01	0.0	1.836D 03
40	2.823D 02	1.257D 03	0.0	0.0	2.365D 06	1.650D-01	0.0	0.0	1.654D-01	0.0	1.957D 03
39	2.751D 02	1.269D 03	0.0	0.0	2.585D 06	1.461D-01	0.0	0.0	1.467D-01	0.0	2.213D 03
38	2.679D 02	1.309D 03	0.0	0.0	3.449D 06	1.692D-01	0.0	0.0	1.693D-01	0.0	2.327D 03
37	2.606D 02	1.371D 03	0.0	0.0	5.220D 06	3.101D-01	0.0	0.0	3.107D-01	2.546D 03	1.486D 03
36	2.534D 02	1.498D 03	2.145D 03	3.591D 03	1.135D 07	5.673D-01	0.0	3.283D 00	5.673D-01	3.830D 03	1.486D 03
35	2.461D 02	1.587D 03	2.178D 03	3.824D 03	3.398D 07	2.168D-01	6.037D-03	1.040D 00	2.248D-01	7.214D 03	7.270D 03
34	2.389D 02	1.625D 03	1.866D 03	3.841D 03	2.724D 07	1.058D-01	3.748D-03	1.749D-01	1.130D-01	7.324D 03	9.243D 03
33	2.317D 02	1.692D 03	2.493D 03	3.897D 03	3.639D 07	9.657D-02	3.553D-03	7.721D-01	1.043D-01	7.040D 03	1.030D 04
32	2.244D 02	1.774D 03	3.085D 03	3.967D 03	4.649D 07	7.264D-02	2.365D-03	1.550D 00	8.035D-02	5.861D 03	8.547D 03
31	2.172D 02	1.823D 03	3.039D 03	4.149D 03	5.509D 07	7.865D-02	2.222D-03	1.265D 00	8.740D-02	4.899D 03	7.391D 03
30	2.099D 02	1.868D 03	3.273D 03	4.180D 03	6.435D 07	8.250D-02	2.093D-03	1.914D 00	9.133D-02	3.878D 03	5.323D 03
29	2.027D 02	1.899D 03	3.220D 03	4.082D 03	6.837D 07	8.616D-02	2.001D-03	2.006D 00	9.540D-02	2.938D 03	4.250D 03
28	1.955D 02	1.922D 03	3.181D 03	4.090D 03	7.149D 07	7.958D-02	1.693D-03	1.697D 00	8.967D-02	1.213D 03	2.909D 03
27	1.882D 02	1.941D 03	3.432D 03	4.171D 03	7.845D 07	8.432D-02	1.731D-03	2.641D 00	9.333D-02	8.112D 02	1.758D 02
26	1.810D 02	1.904D 03	2.391D 03	4.189D 03	7.701D 07	2.409D-01	3.793D-03	9.964D-01	2.501D-01	-9.720D 01	-9.716D 01
25	1.737D 02	1.720D 03	3.652D 03	4.199D 03	4.742D 07	2.613D-02	4.016D-03	1.296D 00	3.518D-02	-1.695D 03	-1.695D 03
24	1.665D 02	1.817D 03	3.154D 03	4.249D 03	6.631D 07	1.295D-01	4.030D-03	2.317D 00	1.380D-01	-1.987D 03	-2.884D 03
23	1.593D 02	1.793D 03	2.881D 03	3.925D 03	6.052D 07	1.504D-01	4.658D-03	2.270D 00	1.589D-01	-2.836D 03	-5.123D 03
22	1.520D 02	1.718D 03	2.335D 03	3.761D 03	4.700D 07	1.301D-01	7.243D-03	7.909D-01	1.417D-01	-4.697D 03	-7.766D 03
21	1.448D 02	1.670D 03	2.342D 03	3.723D 03	2.543D 07	2.549D-01	0.0	1.707D 00	2.569D-01	-5.581D 03	-5.580D 03
20	1.376D 02	1.616D 03	1.953D 03	3.520D 03	1.975D 07	3.363D-01	0.0	9.781D-01	3.378D-01	-4.524D 03	-3.781D 03
19	1.303D 02	1.603D 03	2.157D 03	3.440D 03	1.847D 07	4.851D-01	0.0	2.813D 00	4.851D-01	-4.247D 03	-3.781D 03
18	1.231D 02	1.582D 03	0.0	0.0	1.826D 07	1.281D-01	0.0	0.0	1.284D-01	0.0	-3.709D 03
17	1.158D 02	1.027D 03	0.0	0.0	1.746D 07	7.889D-01	0.0	0.0	7.889D-01	0.0	-3.566D 03
16	1.086D 02	9.558D 02	0.0	0.0	1.662D 07	8.059D-01	0.0	0.0	8.059D-01	0.0	-3.510D 03
15	1.014D 02	8.827D 02	0.0	0.0	1.578D 07	8.146D-01	0.0	0.0	8.146D-01	0.0	-3.480D 03
14	9.411D 01	8.159D 02	0.0	0.0	1.495D 07	8.198D-01	0.0	0.0	8.198D-01	0.0	-3.462D 03
13	8.687D 01	7.622D 02	0.0	0.0	1.411D 07	8.230D-01	0.0	0.0	8.230D-01	0.0	-3.451D 03
12	7.963D 01	7.212D 02	0.0	0.0	1.327D 07	8.249D-01	0.0	0.0	8.249D-01	0.0	-3.445D 03
11	7.240D 01	6.926D 02	0.0	0.0	1.243D 07	8.261D-01	0.0	0.0	8.261D-01	0.0	-3.441D 03
10	6.516D 01	6.738D 02	0.0	0.0	1.159D 07	8.268D-01	0.0	0.0	8.268D-01	0.0	-3.439D 03
9	5.792D 01	6.619D 02	0.0	0.0	1.075D 07	8.272D-01	0.0	0.0	8.272D-01	0.0	-3.437D 03
8	5.068D 01	6.545D 02	0.0	0.0	9.914D 06	8.274D-01	0.0	0.0	8.274D-01	0.0	-3.436D 03
7	4.344D 01	6.501D 02	0.0	0.0	9.076D 06	8.276D-01	0.0	0.0	8.276D-01	0.0	-3.436D 03
6	3.620D 01	6.475D 02	0.0	0.0	8.237D 06	8.278D-01	0.0	0.0	8.278D-01	0.0	-3.435D 03
5	2.896D 01	6.459D 02	0.0	0.0	7.399D 06	8.279D-01	0.0	0.0	8.279D-01	0.0	-3.435D 03
4	2.172D 01	6.450D 02	0.0	0.0	6.560D 06	8.279D-01	0.0	0.0	8.279D-01	0.0	-3.435D 03
3	1.448D 01	6.444D 02	0.0	0.0	5.722D 06	8.280D-01	0.0	0.0	8.280D-01	0.0	-3.434D 03
2	7.240D 00	6.439D 02	0.0	0.0	4.883D 06	8.280D-01	0.0	0.0	8.280D-01	0.0	-3.434D 03
1	0.0	6.436D 02	0.0	0.0	4.045D 06	8.280D-01	0.0	0.0	8.280D-01	0.0	-3.434D 03

SAMPLE PROBLEM FOR LOF-TOP CONDITIONS
INITIALLY 2 FAILURE CELLS, PARTIALLY VOIDED CHANNEL, NORM. POWER AT 439

TIME= 2.9940D-02 DELT= 5.4283D-05 NORMALIZED POWER= 1.1625D-03
FCI BOUNDARIES IN CELLS 6 AND 45 FCIL= 4.0874D 01 FCIU= 3.1953D 02 HIGHEST FAILURE CELL IS 30
6.3767D 01 GRAMS FUEL IN 182 GROUPS XMIN= 4.4917D 01 XMAX= 3.0906D 02 LOWEST FAILURE CELL IS 22
REACTIVITY CHANGES-- SODIUM= 0.0 TOTAL FUEL= 0.0 TOTAL= 0.0 PIN FUEL= 0.0 CHANNEL FUEL= 0.0

*** FUEL PIN QUANTITIES *** *** REACTIVITIES ***

J	POSITION OF CELL BOTTOM	FUEL TEMPRTURE TFUP	CAVITY PRESSURE PF	FUEL DENSITY ROFUP	FIS.GAS DENSITY ROGFP	CAVITY AREA AF	FUEL+FGAS VELOCITY UF	CLAD TEMPRTURE TCL	PIN FUEL REACTIVTY CHANGE	CHAN FUEL REACTIVTY CHANGE	TOTL FUEL REACTIVTY CHANGE
50	3.547D 02	0.0	0.0	0.0	0.0	0.0	0.0	1.129D 03	0.0	0.0	0.0
49	3.475D 02	0.0	0.0	0.0	0.0	0.0	0.0	1.130D 03	0.0	0.0	0.0
48	3.403D 02	0.0	0.0	0.0	0.0	0.0	0.0	1.132D 03	0.0	0.0	0.0
47	3.330D 02	0.0	0.0	0.0	0.0	0.0	0.0	1.133D 03	0.0	0.0	0.0
46	3.258D 02	0.0	0.0	0.0	0.0	0.0	0.0	1.136D 03	0.0	0.0	0.0
45	3.185D 02	0.0	0.0	0.0	0.0	0.0	0.0	1.139D 03	0.0	0.0	0.0
44	3.113D 02	0.0	0.0	0.0	0.0	0.0	0.0	1.160D 03	0.0	0.0	0.0
43	3.041D 02	0.0	0.0	0.0	0.0	0.0	0.0	1.203D 03	0.0	0.0	0.0
42	2.968D 02	0.0	0.0	0.0	0.0	0.0	0.0	1.287D 03	0.0	0.0	0.0
41	2.896D 02	0.0	0.0	0.0	0.0	0.0	0.0	1.418D 03	0.0	0.0	0.0
40	2.823D 02	0.0	0.0	0.0	0.0	0.0	0.0	1.426D 03	0.0	0.0	0.0
39	2.751D 02	0.0	0.0	0.0	0.0	0.0	0.0	1.407D 03	0.0	0.0	0.0
38	2.679D 02	0.0	0.0	0.0	0.0	0.0	0.0	1.413D 03	0.0	0.0	0.0
37	2.606D 02	0.0	0.0	0.0	0.0	0.0	0.0	1.427D 03	0.0	0.0	0.0
36	2.534D 02	0.0	0.0	0.0	0.0	0.0	0.0	1.425D 03	0.0	0.0	0.0
35	2.461D 02	0.0	0.0	0.0	0.0	0.0	0.0	1.419D 03	0.0	0.0	0.0
34	2.389D 02	0.0	0.0	0.0	0.0	0.0	0.0	1.425D 03	0.0	0.0	0.0
33	2.317D 02	0.0	0.0	0.0	0.0	0.0	0.0	1.476D 03	0.0	0.0	0.0
32	2.244D 02	3.321D 03	2.692D 07	4.453D 00	5.831D-03	2.319D-02	-1.865D 02	1.675D 03	0.0	0.0	0.0
31	2.172D 02	3.464D 03	2.534D 07	3.752D 00	6.140D-03	1.391D-01	-6.892D 01	1.700D 03	0.0	0.0	0.0
30	2.099D 02	3.634D 03	3.124D 07	3.950D 00	6.853D-03	1.855D-01	-2.403D 02	1.700D 03	0.0	0.0	0.0
29	2.027D 02	3.870D 03	3.289D 07	3.832D 00	6.737D-03	2.087D-01	7.706D 01	1.700D 03	0.0	0.0	0.0
28	1.955D 02	4.065D 03	3.527D 07	3.872D 00	6.491D-03	2.087D-01	6.074D 01	1.700D 03	0.0	0.0	0.0
27	1.882D 02	4.175D 03	3.322D 07	3.612D 00	5.925D-03	2.087D-01	-1.433D 02	1.700D 03	0.0	0.0	0.0
26	1.810D 02	4.218D 03	2.922D 07	3.205D 00	5.288D-03	2.087D-01	-4.600D 02	1.700D 03	0.0	0.0	0.0
25	1.737D 02	4.170D 03	2.972D 07	3.279D 00	5.569D-03	2.087D-01	-5.259D 02	1.700D 03	0.0	0.0	0.0
24	1.665D 02	4.089D 03	2.756D 07	3.140D 00	5.601D-03	2.087D-01	-7.322D 02	1.685D 03	0.0	0.0	0.0
23	1.593D 02	3.959D 03	2.748D 07	3.187D 00	6.043D-03	2.087D-01	-5.806D 02	1.638D 03	0.0	0.0	0.0
22	1.520D 02	3.698D 03	2.459D 07	3.151D 00	6.150D-03	1.855D-01	2.141D 01	1.587D 03	0.0	0.0	0.0
21	1.448D 02	3.376D 03	2.357D 07	3.298D 00	6.439D-03	1.623D-01	3.894D 02	1.519D 03	0.0	0.0	0.0
20	1.376D 02	3.275D 03	2.324D 07	3.357D 00	6.490D-03	4.638D-02	0.0	1.434D 03	0.0	0.0	0.0
19	1.303D 02	0.0	0.0	0.0	0.0	0.0	0.0	1.347D 03	0.0	0.0	0.0
18	1.231D 02	0.0	0.0	0.0	0.0	0.0	0.0	1.074D 03	0.0	0.0	0.0
17	1.158D 02	0.0	0.0	0.0	0.0	0.0	0.0	9.892D 02	0.0	0.0	0.0
16	1.086D 02	0.0	0.0	0.0	0.0	0.0	0.0	9.410D 02	0.0	0.0	0.0
15	1.014D 02	0.0	0.0	0.0	0.0	0.0	0.0	9.214D 02	0.0	0.0	0.0
14	9.411D 01	0.0	0.0	0.0	0.0	0.0	0.0	8.935D 02	0.0	0.0	0.0
13	8.687D 01	0.0	0.0	0.0	0.0	0.0	0.0	9.095D 02	0.0	0.0	0.0
12	7.963D 01	0.0	0.0	0.0	0.0	0.0	0.0	8.960D 02	0.0	0.0	0.0
11	7.240D 01	0.0	0.0	0.0	0.0	0.0	0.0	8.760D 02	0.0	0.0	0.0
10	6.516D 01	0.0	0.0	0.0	0.0	0.0	0.0	8.462D 02	0.0	0.0	0.0
9	5.792D 01	0.0	0.0	0.0	0.0	0.0	0.0	7.992D 02	0.0	0.0	0.0
8	5.068D 01	0.0	0.0	0.0	0.0	0.0	0.0	7.576D 02	0.0	0.0	0.0
7	4.344D 01	0.0	0.0	0.0	0.0	0.0	0.0	7.184D 02	0.0	0.0	0.0
6	3.620D 01	0.0	0.0	0.0	0.0	0.0	0.0	6.850D 02	0.0	0.0	0.0
5	2.896D 01	0.0	0.0	0.0	0.0	0.0	0.0	6.754D 02	0.0	0.0	0.0
4	2.172D 01	0.0	0.0	0.0	0.0	0.0	0.0	6.683D 02	0.0	0.0	0.0

3	1.448D 01	0.0	0.0	0.0	0.0	0.0	0.0	6.622D 02	0.0	0.0	0.0
2	7.240D 00	0.0	0.0	0.0	0.0	0.0	0.0	6.573D 02	0.0	0.0	0.0
1	0.0	0.0	0.0	0.0	0.0	0.0	0.0	6.534D 02	0.0	0.0	0.0

*** CHANNEL QUANTITIES ***

J	POSITION OF CELL BOTTOM	SODIUM TEMPRTURE TNA	FIS.GAS TEMPRTURE TFG	FUEL TEMPRTURE TFU	TOTAL PRESSURE PM	LIQ. NA DENSITY ROSLC	FIS.GAS DENSITY ROFGC	FUEL DENSITY ROFPC	NA+FISGAS DENSITY ROMC	FUEL VELOCITY UP	NA+FISGAS VELOCITY UM
50	3.547D 02	1.136D 03	0.0	0.0	2.016D 06	7.182D-01	0.0	0.0	7.182D-01	0.0	1.317D 03
49	3.475D 02	1.138D 03	0.0	0.0	2.306D 06	7.180D-01	0.0	0.0	7.180D-01	0.0	1.318D 03
48	3.403D 02	1.141D 03	0.0	0.0	2.595D 06	7.176D-01	0.0	0.0	7.176D-01	0.0	1.318D 03
47	3.330D 02	1.143D 03	0.0	0.0	2.885D 06	7.173D-01	0.0	0.0	7.173D-01	0.0	1.318D 03
46	3.258D 02	1.146D 03	0.0	0.0	3.175D 06	7.184D-01	0.0	0.0	7.184D-01	0.0	1.305D 03
45	3.185D 02	1.301D 03	0.0	0.0	3.462D 06	8.842D-02	0.0	0.0	8.843D-02	0.0	1.268D 03
44	3.113D 02	1.314D 03	0.0	0.0	3.570D 06	6.927D-01	0.0	0.0	[illegible]D-01	0.0	9.963D 02
43	3.041D 02	1.567D 03	1.999D 03	3.071D 03	1.547D 07	6.464D-01	0.0	3.577	[illegible]64D-01	1.800D 03	9.963D 02
42	2.968D 02	1.788D 03	2.040D 03	3.168D 03	3.921D 07	4.555D-01	0.0	1.39	[illegible]560D-01	8.793D 02	8.732D 02
41	2.896D 02	1.766D 03	2.525D 03	3.593D 03	3.876D 07	1.961D-01	1.666D-03	2.03	[illegible]09D-01	1.567D 03	1.556D 03
40	2.823D 02	1.726D 03	2.139D 03	3.777D 03	3.814D 07	1.374D-01	3.129D-03	4.56	[illegible]1D-01	-6.140D 01	-6.516D 01
39	2.751D 02	1.664D 03	2.673D 03	3.934D 03	4.445D 07	1.666D-01	5.404D-03	1.84	[illegible].745D-01	6.711D 02	-6.526D 02
38	2.679D 02	1.593D 03	2.463D 03	3.833D 03	4.038D 07	1.831D-01	7.172D-03	1.570	[illegible].922D-01	1.682D 03	1.689D 03
37	2.606D 02	1.607D 03	3.015D 03	3.827D 03	3.535D 07	1.008D-01	4.360D-03	2.355D	[illegible]074D-01	1.832D 03	1.060D 03
36	2.534D 02	1.589D 03	2.871D 03	3.756D 03	3.286D 07	1.010D-01	4.781D-03	1.924D	[illegible].080D-01	2.456D 03	1.464D 03
35	2.461D 02	1.561D 03	2.923D 03	3.690D 03	3.015D 07	8.831D-02	4.609D-03	2.097D 00	9.492D-02	3.607D 03	6.903D 02
34	2.389D 02	1.512D 03	2.917D 03	3.843D 03	1.956D 07	5.009D-02	2.700D-03	9.814D-01	5.488D-02	6.758D 03	1.756D 02
33	2.317D 02	1.534D 03	2.286D 03	3.797D 03	1.601D 07	1.808D-02	1.108D-03	1.158D-01	2.193D-02	4.456D 03	2.616D 04
32	2.244D 02	1.731D 03	3.791D 03	3.934D 03	3.255D 07	1.323D-03	6.469D-05	3.384D-01	7.429D-03	2.274D 03	7.151D 03
31	2.172D 02	1.703D 03	3.963D 03	4.041D 03	3.210D 07	3.185D-03	1.824D-04	1.239D 00	8.407D-03	5.300D 02	2.730D 03
30	2.099D 02	1.717D 03	3.734D 03	3.931D 03	3.348D 07	9.738D-03	5.480D-04	1.451D 00	1.533D-02	1.040D 03	-1.596D 03
29	2.027D 02	1.713D 03	2.502D 03	3.874D 03	3.289D 07	2.244D-02	1.149D-03	1.808D-01	2.932D-02	6.003D 02	4.332D 03
28	1.955D 02	1.722D 03	3.816D 03	4.068D 03	3.527D 07	1.289D-02	5.076D-04	1.486D 00	1.847D-02	3.354D 02	1.138D 03
27	1.882D 02	1.717D 03	2.031D 03	4.043D 03	3.711D 07	8.892D-02	2.619D-03	1.965D-01	9.668D-02	4.983D 02	5.006D 02
26	1.810D 02	1.713D 03	2.364D 03	4.031D 03	3.455D 07	3.915D-02	1.382D-03	2.136D-01	4.607D-02	4.127D 01	4.552D 01
25	1.737D 02	1.700D 03	1.700D 03	0.0	2.972D 07	9.735D-03	5.719D-04	0.0	1.601D-02	-9.191D 02	3.319D 03
24	1.665D 02	1.685D 03	4.130D 03	4.153D 03	3.081D 07	8.050D-04	4.318D-05	1.329D 00	5.452D-03	-1.857D 03	-9.382D 03
23	1.593D 02	1.665D 03	3.801D 03	4.008D 03	2.751D 07	2.886D-03	2.866D-04	4.254D-01	7.940D-03	-7.926D 02	-7.548D 03
22	1.520D 02	1.621D 03	3.766D 03	3.828D 03	2.459D 07	3.644D-03	1.064D-03	1.769D 00	8.021D-03	-2.052D 03	-8.883D 03
21	1.448D 02	1.570D 03	3.634D 03	3.698D 03	1.905D 07	3.160D-03	8.792D-04	1.310D 00	6.898D-03	-3.516D 03	-1.071D 04
20	1.376D 02	1.536D 03	3.626D 03	3.689D 03	1.551D 07	2.404D-03	5.943D-04	1.145D 00	5.468D-03	-4.511D 03	-1.527D 04
19	1.303D 02	1.492D 03	3.507D 03	3.600D 03	1.195D 07	1.573D-03	3.815D-04	4.704D-01	4.157D-03	-5.965D 03	-2.667D 04
18	1.231D 02	1.211D 03	3.306D 03	3.577D 03	4.480D 06	4.253D-03	1.042D-03	3.742D-01	5.694D-03	-7.223D 03	-1.161D 04
17	1.158D 02	1.035D 03	2.671D 03	3.573D 03	6.844D 06	1.271D-02	3.292D-03	2.991D-01	1.608D-02	-7.610D 03	-8.478D 03
16	1.086D 02	9.707D 02	1.638D 03	3.566D 03	6.698D 06	1.933D-02	5.497D-03	7.705D-02	2.487D-02	-6.979D 03	-1.973D 03
15	1.014D 02	9.264D 02	2.409D 03	3.563D 03	5.530D 06	9.080D-03	3.094D-03	1.230D-01	1.220D-02	-6.885D 03	-6.889D 03
14	9.411D 01	9.046D 02	2.522D 03	3.561D 03	1.013D 07	1.525D-02	5.515D-03	2.752D-01	2.078D-02	-7.627D 03	-5.014D 03
13	8.687D 01	9.157D 02	2.513D 03	3.577D 03	8.582D 06	1.676D-02	4.638D-03	2.341D-01	2.141D-02	-6.826D 03	-6.823D 03
12	7.963D 01	1.051D 03	1.962D 03	3.582D 03	6.522D 06	4.754D-02	3.949D-03	3.603D-01	5.158D-02	0.0	-3.749D 03
11	7.240D 01	1.297D 03	2.512D 03	3.850D 03	1.654D 07	1.728D-01	4.002D-03	1.667D 00	1.772D-01	-7.214D 03	-7.210D 03
10	6.516D 01	1.357D 03	2.352D 03	4.055D 03	8.005D 06	2.141D-01	2.157D-04	1.779D 00	2.143D-01	-4.065D 03	-2.881D 03
9	5.792D 01	1.625D 03	2.135D 03	3.375D 03	2.034D 07	3.028D-01	0.0	1.439D 00	3.043D-01	-4.479D 03	-4.546D 03
8	5.068D 01	1.674D 03	2.315D 03	3.193D 03	2.507D 07	3.431D-01	0.0	3.827D 00	3.431D-01	-4.979D 03	-5.014D 03
7	4.344D 01	1.626D 03	2.227D 03	3.071D 03	2.025D 07	3.780D-01	0.0	3.721D 00	3.780D-01	-4.857D 03	-5.014D 03
6	3.620D 01	1.596D 03	0.0	0.0	1.970D 07	1.312D-01	0.0	0.0	1.318D-01	0.0	-4.995D 03
5	2.896D 01	7.586D 02	0.0	0.0	1.721D 07	8.222D-01	0.0	0.0	8.222D-01	0.0	-4.930D 03
4	2.172D 01	7.467D 02	0.0	0.0	1.456D 07	8.266D-01	0.0	0.0	8.266D-01	0.0	-4.915D 03
3	1.448D 01	7.321D 02	0.0	0.0	1.190D 07	8.276D-01	0.0	0.0	8.276D-01	0.0	-4.911D 03
2	7.240D 00	7.166D 02	0.0	0.0	9.249D 06	8.278D-01	0.0	0.0	8.278D-01	0.0	-4.910D 03
1	0.0	7.017D 02	0.0	0.0	6.595D 06	8.279D-01	0.0	0.0	8.279D-01	0.0	-4.910D 03

SAMPLE PROBLEM FOR LOF-TOP CONDITIONS
INITIALLY 2 FAILURE CELLS, PARTIALLY VOIDED CHANNEL, NORM. POWER AT 439

TIME= 4.9932D-02 DELT= 2.8958D-05 NORMALIZED POWER= 2.3098D-04
FCI BOUNDARIES IN CELLS 1 AND 50 FCIL= 7.2395D-01 FCIU= 3.5727D 02 HIGHEST FAILURE CELL IS 30
6.7847D 01 GRAMS FUEL IN 87 GROUPS XMIN= 7.2395D-01 XMAX= 3.5667D 02 LOWEST FAILURE CELL IS 22
REACTIVITY CHANGES-- SODIUM= 0.0 TOTAL FUEL= 0.0 TOTAL= 0.0 PIN FUEL= 0.0 CHANNEL FUEL= 0.0

*** FUEL PIN QUANTITIES ***

*** REACTIVITIES ***

J	POSITION OF CELL BOTTOM	FUEL TEMPRTURE TFUP	CAVITY PRESSURE PF	FUEL DENSITY ROFUP	FIS.GAS DENSITY ROGFP	CAVITY AREA AF	FUEL+FGAS VELOCITY UF	CLAD TEMPRTURE TCL	PIN FUEL REACTIVTY CHANGE	CHAN FUEL REACTIVTY CHANGE	TOTL FUEL REACTIVTY CHANGE
50	3.547D 02	0.0	0.0	0.0	0.0	0.0	0.0	1.184D 03	0.0	0.0	0.0
49	3.475D 02	0.0	0.0	0.0	0.0	0.0	0.0	1.214D 03	0.0	0.0	0.0
48	3.403D 02	0.0	0.0	0.0	0.0	0.0	0.0	1.230D 03	0.0	0.0	0.0
47	3.330D 02	0.0	0.0	0.0	0.0	0.0	0.0	1.254D 03	0.0	0.0	0.0
46	3.258D 02	0.0	0.0	0.0	0.0	0.0	0.0	1.285D 03	0.0	0.0	0.0
45	3.185D 02	0.0	0.0	0.0	0.0	0.0	0.0	1.328D 03	0.0	0.0	0.0
44	3.113D 02	0.0	0.0	0.0	0.0	0.0	0.0	1.371D 03	0.0	0.0	0.0
43	3.041D 02	0.0	0.0	0.0	0.0	0.0	0.0	1.422D 03	0.0	0.0	0.0
42	2.968D 02	0.0	0.0	0.0	0.0	0.0	0.0	1.467D 03	0.0	0.0	0.0
41	2.896D 02	0.0	0.0	0.0	0.0	0.0	0.0	1.521D 03	0.0	0.0	0.0
40	2.823D 02	0.0	0.0	0.0	0.0	0.0	0.0	1.528D 03	0.0	0.0	0.0
39	2.751D 02	0.0	0.0	0.0	0.0	0.0	0.0	1.497D 03	0.0	0.0	0.0
38	2.679D 02	0.0	0.0	0.0	0.0	0.0	0.0	1.497D 03	0.0	0.0	0.0
37	2.606D 02	0.0	0.0	0.0	0.0	0.0	0.0	1.510D 03	0.0	0.0	0.0
36	2.534D 02	0.0	0.0	0.0	0.0	0.0	0.0	1.511D 03	0.0	0.0	0.0
35	2.461D 02	0.0	0.0	0.0	0.0	0.0	0.0	1.505D 03	0.0	0.0	0.0
34	2.389D 02	0.0	0.0	0.0	0.0	0.0	0.0	1.504D 03	0.0	0.0	0.0
33	2.317D 02	0.0	0.0	0.0	0.0	0.0	0.0	1.544D 03	0.0	0.0	0.0
32	2.244D 02	3.362D 03	2.001D 07	3.664D 00	5.101D-03	2.319D-02	1.233D 02	1.700D 03	0.0	0.0	0.0
31	2.172D 02	3.484D 03	1.924D 07	3.176D 00	5.172D-03	1.391D-01-6.113D 01		1.700D 03	0.0	0.0	0.0
30	2.099D 02	3.623D 03	2.017D 07	3.068D 00	5.252D-03	1.855D-01-6.187D 01		1.700D 03	0.0	0.0	0.0
29	2.027D 02	3.781D 03	2.074D 07	2.953D 00	5.141D-03	2.087D-01-1.151D 02		1.700D 03	0.0	0.0	0.0
28	1.955D 02	3.942D 03	2.265D 07	2.993D 00	5.122D-03	2.087D-01-2.108D 02		1.700D 03	0.0	0.0	0.0
27	1.882D 02	4.069D 03	2.505D 07	3.078D 00	5.154D-03	2.087D-01-1.746D 02		1.700D 03	0.0	0.0	0.0
26	1.810D 02	4.155D 03	2.805D 07	3.219D 00	5.328D-03	2.087D-01-1.172D 02		1.700D 03	0.0	0.0	0.0
25	1.737D 02	4.185D 03	2.935D 07	3.260D 00	5.430D-03	2.087D-01 4.151D 00		1.700D 03	0.0	0.0	0.0
24	1.665D 02	4.150D 03	2.916D 07	3.247D 00	5.574D-03	2.087D-01 2.364D 02		1.700D 03	0.0	0.0	0.0
23	1.593D 02	4.059D 03	2.991D 07	3.353D 00	6.030D-03	2.087D-01 2.374D 02		1.700D 03	0.0	0.0	0.0
22	1.520D 02	3.883D 03	2.897D 07	3.407D 00	6.393D-03	1.855D-01 1.218D 02		1.700D 03	0.0	0.0	0.0
21	1.448D 02	3.478D 03	2.859D 07	3.643D 00	7.060D-03	1.623D-01-9.875D 01		1.692D 03	0.0	0.0	0.0
20	1.376D 02	3.335D 03	2.852D 07	3.737D 00	7.239D-03	4.638D-02 0.0		1.619D 03	0.0	0.0	0.0
19	1.303D 02	0.0	0.0	0.0	0.0	0.0	0.0	1.545D 03	0.0	0.0	0.0
18	1.231D 02	0.0	0.0	0.0	0.0	0.0	0.0	1.257D 03	0.0	0.0	0.0
17	1.158D 02	0.0	0.0	0.0	0.0	0.0	0.0	1.102D 03	0.0	0.0	0.0
16	1.086D 02	0.0	0.0	0.0	0.0	0.0	0.0	1.007D 03	0.0	0.0	0.0
15	1.014D 02	0.0	0.0	0.0	0.0	0.0	0.0	9.572D 02	0.0	0.0	0.0
14	9.411D 01	0.0	0.0	0.0	0.0	0.0	0.0	9.095D 02	0.0	0.0	0.0
13	8.687D 01	0.0	0.0	0.0	0.0	0.0	0.0	9.131D 02	0.0	0.0	0.0
12	7.963D 01	0.0	0.0	0.0	0.0	0.0	0.0	9.040D 02	0.0	0.0	0.0
11	7.240D 01	0.0	0.0	0.0	0.0	0.0	0.0	9.020D 02	0.0	0.0	0.0
10	6.516D 01	0.0	0.0	0.0	0.0	0.0	0.0	8.941D 02	0.0	0.0	0.0
9	5.792D 01	0.0	0.0	0.0	0.0	0.0	0.0	8.817D 02	0.0	0.0	0.0
8	5.068D 01	0.0	0.0	0.0	0.0	0.0	0.0	8.789D 02	0.0	0.0	0.0
7	4.344D 01	0.0	0.0	0.0	0.0	0.0	0.0	8.721D 02	0.0	0.0	0.0
6	3.620D 01	0.0	0.0	0.0	0.0	0.0	0.0	8.643D 02	0.0	0.0	0.0
5	2.896D 01	0.0	0.0	0.0	0.0	0.0	0.0	8.566D 02	0.0	0.0	0.0
4	2.172D 01	0.0	0.0	0.0	0.0	0.0	0.0	8.505D 02	0.0	0.0	0.0

3	1.448D 01	0.0	0.0	0.0	0.0	0.0	0.0	8.426D 02	0.0	0.0	0.0
2	7.240D 00	0.0	0.0	0.0	0.0	0.0	0.0	8.340D 02	0.0	0.0	0.0
1	0.0	0.0	0.0	0.0	0.0	0.0	0.0	1.362D 03	0.0	0.0	0.0

*** CHANNEL QUANTITIES ***

J	POSITION OF CELL BOTTOM	SODIUM TEMPRTURE TNA	FIS.GAS TEMPRTURE TFG	FUEL TEMPRTURE TFU	TOTAL PRESSURE PM	LIQ. NA DENSITY ROSLC	FIS.GAS DENSITY ROFGC	FUEL DENSITY ROFPC	NA+FISGAS DENSITY ROMC	FUEL VELOCITY UP	NA+FISGAS VELOCITY UM
50	3.547D 02	1.582D 03	2.091D 03	2.857D 03	9.024D 06	1.730D-01	0.0	1.544D 00	1.730D-01	-5.425D 01	-3.967D 02
49	3.475D 02	1.490D 03	1.810D 03	2.857D 03	1.042D 07	3.405D-01	0.0	1.349D 00	3.412D-01	0.0	-4.792D 02
48	3.403D 02	1.469D 03	1.894D 03	3.070D 03	9.355D 06	4.497D-01	0.0	2.078D 00	4.499D-01	1.533D 03	1.578D 03
47	3.330D 02	1.474D 03	0.0	0.0	9.596D 06	2.171D-01	0.0	0.0	2.185D-01	2.245D 03	2.243D 03
46	3.258D 02	1.527D 03	1.750D 03	3.071D 03	1.525D 07	5.150D-01	6.217D-04	1.142D 00	5.159D-01	0.0	1.420D 03
45	3.185D 02	1.522D 03	1.748D 03	3.476D 03	1.802D 07	2.939D-01	2.289D-03	5.208D-01	2.975D-01	1.834D 03	2.568D 03
44	3.113D 02	1.554D 03	2.254D 03	3.474D 03	1.751D 07	1.148D-01	1.357D-03	8.546D-01	1.184D-01	1.538D 03	1.079D 03
43	3.041D 02	1.527D 03	2.102D 03	3.696D 03	1.996D 07	1.656D-01	3.064D-03	7.996D-01	1.705D-01	1.283D 03	1.284D 03
42	2.968D 02	1.549D 03	2.895D 03	3.717D 03	1.816D 07	4.858D-02	1.358D-03	1.016D 00	5.240D-02	1.595D 03	2.921D 03
41	2.896D 02	1.566D 03	1.859D 03	3.347D 03	1.924D 07	8.290D-02	2.567D-03	2.177D-01	8.828D-02	0.0	2.927D 03
40	2.823D 02	1.604D 03	2.965D 03	3.705D 03	2.244D 07	4.211D-02	1.350D-03	1.056D 00	4.663D-02	-5.580D 02	-5.578D 02
39	2.751D 02	1.529D 03	1.979D 03	3.596D 03	1.981D 07	1.041D-01	3.965D-03	3.922D-01	1.103D-01	1.215D 03	3.294D 03
38	2.679D 02	1.585D 03	3.244D 03	3.707D 03	2.312D 07	4.132D-02	1.818D-03	1.963D 00	4.567D-02	1.163D 03	3.088D 03
37	2.606D 02	1.609D 03	2.725D 03	3.639D 03	2.630D 07	6.511D-02	2.969D-03	1.082D 00	7.115D-02	1.980D 03	4.156D 03
36	2.534D 02	1.645D 03	2.683D 03	3.602D 03	2.880D 07	5.357D-02	2.516D-03	1.238D 00	5.966D-02	2.007D 03	3.626D 03
35	2.461D 02	1.674D 03	3.149D 03	3.565D 03	3.251D 07	4.690D-02	2.236D-03	2.325D 00	5.253D-02	4.844D 02	4.803D 02
34	2.389D 02	1.679D 03	3.078D 03	3.770D 03	3.642D 07	6.681D-02	3.259D-03	1.869D 00	7.366D-02	-9.293D 01	-9.344D 01
33	2.317D 02	1.686D 03	3.067D 03	3.863D 03	3.751D 07	6.844D-02	3.354D-03	1.646D 00	7.560D-02	-3.869D 02	-3.883D 02
32	2.244D 02	1.726D 03	2.373D 03	3.789D 03	4.102D 07	9.483D-02	4.439D-03	6.158D-01	1.042D-01	1.173D 03	-6.579D 01
31	2.172D 02	1.735D 03	3.236D 03	4.048D 03	3.993D 07	4.210D-02	1.801D-03	1.100D 00	4.922D-02	8.991D 02	9.031D 02
30	2.099D 02	1.704D 03	3.343D 03	4.024D 03	3.195D 07	1.066D-02	3.336D-04	3.584D-01	1.654D-02	7.212D 02	7.215D 02
29	2.027D 02	1.702D 03	2.381D 03	3.962D 03	3.136D 07	2.095D-02	6.574D-04	1.246D-01	2.716D-02	0.0	2.171D 03
28	1.955D 02	1.701D 03	2.465D 03	4.020D 03	3.148D 07	1.428D-02	4.574D-04	9.939D-02	2.035D-02	5.270D 02	5.272D 02
27	1.882D 02	1.701D 03	2.759D 03	3.993D 03	3.121D 07	1.128D-02	3.816D-04	1.342D-01	1.728D-02	9.899D 01	4.717D 02
26	1.810D 02	1.702D 03	2.165D 03	3.939D 03	3.132D 07	2.408D-02	8.259D-04	8.797D-02	3.045D-02	8.475D 01	8.444D 01
25	1.737D 02	1.700D 03	4.131D 03	4.131D 03	3.202D 07	0.0	0.0	2.219D-04	5.801D-03	0.0	-1.342D 04
24	1.665D 02	1.700D 03	1.700D 03	0.0	2.916D 07	1.690D-02	1.066D-03	0.0	2.361D-02	0.0	7.554D 03
23	1.593D 02	1.709D 03	3.689D 03	3.914D 03	3.073D 07	9.330D-05	4.689D-07	1.167D-02	6.091D-03	-2.988D 01	-7.396D 03
22	1.520D 02	1.700D 03	3.897D 03	3.905D 03	2.969D 07	7.507D-05	1.753D-05	3.517D-01	5.653D-03	-6.650D 02	-1.010D 04
21	1.448D 02	1.692D 03	3.565D 03	3.879D 03	2.863D 07	9.490D-04	5.870D-05	7.843D-02	6.552D-03	-1.797D 03	-7.795D 03
20	1.376D 02	1.649D 03	3.555D 03	3.847D 03	2.391D 07	1.167D-03	1.652D-05	1.051D-01	5.831D-03	-2.350D 03	-6.410D 03
19	1.303D 02	1.639D 03	3.649D 03	3.848D 03	2.294D 07	3.142D-04	1.312D-06	4.098D-02	4.820D-03	-5.547D 03	-2.883D 04
18	1.231D 02	1.471D 03	4.124D 03	4.130D 03	1.382D 07	5.885D-05	1.461D-06	1.283D 00	1.887D-03	-5.982D 03	-3.440D 04
17	1.158D 02	1.359D 03	3.603D 03	3.822D 03	6.159D 06	3.898D-04	1.015D-06	4.919D-02	1.524D-03	-8.557D 03	-5.000D 04
16	1.086D 02	1.183D 03	3.730D 03	3.814D 03	2.580D 06	3.451D-04	1.449D-06	1.410D-01	6.801D-04	-1.063D 04	-5.000D 04
15	1.014D 02	9.835D 02	3.434D 03	3.806D 03	1.393D 06	1.866D-03	3.706D-06	1.502D-01	1.917D-03	-1.058D 04	-3.361D 04
14	9.411D 01	9.304D 02	2.623D 03	3.798D 03	1.273D 06	4.845D-03	6.008D-06	7.037D-02	4.875D-03	-1.088D 04	-1.873D 04
13	8.687D 01	9.191D 02	2.131D 03	3.796D 03	1.251D 06	3.947D-03	5.267D-06	3.312D-02	3.974D-03	-1.261D 04	-1.505D 04
12	7.963D 01	9.077D 02	2.396D 03	3.792D 03	1.395D 06	6.822D-03	1.142D-04	8.539D-02	6.954D-03	-1.251D 04	-1.117D 04
11	7.240D 01	9.079D 02	2.497D 03	3.774D 03	2.983D 06	2.543D-02	1.044D-03	3.471D-01	2.649D-02	-1.310D 04	-5.389D 03
10	6.516D 01	8.979D 02	9.231D 02	3.758D 03	1.803D 06	1.741D-02	1.212D-03	2.422D-03	1.863D-02	0.0	-2.335D 03
9	5.792D 01	8.913D 02	3.424D 03	3.794D 03	4.181D 06	1.016D-02	1.186D-03	7.346D-01	1.136D-02	-7.362D 03	-3.295D 03
8	5.068D 01	8.875D 02	3.593D 03	3.814D 03	5.046D 06	7.578D-03	1.378D-03	9.964D-01	8.968D-03	-8.277D 03	-4.352D 03
7	4.344D 01	8.801D 02	3.349D 03	3.767D 03	6.297D 06	1.012D-02	2.150D-03	6.581D-01	1.228D-02	-7.421D 03	-6.660D 03
6	3.620D 01	8.724D 02	3.285D 03	3.697D 03	5.486D 06	1.004D-02	1.995D-03	5.601D-01	1.205D-02	-6.248D 03	-3.102D 03
5	2.896D 01	8.798D 02	3.595D 03	3.836D 03	7.351D 06	1.286D-02	1.972D-03	1.662D 00	1.484D-02	-5.569D 03	-5.571D 03
4	2.172D 01	8.720D 02	3.016D 03	3.702D 03	9.085D 06	2.963D-02	3.492D-03	1.044 00	3.313D-02	-5.895D 03	-4.036D 03
3	1.448D 01	8.654D 02	1.968D 03	3.584D 03	6.411D 06	4.737D-02	4.116D-03	3.304D-01	5.150D-02	-5.684D 03	-5.684D 03
2	7.240D 00	8.586D 02	1.425D 03	3.568D 03	5.548D 06	7.632D-02	4.761D-03	2.273D-01	8.109D-02	-5.668D 03	-5.684D 03
1	0.0	2.035D 03	2.274D 03	3.071D 03	5.535D 06	1.561D 00	1.562D-02	7.652D 00	1.576D 00	-5.674D 03	-5.684D 03

are displayed. Next, data for the whole r-z fuel mesh is displayed when NPRAD > 0. This data includes, for each axial cell, the fuel outer radius, the outermost radial subcell that is fully molten, the outer radius of each radial cell, the total cross-sectional area out to and including each radial subcell, the temperature fraction of heat of fusion satisfied, mass and fission gas to fuel mass ratio for each radial subcell.

Some selections from the output for the transient are provided. The printout at t = 0 shows conditions as input but after the first ejection of fuel and fission gas into the coolant channel. Notice that the lower sodium slug interface has moved from 194.7 in cell 27 to 181.4 in cell 26 because fuel was ejected into the channel at 181.4 cm and the slug interface was automatically redefined to be at that location. About 0.9 gm of fuel was ejected at t = 0 and this was divided into 10 particle groups. The cavity pressure reflects the final equilibrated values after ejection in ejection cells 26 and 27. The same is true of the fission gas and fuel smear densities in the pin. The smear density of fission gas and fuel in the coolant channel reflects the ejection as well. The channel pressure in the lower slug is entirely changed as a result of the ejection. The pressure in cells 26 and 27 is the equilibrated pressure after ejection but the pressures in the single-phase lower slug are merely linear interpolations between the inlet pressure and the interface cell pressure (in this case 1.15×10^8 dynes/cm^2 in cell 26). This interpolation and linear pressure drop in the slugs is assumed throughout the calculation.

The next printout is from approximately 5 msec. The upper slug interface has not moved much since it has been essentially insulated from the high pin failure pressures by the long voided portion of the channel. The lower slug interface has moved downward partially as a result of the extension of the clad rip downwards (it has also extended upwards) as the molten fuel cavity expanded (the option of extending the clad rip to cells with 8 radial subcells fully molten was specified and this extended the failure upwards to cell 30 and downwards to cell 22) considerably with the high power level. It is noted from the printout of the cavity area that the cavity has expanded radially significantly and axially it was extended 2 cells on the bottom and 1 on the top. In the coolant channel, it is seen that considerable fuel and fission gas has been ejected (36 gm fuel) and there is a significant FCI (peak sodium temperature 1789K).

The printout at about 10 msec shows somewhat similar conditions in the pin cavity as at 5 msec. There has been considerable motion of material in the coolant channel, however and the FCI has increased (1941K peak sodium temperature. By about 30 msec into the transient, the pin pressure has been considerably reduced, and there has been extensive material motion in the coolant channel. The fuel moving upwards in the coolant channel has almost caught up with the upper slug interface (XMAX = 309.1, FCIU = 319.5). The printout at 49 msec shows a further progression of essentially the same trends.

APPENDIX A

ENERGY DIVISION ALGORITHM FOR SODIUM: ENERGY REQUIRED FOR BOILING VERSUS HEATING THE LIQUID PHASE

Assumptions

1. The vapor phase can be treated like an ideal gas.

2. The two-phase mixture follows the saturation line [for which we have an expression: $P_{sat} = P_{sat}(T)$].

3. Changes in volume fractions can be ignored as an effect.

4. Condensation on cladding does not affect the energy apportionment between the two phases.

Since the ideal gas law gives PV = MRT, and M_{vap}, the mass of the vapor, is changing due to boiling and due to ΔT,

$$\frac{M^2_{vap}}{M^1_{vap}} = \frac{T^1}{T^2}\frac{P^2}{P^1} = \frac{T^1}{P^1}\frac{P_{sat}(T^2)}{P_{sat}(T^1)}, \tag{A.1}$$

Then,

$$\frac{M^2_{vap}}{M^1_{vap}} = \left(\frac{T^1}{T^1 + \Delta T}\right)\cdot\left[\frac{P_{sat}(T^1 + \Delta T)}{P_{sat}(T^1)}\right] \tag{A.2}$$

or

$$\frac{M^2_{vap}}{M^1_{vap}} = \frac{1}{1 + \frac{\Delta T}{T^1}} \times \frac{P_{sat}\,[T^1 + \Delta T]}{P_{sat}(T^1)}\ ; \tag{A.3}$$

now,

$$\frac{M^2_{vap}}{M^1_{vap}} = \frac{M^1_{vap} + \Delta M_{vap}}{M^1_{vap}} \tag{A.4}$$

and

$$P_{sat}(T^1 + \Delta T) \simeq P_{sat}(T^1) + \Delta T \frac{dP_{sat}(T^1)}{dT} , \tag{A.5}$$

so that

$$\frac{M^2_{vap}}{M^1_{vap}} = \frac{M^1_{vap} + \Delta M_{vap}}{M^1_{vap}} \simeq \left(\frac{1}{1 + \frac{\Delta T}{T^1}}\right) \cdot \left[\frac{P_{sat}(T^1) + \Delta T \frac{dP_{sat}(T^1)}{dT}}{P_{sat}(T^1)}\right] \tag{A.6}$$

$$\frac{M^1_{vap} + \Delta M_{vap}}{M^1_{vap}} \simeq \left(1 - \frac{\Delta T}{T^1}\right) \cdot \left[1 + \Delta T \cdot \frac{\frac{dP_{sat}(T^1)}{dT}}{P_{sat}(T^1)}\right] \tag{A.7}$$

so that

$$\frac{M^1_{vap} + \Delta M_{vap}}{M^1_{vap}} \simeq 1 + \Delta T \left[\frac{dP_{sat}(T^1)}{dT} \cdot \frac{1}{P_{sat}(T^1)} - \frac{1}{T^1}\right] , \tag{A.8}$$

$$\Delta M_{vap} \simeq M^1_{vap} \Delta T \left[\frac{dP_{sat}(T^1)}{dT} \cdot \frac{}{P_{sat}(T^1)} - \frac{1}{T^1}\right] . \tag{A.9}$$

Now, from the Clausius-Clapyron equation,

$$\rho_{vap} \cdot H_{fg} = T \frac{dP_{sat}}{dT} , \tag{A.10}$$

and we realize that energy that goes into generating ΔM_{vap} is

$$\Delta E_{vap} = H_{fg} \Delta M_{vap} \text{ and } M^1_{vap} = \rho^1_{vap} \cdot V^1_{vap} \tag{A.11}$$

so,

$$\Delta E_{vap} = H_{fg} \cdot \rho^{1}_{vap} \cdot V^{1}_{vap} \cdot \Delta T \times \left[\frac{dP_{sat}(T^{1})}{T} \cdot \frac{1}{P_{sat}(T^{1})} - \frac{1}{T^{1}} \right] \quad (A.12)$$

and

$$H_{fg} \rho^{1}_{vap} = T^{1} \cdot \frac{dP_{sat}(T^{1})}{dT} \cdot \quad (A.13)$$

so

$$\Delta E_{vap} = T^{1} \cdot \frac{dP_{sat}(T^{1})}{dT} \cdot V^{1}_{vap} \times \left[\frac{dP_{sat}(T^{1})}{dT} \cdot \frac{1}{P_{sat}(T^{1})} - \frac{1}{T^{1}} \right] \cdot \Delta T. \quad (A.14)$$

Now we realize that to heat up the liquid (ignoring ΔM_{vap}) that

$$\Delta E_{liq} = \rho_{liq} \cdot V_{liq} \cdot C_{P,liq} \cdot \Delta T \, , \quad (A.15)$$

and since we follow the saturation curve, $\Delta T = \Delta T_{vap} = \Delta T_{liq}$, so

$$\frac{\Delta E_{vap}}{\Delta E_{liq}} = \frac{T^{1} \cdot \frac{dP_{sat}(T^{1})}{dT} \cdot V^{1}_{vap} \cdot \left[\frac{dP_{sat}(T^{1})}{dT} \cdot \frac{1}{P_{sat}(T^{1})} - \frac{1}{T^{1}} \right]}{\rho_{liq} V_{liq} C_{p,liq}} \cdot \quad (A.16)$$

This expression is accurate up to ~90% of the critical temperature.

APPENDIX B

MATERIAL PROPERTIES USED IN THE PROGRAM

Fuel

The following material properties are treated as constants throughout the calculation and are specified in the input:

Melting temperature
Heat of vaporization
Heat of fusion
Specific heat of liquid fuel
Thermal conductivity for liquid fuel
Gas constant for fuel vapor
Absolute fuel viscosity

The theoretical density of liquid fuel is treated as a constant in the program but the user specifies a temperature as input with which the constant fuel density is calculated from the following function:[19]

$$\rho = \frac{11.08}{1 + 9.3 \cdot 10^{-5} \cdot (T-273)} \qquad (B.1)$$

where ρ is in g/cm^3 and T is in K.

The specific heat of solid fuel is given by the following:[19]

$$C_p = (12.54 + 0.017 \cdot T - 0.117 \cdot 10^{-4} \cdot T^2 + 0.307 \cdot 10^{-8} \cdot T^3) \cdot \frac{4.184 \cdot 10^7}{270.25} \qquad (B.2)$$

where C_p is in ergs/g·K and T is in K.

The vapor pressure of fuel is given by:[20]

$$P_{sat} = \exp[69.979 - \frac{76800}{T} - 4.34 \ln(T)] \qquad (B.3)$$

where P is in $dynes/cm^2$ and T in K.

Sodium

The following material properties are treated as constants throughout the calculation and are specified in the input:

Compressibility of liquid sodium
Speed of sound in liquid sodium
Absolute viscosity of liquid sodium
Absolute viscosity of two-phase sodium

The theoretical density of liquid sodium is given by the following function:[6]

$$\rho_{liq} = 0.1818 + 0.756428 \cdot (1.0 - T \cdot 0.0003659)^{0.586885} \qquad (B.4)$$

where ρ is in g/cm^3 and T in K

The theoretical density of sodium vapor is given by the following funtion:[19]

$$\rho_{vap} = \left(\frac{H_{fg}}{T \cdot \frac{dP_{sat}}{dT}} + \frac{1}{\rho_{liq}} \right)^{-1} \qquad (B.5)$$

where H_{fg} and P_{sat} are given below and T is in K.

The specific heat of liquid sodium is given by the following:[19]

$$C_p = 0.85563 \cdot 10^7 + 0.3808 \cdot 10^7 / (1.0 - T/2733)^{0.5738} \qquad (B.6)$$

where C_p is in ergs/g·K and T is in K.

The specific heat of sodium vapor is given by the following:[19]

$$C_p = 0.85563 \cdot 10^7 - 0.3808 \cdot 10^7 / (1.0 - T/2733)^{0.5738} \qquad (B.7)$$

where C_p is in ergs/g·K and T is in K.

The vapor pressure of sodium is given by[21]

$T < 1144$ K

$$P_{sat} = \exp\left[28.4597 - \frac{12818.5}{T} - 0.5 \ln(T)\right] \qquad (B.8)$$

1144 K < T < 1644 K

$$P_{sat} = \exp\left[29.2125 - \frac{12767.8}{T} - 0.61344 \ln(T)\right] \quad (B.9)$$

T > 1644 K

$$P_{sat} = \exp\left[17.4249 - \frac{10461.8}{T} + 0.789 \ln(T)\right] \quad (B.10)$$

where P_{sat} is in dyne/cm^2 and T in K.

The heat of vaporization for sodium is given by [21]

$$H_{fg} = 4.99141.(1.0-T_{Na}/2733)^{0.4262} \quad (B.11)$$

where H_{fg} is in ergs/gm and T is in K.

Cladding

The following material properties are treated as constants throughout the calculation and are specified in the input.

Theoretical density
Melting temperature
Specific heat
Heat of fusion

Fission Gas

The user must specify a gas constant for the ideal gas formulation of fission gas pressure.

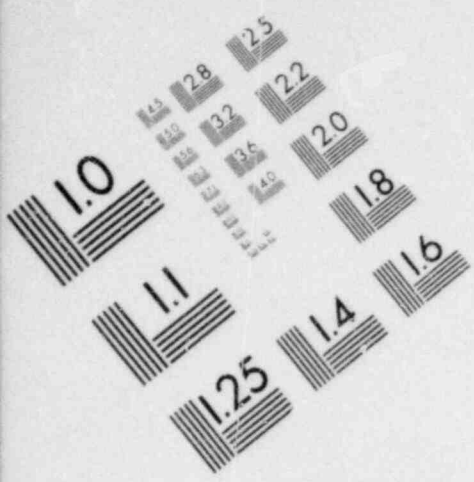

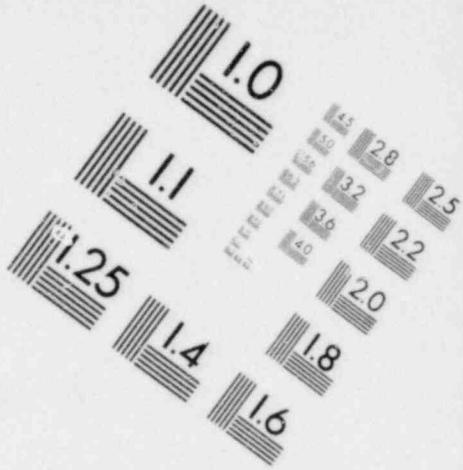

IMAGE EVALUATION
TEST TARGET (MT-3)

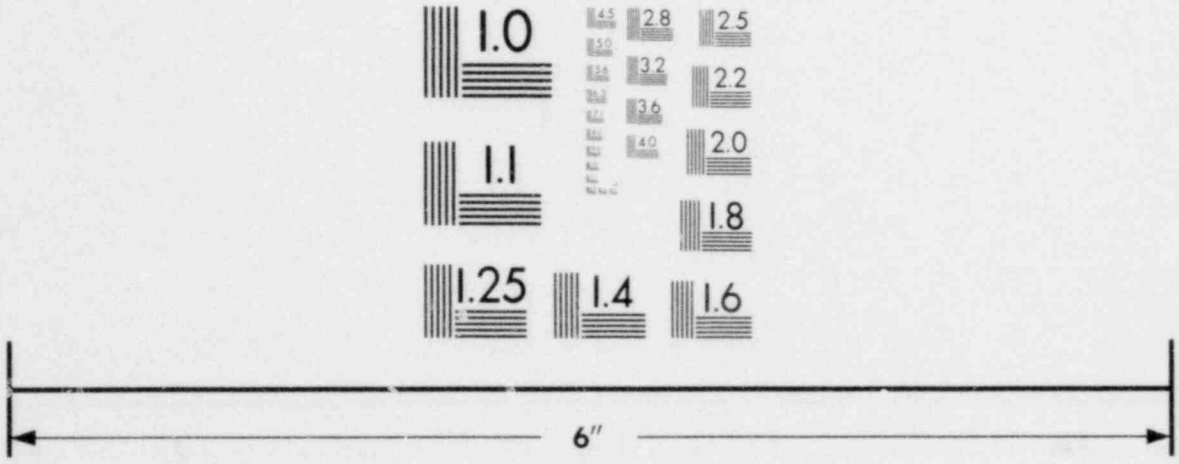

MICROCOPY RESOLUTION TEST CHART

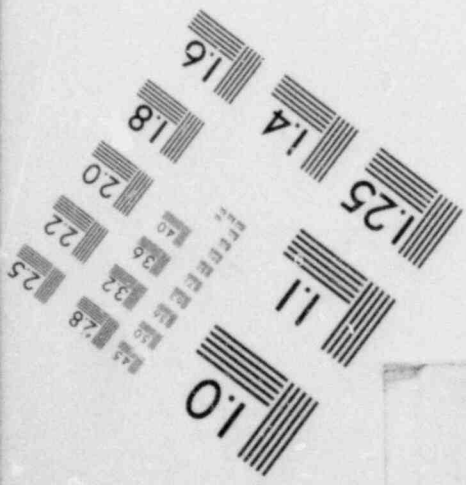

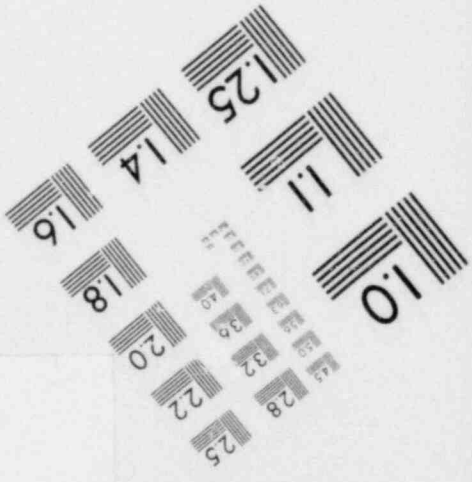

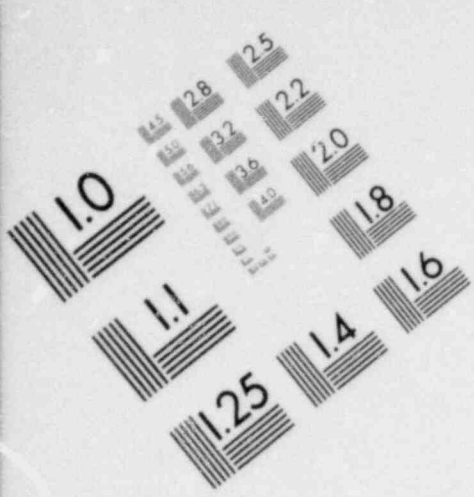

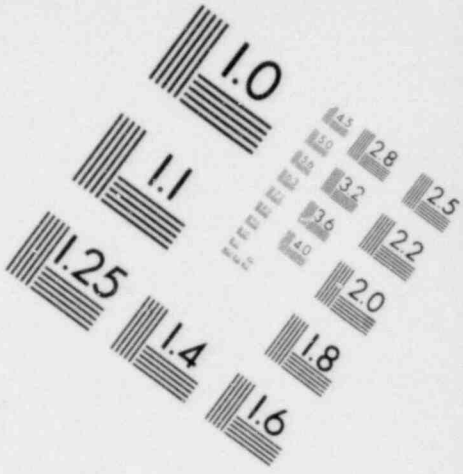

IMAGE EVALUATION
TEST TARGET (MT-3)

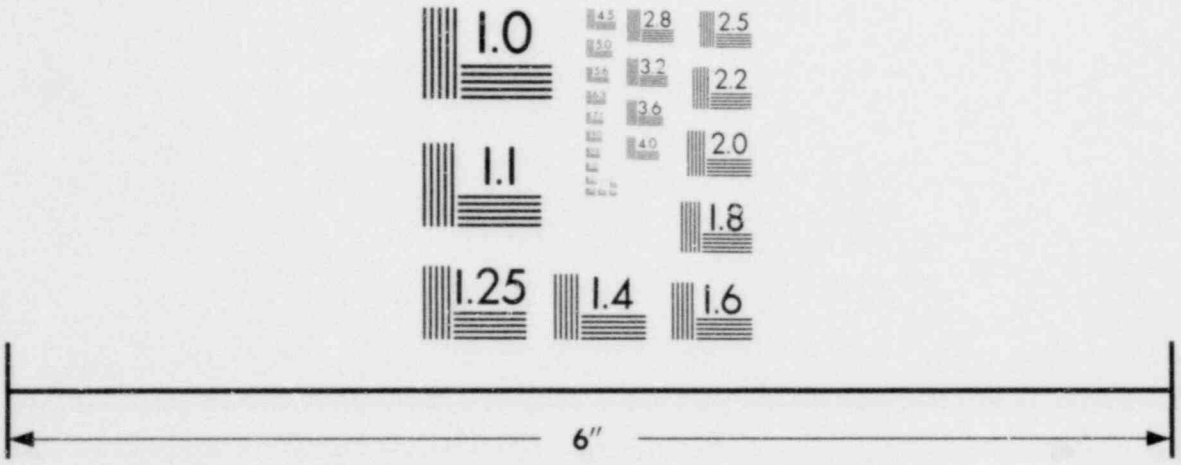

MICROCOPY RESOLUTION TEST CHART

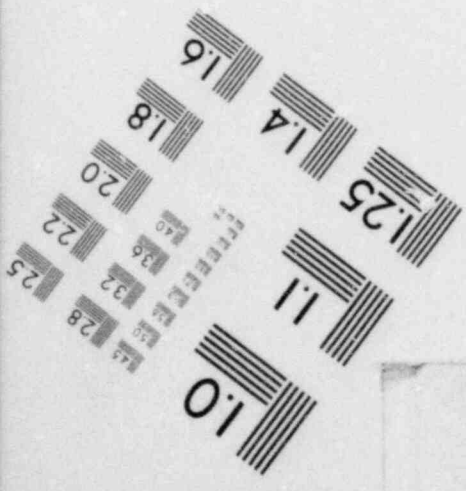

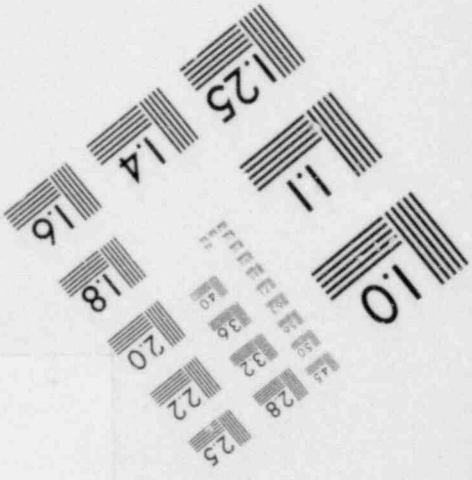

APPENDIX C

DICTIONARY OF VARIABLES IN COMMON STORAGE IN EPIC

Note that for all smear densities in the coolant channel in the slug interface cells, the smear density is the mass of the material in the partial cell on the interaction zone side of the partial cell divided by the total cell volume, not by the partial cell volume. All velocities are values at the bottom edge of their respective cells, i.e., U^i is the velocity of the bottom edge of cell i. With respect to all variables whose values are heights, the bottom of the channel mesh is zero.

The following variables e. have three time values. The variable names ending in 1 are for the beginning of time step values. The variable names ending in 2 are for the beginning of time step values on the first (explicit) pass and on the second pass are for the end of time step values which were calculated during the first (explicit) pass and which are used to form the semi-implicit average values on the second pass. The variable names ending in 3 are for the current end of step value being calculated on each step. Therefore, at the end of the first pass, the 3 values become the 2 values for the second pass. When the differencing in time is strictly explicit, this scheme becomes irrelevant, but the 1, 2 and 3 values function as they do on the first (explicit) pass when the differencing is semi-implicit in time.

Name	Dim.	Unit	Description
AC1	(100)	cm^2	Cross-sectional area of coolant channel by axial cell.
AC2	(100)	cm^2	
AC3	(100)	cm^2	
AF1	(100)	cm^2	Cross-sectional area of molten fuel cavity in the fuel pin by axial cell.
AF2	(100)	cm^2	
AF3	(100)	cm^2	
AM1	(100)	cm^2	Total cross-sectional area of coolant channel minus equivalent cross-sectional area of fuel, i.e., $A_m = A_c - V_{fu}/\Delta z$ where V_{fu} is the volume of all fuel in the cell, Δz the cell height.
AM2	(100)	cm^2	
AM3	(100)	cm^2	
FCIL1	-	cm	Interaction zone/lower sodium slug interface location.
FCIL2	-	cm	
FCIL3	-	cm	
FCIU1	-	cm	Interaction zone/upper sodium slug interface location.
FCIU2	-	cm	
FCIU3	-	cm	
ROFGC1	(100)	g/cm^3	Smear density of fission gas in coolant channel by axial cell.
ROFGC2	(100)	g/cm^3	
ROFGC3	(100)	g/cm^3	

Name	Dim.	Unit	Description
ROFPC1 ROFPC2 ROFPC3	(100) (100) (100)	g/cm3 g/cm3 g/cm3	Smear density of fuel in coolant channel by axial cell obtained by summing all fuel particle groups in a cell and dividing by cell volume.
ROFUP1 ROFUP2 ROFUP3	(100) (100) (100)	g/cm3 g/cm3 g/cm3	Smear density of fuel in the molten fuel cavity in the fuel pin by axial cell.
ROGFP1 ROGFP2 ROGFP3	(100) (100) (100)	g/cm3 g/cm3 g/cm3	Smear density of fission gas in the molten fuel cavity in the fuel pin by axial cell.
ROMC1 ROMC2 ROMC3	(100) (100) (100)	g/cm3 g/cm3 g/cm3	Smear density of two-phase sodium plus fission gas in coolant channel by axial cell.
ROSLC1 ROSLC2 ROSLC3	(100) (100) (100)	g/cm3 g/cm3 g/cm3	Smear density of sodium liquid in the coolant channel by axial cell.
ROSVC1 ROSVC2 ROSVC3	(100) (100) (100)	g/cm3 g/cm3 g/cm3	Smear density of sodium vpaor in the coolant channel by axial cell. (This is not bookkept but calculated every timestep from void fraction and saturation conditions.)
TCL1 TCL2 TCL3	(100) (100) (100)	K K K	Temperature of cladding by axial cell.
TFG1 TFG2 TFG3	(100) (100) (100)	K K K	Temperature of fission gas in coolant channel by axial cell.
TFU1 TFU2 TFU3	(100) (100) (100)	K K K	Average temperature of all fuel particle groups in an axial cell in the coolant channel.
TFUP1 TFUP2 TFUP3	(100) (100) (100)	K K K	Temperature of the fuel/fission gas froth in the molten fuel cavity in the fuel pin by axial cell.
TNA1 TNA2 TNA3	(100) (100) (100)	K K K	Temperature of the two-phase sodium in the coolant channel. In slug interface cells, this is the temperature on the interaction zone side.

Name	Dim.	Unit	Description
UF1 UF2 UF3	(100) (100) (100)	cm/s cm/s cm/s	Velocity of fuel in the molten fuel cavity in the fuel pin by axial cell.
UG1 UG2 UG3	(100) (100) (100)	cm/s cm/s cm/s	Velocity of fission gas in the molten fuel cavity in the fuel pin by axial cell. (At the present time, this is the same as that of the fuel, UF, because no mechanistic calculation of fuel/fission gas slip is done.)
UM1 UM2 UM3	(100) (100) (100)	cm/s cm/s cm/s	Velocity of two-phase sodium and fission gas mixture in coolant channel by axial cell.
UP1 UP2 UP3	(100) (100) (100)	cm/s cm/s cm/s	Average velocity of particle groups centered one-half cell above to one-half cell below node edge by axial cell.

The following variables have only two time values. For these variables, there is no need to store the current calculated end of step value separately, so the newly calculated end of step value is placed immediately in the 2 value, replacing the beginning of time step value on the first pass and replacing the old end of time step value on the second pass.

Name	Dim.	Unit	Description
APER1 APER2	(100) (100)	cm^2 cm^2	The area of cladding available for condensation of sodium or fuel vapor. Set to $2\pi r_{cl} \cdot F/\Delta z$, where r_{cl} is the cladding outer radius, and F is Δz for all axial cells except the interface cells where it is the length of the portion of the cell in the interaction zone.
FGIL1 FGIL2	- -	cm cm	Lower interface position of fission gas within interaction zone.
HFPRZ1 HFPRZ2	(10,100) (10,100)	- -	Fraction of heat of fusion satisfied for each r-z cell in the fuel pin, the first index being for radial subcell.
MELTR1 MELTR2	(100) (100)	- -	The outermost fully molten radial subcell by axial cell.

Name	Dim.	Unit	Description
NFCIL1 NFCIL2	- -	- -	Cell number of lower slug/ interaction zone interface.
NFCIU1 NFCIU2	- -	- -	Cell number of upper slug/ interaction zone interface.
NMP1 NMP2	- -	- -	Number of fuel particle groups in the coolant channel.
PF1 PF2	(100) (100)	dynes/cm^2	Total pressure in the molten fuel cavity in the fuel pin by axial cell.
PM1 PM2	(100) (100)	dynes/cm^2	Total pressure in the coolant channel by axial cell.
PPOS1 PPOS2	(1000)	cm cm	The position of the center of each fuel particle group.
PTMP1 PTMP2	(1000) (1000)	K K	The temperature of each fuel particle group.
PVEL1 PVEL2	(1000) (1000)	cm/s cm/s	The velocity of each fuel particle group.
SVLSI1 SVLSI2	- -	cm^3 cm^3	Volume of single-phase portion of interaction zone/lower slug interface cell except when the interface cell is an ejection cell, in which case this is zero.
SVUSI1 SVUSI2	- -	cm^3 cm^3	Volume of single-phase portion of interaction zone/upper slug interface cell except when the interface cell is an ejection cell, in which case this is zero.
TFPRZ1 TFPRZ2	(10,100) (10,100)	K K	Temperature of each r-z cell in the fuel pin, the first index being for radial subcell. (Only the solid fuel cells are updated during the calculation.)
TLSI1 TLSI2	- -	K K	Temperature of single-phase portion of interaction zone/lower slug interface cell.
TMPPL1 TMPPL2	- -	g/cm^3 g/cm^3	Adjusted smear density of liquid sodium in lower interface cell to provide correct local density in interaction zone portion. TMPPL = ρ_{Na}/ (1 - SVLSI/($A_c \cdot \Delta z$)).

Name	Dim.	Unit	Description
TMPPU1 TMPPU2	- -	g/cm^3 g/cm^3	Adjusted smear density of liquid sodium in upper interface cell to provide correct local density in interaction zone portion. TMPPU = ρ_{Na}/(1 - SVUSI/($A_c \cdot \Delta z$)).
TOTMS1 TOTMS2	- -	g g	Total mass of fuel ejected into coolant channel.
TUSI1 TUSI2	- -	K K	Temperature of single-phase portion of interaction zone/upper slug interface cell.

The following are miscellaneous arrays and variables.

Name	Dim.	Unit	Description
ACLEND	-	cm^2	Area of coolant channel between end of mesh and HLPLEN.
ACUEND	-	cm^2	Area of coolant channel between end of mesh and HUPLEN.
ATEMPX	(10,000)	-	Temporary storage for elements of tri-diagonal matrix used for solution of momentum equations in pin and channel.
ATMP	(1000)	-	Temporary storage
BTEMPX	(100)	-	Temporary storage for constant vector and solution vector in solution of momentum equations in pin and channel.
CLDEN	-	g/cm^3	Cladding density
CLMELT	-	K	Cladding melting temperature
CPCL	-	ergs/g-K	Cladding specific heat
CPFU	-	ergs/g·K	Specific heat of liquid fuel.
CSNDNA	-	cm/s	Speed of sound in liquid sodium.
DCHANL	-	cm	Hydraulic diameter of lower slug.
DCHANU	-	cm	Hydraulic diameter of upper slug.

Name	Dim.	Unit	Description
DELA	(100)	cm^2	Effective area (volume/Δz) of material ejected by axial cell.
DELT	-	s	Time step size.
DELT1	-	s	First time step specified. See input description.
DELT2	-	s	Second time step specified. See input description.
DELT3	-	s	Third time step specified. See input description.
DELZ	-	cm	Eulerian cell height.
EXTIME	-	s	Time after which calculation is explicit in time.
FCI	(100)	ergs/s·cm	Fuel-coolant heat transfer per unit height over a time step.
FDEN	-	g/cm^3	Theoretical density of liquid fuel.
FFCI	-	-	Multiplier applied to heat transfer coefficient between fuel and sodium.
FGFUF	(10,100)	-	Ratio of mass of fission gas to mass of fuel in each r-z cell in fuel pin.
FRACHF	-	-	Not presently used.
FUCOND	-	ergs/cm·K·s	Thermal conductivity of liquid fuel.
GMPN	(10,100)	g	Mass of fuel in each r-z cell in the fuel pin.
HBOND	-	$ergs/K \cdot s \cdot cm^2$	Gap conductance between solid fuel and cladding at cladding inner surface.
HBONDM	-	$ergs/K \cdot s \cdot cm^2$	Gap conductance between molten fuel and cladding at cladding inner surface.
HCFV	-	$ergs/K \cdot s \cdot cm^2$	Condensation heat transfer coefficient for fuel vapor.

Name	Dim.	Unit	Description
HCSL	-	ergs/K•s•cm^2	Heat transfer coefficient between cladding and liquid sodium.
HCSV	-	ergs/K•s•cm^2	Condensation heat transfer coefficient for sodium vapor.
HFGFU	-	ergs/g	Heat of vaporization for fuel.
HLPEN	-	cm	Height of lower plenum free surface.
HSFCL	-	ergs/g	Heat of fusion for cladding.
HSFFU	-	ergs/g	Heat of fusion for fuel.
HUPLEN	-	cm	Height of upper free surface.
ICT	-	-	Counter for turning on printout according to number of time steps between printouts.
ICYCLE	-	-	Counter for turning on plotting data writeout according to number of time steps between writeouts.
IFAIL	(100)	-	Set to one for ejection cells, otherwise zero by axial cell.
IFMAX	-	-	Highest ejection cell.
IFMIN	-	-	Lowest ejection cell.
IIL	-	-	Index of last cell with full density sodium in lower slug at end opposite interaction zone.
IILSLG	-	-	Index of first cell with less than full density sodium on the end of the lower sodium slug opposite to the interaction zone or zero if the slug extends to the bottom of the channel.
IIU	-	-	Index of last cell with full density sodium in upper slug at end opposite interaction zone.

Name	Dim.	Unit	Description
IIUSLG	-	-	Index of first cell with less than full density sodium on the end of the upper sodium slug opposite to the interaction zone or zero if the slug extends to the top of the channel.
ILIM	-	-	Set to the dimension of the arrays for the pin and channel mesh, presently 100.
ILIMP	-	-	Set to the dimension of the fuel particle group arrays, presently 1000.
INTPO	-	-	Interval between printouts. See input.
INTPO1	-	-	Switch to turn on double printouts every time step. See input.
IOPT5	-	-	Option for fuel ejection. See input.
IOPT6	-	-	Option for clad rip extension. See input.
IPASS	-	-	Counter for indicating which of two semi-implicit passes is being done.
IPCYCL	-	-	Number of time steps between writeouts of plot data.
IPLOT	-	-	If non-zero, unit number for plot data set.
IPR10	-	-	If non-zero, option for writing short form of output on unit 10.
IRST	-	-	Set non-zero in EQUILN when time step is to be repeated because of overcompaction or because of drastic increase in pin pressure.
IRST1	-	-	Set non-zero if time step is in the process of being repeated.

Name	Dim.	Unit	Description
IY	-	-	Seed for "random number" generator subroutine initially and on each call.
JOBID	(72,2)	-	Alphanumeric case identification.
MAXPRT	-	-	Maximum number of fuel particle groups allowed.
MPPART	-	-	Number of fuel particle per particle group at ejection.
NCL	-	-	Lowest cell in channel mesh.
NCU	-	-	Highest cell in channel mesh.
NCU1	-	-	NCU + 1.
NDIV	-	-	Number of cell subdivisions for particle recombination.
NFL1	-	-	Number of arrays in COMMON/FLOAT2/divided by 3.
NFL2	-	-	Number of arrays in COMMON/FLOAT2/divided by 2 assuming TFPRZ and HFPRZ each count as 10.
NFL3	-	-	Number of time dependent arrays in COMMON/FLOAT3/ divided by 2.
NFL4	-	-	Number of undimensioned variables is COMMON/FLOAT1/ divided by 3.
NFL5	-	-	Number of undimensioned variables in COMMON/FLOAT2/ divided by 2.
NPL	-	-	Lowest pin cavity cell.
NPLC	-	-	Lowest cell in fuel mesh.
NPL1	-	-	NPL + 1.
NPRAD	-	-	Number of radial cells in fuel mesh.

Name	Dim.	Unit	Description
NPU	-	-	Highest cell in in cavity.
NPUC	-	-	Highest cell in fuel mesh.
ON	-	-	Set to 1.0DO.
PHI	-	-	Current value of normalized power.
PI	-	-	Set to π.
PLINT	-	-	Time interval for plotting.
PLPLEN	-	dynes/cm^2	Pressure of lower plenum.
PMAS	(1000)	g	The mass of each fuel particle group.
PMASS	-	g	The mass of one fuel particle.
POINT	-	s	Time interval for printouts.
PTIME1	-	s	Time to initiate full printouts.
PTIME2	-	s	Time to end full printout.
PUPLEN	-	dynes/cm^2	Pressure of upper plenum.
P1	-	-	Set to 0.1 DO.
P125	-	-	Set to 0.125 DO.
P25	-	-	Set to 0.25 DO
P5	-	-	Set to 0.5 DO.
RAF	-	-	Coefficient in RAF(Re)^{RBF} for sodium liquid and pin cavity friction factor.
RAM	-	-	Coefficient in RAM(Re)^{RBM} for two-phase sodium friction factor.
RBF	-	-	Exponent in RAF(Re)^{RBF} for sodium liquid and pin cavity friction factor.
RBM	-	-	Exponent in RAM(Re)^{RBM} for two-phase sodium friction factor.

Name	Dim.	Unit	Description
RCL	(100)	cm	Outer cladding radius by axial cell.
RCIN	(100)	cm	Inner Cladding radius by axial cell.
RFG	-	ergs/cm·K	Gas constant for fission gas.
RFOUT	(100)	cm	Outer radius of solid fuel by axial cell.
RFPCN	(100)	K	Channel fuel reactivity component by axial cell.
RFPN	(100)	K	Total fuel reactivity by axial cell.
RFPPN	(100)	K	Pin fuel reactivity component by axial cell.
RFPO	-	K	Total fuel reactivity at t=0.
RFPON	(100)	K	Total fuel reactivity by axial cell a t=0.
RFU	-	ergs/cm·K	Gas constant for fuel vapor.
RNAO	-	K	Total sodium void reactivity at t=0.
RPART	-	cm	Radius of fuel particles in channel.
RVOID	(100)	cm	Radius of central void in each pin cavity cell.
SCOMP	-	cm^2/dyne	Sodium liquid compressibility.
SMELT	(100)	g/s	Rate of fuel melt-in for a time step by axial cell.
SVCON	(100)	g/s	Rate of sodium vapor condensation for a time step by axial cell.
TCL	(100)	K	Cladding temperature by axial cell. This includes the temperature-equivalent of the heat of fusion satisfied when the energy content has raised the temperature above the solidus.

Name	Dim.	Unit	Description
TIMAX	-	s	Maximum problem time.
TIME	-	s	Current time.
TIME01	-	s	First time step limit. See input.
TIME02	-	s	Second time step limit. See input.
TIME03	-	s	Third time step limit. See input.
TIME04	-	s	Fourth time step limit. See input.
TLPLEN	-	K	Temperature at upper free surface.
TMELT	-	K	Fuel melting temperature.
TNASS	(100)	K	Steady state sodium temperature for reactivity calculation by axial cell.
TO	-	-	Set to 2.0 DO.
TUPLEN	-	K	Temperature at upper free surface.
VAPS	(100)	-	Ratio of $\Delta E_{vap}/\Delta E_{liq}$. See Appendix A.
VFC	-	-	Volume fraction of coolant.
VISCF	-	g/s•cm	Absolute fuel viscosity.
VISCM	-	g/s•cm	Absolute viscosity of two-phase sodium and fission gas mixture.
VISCSL	-	g/s•cm	Absolute viscosity of sodium liquid.
VPFRO	(100)	-	Void fraction in coolant channel by axial cell.
WCOOL	(100)	$\frac{dk}{kgNa}\times 10^5$	Coolant reactivity worth by axial cell.

Name	Dim.	Unit	Description
WFUEL	(100)	$\frac{\Delta\rho}{a}\times 10^5$	Fuel reactivity worth by axial cell.
WPGM	(100)	W/g	Watts per gram of fuel by axial cell.
XMAX	-	cm	Highest fuel particle position in coolant channel.
XMAXO	-	cm	Highest fuel particle position in coolant channel at t = zero.
XMIN	-	cm	Lowest fuel particle position in coolant channel.
XMINO	-	cm	Lowest fuel particle position in coolant channel at t = zero.
YFL	-	-	"Random Number" from 0.0 to 1.0 resulting from RANDU call.
ZO	-	-	Set to 0.0 DO
ZPART	-	cm	Length of DPIC particle group.

APPENDIX D

LIST OF SYMBOLS USED IN TEXT

Quantities

English Letters

a	coefficient of Reynold's number in a Re^b formulation
A	area
b	exponent of Reynold's number in a Re^b formulation
c	speed of sound
C_D	drag function
C_p	specific heat
D	displacement
D_c	hydraulic diameter
E	energy
F	fraction of heat of fusion satisfied
FAC	multiplicative factor on FCI heat transfer term
g	gravitational acceleration
h_c	heat transfer coefficient
H_{fg}	heat of vaporization
H_{sf}	heat of fusion
k	thermal conductivity
L	length of slug
m	mass
M	mass
MU	momentum
P	pressure
Q	heat
R	gas constant

English Letters (Contd)

Re	Reynold's number
S	mass source or sink
t	time
T	temperature
U	velocity
V	volume
W	axial power distribution
X	ratio of fission gas mass to fuel mass in fuel pin
Y	factor determining amount of fission gas-fuel slip
z	space

Greek Letters

α	void fraction
β	compressibility
μ	viscosity
ρ	density
Φ	normalized power level
ψ	constant factor in particle momentum equation

Subscripts

b	bond
c	channel
cl	clad
con	condensation
ej	ejection
END	end of slug
ex	excess or remainder
fg	fission gas

Subscripts (Contd)

fp	fuel particle
fr	froth
fu	fuel
in	inner
liq	liquid
m	mixture
max	maximum
melt	melt-in
Na	sodium
p	pin cavity
ps	pin fuel surface
s	slug
sat	saturation
tot	total
vap	vapor

Superscripts

i,j,k	axial cell index
l	radial cell index
L	lower slug
m	particle group
n	time step
o	end of time step but before ejection
p	physical
U	upper slug

ACKNOWLEDGEMENTS

Acknowledgement must be made of the large amount of time and effort provided in the preparation of this document for publication by Dr. B. Burson of NRC/RSR.

Acknowledgement is also due to Dr. H. H. Hummel who provided needed i..sight and guidance in the production of this model, to Dr. H. U. Wider for many helpful conversations and to Dr. J. J. Sienicki for running a series of parametric cases which aided in the development of the code.

Special thanks is due to Ms. T. Maytan for her diligence and patience in typing this document.

REFERENCES

1. P. A. Pizzica and P. B. Abramson, *A Numerical Model of Reactor Fuel and Coolant Motions Following Pin Failure*, Nucl. Sci. Eng., *64*, p. 465-479 (1977).

2. P. A. Pizzica and P. B. Abramson, *EPIC, A Computer Program for Fuel-Coolant Interactions*, Proc. Int. Mtg. Fast Reactor Safety and Related Physics, Chicago, October 1976, CONF-761001, U.S. Energy Research and Development Administration (1977).

3. H. H. Hummel, P. A. Pizzica and Kalimullah, *Studies of Unprotected Loss-of-Flow Accidents for the Clinch River Breeder Reactor*, ANL-76-51 (April 1976).

4. H. H. Hummel, Kalimullah and P. A. Pizzica, *Physics and Pump Coastdown Calculations for a Model of a 4000 MWe Oxide-Fueled LMFBR*, ANL-76-77 (June 1976).

5. P. A. Pizzica and H. H. Hummel, *The Importance of Axial Propagation of Fuel Failure in LOF-TOP Scenarios for a Commercial-Sized LMFBR*, Trans. Am. Nucl. Soc., 33, p. 541 (November 1979).

6. D. R. Ferguson et al., *The Status and Experimental Basis of the SAS4A Accident Analysis Code System*, Proc. ANS/ENS International Mtg. Fast Reactor Safety Tech., Seattle, Washington, August 1979.

7. P. B. Abramson, *A Numerical Hydrodynamics Treatment of Fuel/Steel Pools with Density Variations from Nearly Pure Vapor to Incompressible Liquid*, Trans. Am. Nucl. Soc., *23*, 192 (June 1976).

8. P. J. Roache, *Computational Fluid Dynamics*, Hermosa Publishers, Albuquerque (1972).

9. D. H. Cho, R. O. Ivins and R. W. Wright, *Pressure Generation Under LMFBR Accident Conditions*, Proc. Conf. New Developments in Reactor Mathematics and Applications, Idaho Falls, March 1971, CONF-710302, U.S. Atomic Energy Commission (1971).

10. H. U. Wider, *An Improved Analysis of Fuel Motion During an Overpower Excursion*, PhD Thesis, Northwestern University, p. 45, (June 1974).

11. Graham B. Wallis, *One-Dimensional Two-Phase Flow*, McGraw-Hill Book Company, New York (1969).

12. M. E. Evans and F. H. Harlow, *The Particle in Cell Method for Hydrodynamics Calculations*, LA-2139, Los Alamos Scientific Laboratory (1957).

13. P. B. Abramson and J. J. Sienicki, *The Value of Distributed Particle in Cell Techniques*, Trans. Am. Nucl. Soc., *28*, p. 277 (1978).

14. H. U. Wider et al., *An Improved Analysis of Fuel Motion During an Overpower Excursion*, Proc. Conf. Fast Reactor Safety, Beverly Hills, California, April 2-4, 1974, CONF-740401, p. 1541, U.S. Atomic Energy Commission (1974).

15. S. L. Soo, *Fluid Dynamics of Multiphase Systems*, Blaisdell Publishing Company (1967).

16. *Reactor Development Program and Progress Report*, ANL-RDP-41, Argonne National Laboratory (1975).

17. H. E. Rose and H. E. Barnacle, *Flow of Suspensions of Non-Cohesive Spherical Particles in Pipes*, Parts 1 and 2, The Engineer (June 1957).

18. H. U. Wider, op. cit. (Reference 10), pp. 47-48.

19. L. Liebowitz et al., *Properties for LMFBR Safety Analysis*, ANL-CEN-RSD-76-1.

20. D. C. Menzies, *The Equation of State of Uranium Dioxide at High Temperatures and Pressures*, TRG Report 1119(D), UKAEA (1966).

21. A. Padilla, Jr., *High-Temperature Thermodynamic Properties of Sodium*, ANL-8095, Argonne National Laboratory (April 1974).

Distribution for NUREG/CR-1504 (ANL-80-47)

Internal:

W. E. Massey
J. A. Kyger
C. E. Till
... Avery
P. B. Abramson
C. E. Dickerman
D. Ferguson
L. Baker
P. L. Garner
H. Henryson
H. H. Hummel
Kalimullah
M. F. Kennedy
D. H. Lennox
P. A. Pizzica (16)
D. Rose
A. J. Goldman
J. F. Marchaterre
J. J. Sienicki
W. J. Sturm
D. Weber
H. Wider
W. T. Sha
L. G. LeSage
J. B. Wozniak
ANL Contract File
ANL Libraries (3)
TIS Files (3)

External:

USNRC, Washington, for distribution per R7 (360)
DOE-TIC, Oak Ridge (2)
Manager, Chicago Operations and Regional Office, DOE
Chief, Office of Patent Counsel, DOE-CORO
President, Argonne Universities Association, Argonne, Ill.
Applied Physics Division Review Committee:
P. W. Dickson, Jr., Westinghouse Electric Corp., 3300 Appel Rd., Bethel Park, Pa. 15102
R. L. Hellens, Combustion Engineering, Inc., Windsor, Conn. 06095
K. D. Lathrop, Los Alamos Scientific Lab., P. O. Box 1663, Los Alamos, N.M. 87545
W. B. Loewenstein, Electric Power Research Inst., P. O. Box 10412, Palo Alto, Calif. 94303
R. F. Redmond, College of Engineering, The Ohio State University, 2070 Neil Ave., Columbus, O. 43210
R. Sher, Dept. Mechanical Engineering, Stanford U., Stanford, Calif. 94305
D. B. Wehmeyer, The Detroit Edison Co., 2000 Second Ave., Detroit, Mich. 48226
C. Erdman, U. Virginia, Charlottesville, Va. 22904
K. O. Ott, Purdue U., West Lafayette, Ind. 47906
R. Lancet, Atomics International, P. O. Box 309, Canoga Park, Calif. 91304